Isabel Bevilacqua, BSc.

"Thermal Regime of the Uppermost Blocky Layer of Intact and Relict Rock Glaciers"

MASTER'S THESIS

To achieve the university degree of

Master of Science

Master's degree programme: Earth Science

Submitted to

Graz University of Technology

and

University of Graz

Supervisor

Assoz.-Prof. Mag. Dr.rer.nat., Gerfried Winkler

Institute for Earth Science

Graz, December 2019

AFFIDAVIT

I declare that I have authored this thesis independently, that I have not used other than the declared sources/ resources and that I have explicitly marked all material which has been quoted either literally or by content from the used sources. The text document uploaded to TUGRAZonline is identical to the present master's thesis.

Graz, December 2019

EIDESSTATTLICHE ERKLÄRUNG

Ich erkläre ehrenwörtlich, dass die ich die wissenschaftliche Arbeit selbstständig verfasst, andere als die angegebenen Quellen/Hilfsmittel nicht benutzt und die den Quellen wörtlich oder inhaltlich entnommenen Stellen als solche kenntlich gemacht habe. Das in TUGRAZonline hochgeladene Textdokument ist mit der vorliegenden Masterarbeit identisch.

Graz, Dezember 2019

Isabel Bevilacqua, BSc.

ACKNOWLEDGEMENTS

I would like to acknowledge everyone who supported me during the realization of this thesis. My deep appreciation I would like to give to my supervisor Gerfried Winkler for the valuable suggestions, ideas, discussions and support throughout this time. Furthermore, a special gratitude to Tom Wagner, whose encouraging suggestions, discussions and remarks helped me to accomplish the thesis. I am also thankful to Thomas Pedevilla for the help and consultations during this work. A special thanks goes to Renato R. Colucci and Raoul A. Collenteur for their important suggestions and remarks. Also, I would like to thank Karl Krainer of the University of Innsbruck for providing the data set of the temperature loggers installed at the rock glaciers in Tyrol.

Digital elevation models and the topographic maps were provided by the GIS Service of the Federal Government of Styria and Tyrol. The data of the weather station at Ischgl/Idalpe was kindly provided by ZAMG ("Zentralanstalt für Meteorologie und Geophysik"). This work was co-founded by the Austrian Federal Ministry of Sustainability and Tourism and the Federal States of Styria, Carinthia, Vorarlberg and Tyrol (BBK – Nr. 101093).

A particular thanks I would like to give to all of my study colleagues for the unforgettable time. A special thank goes to my friends Diana, Karin, Katja, Anna, Alina and Markus, who supported me throughout good as well as hard times during these last years of my study. For the encouragement, the patience, the motivation and the help I would like to thank my girlfriend Giada. Last but not least I would like to express my deepest gratitude to my family for the confidence, the strength and the support they sent me every single day of my study despite the big distance that lies between us.

Table of Content

Abstract

Rock glaciers are a common periglacial landform in Alpine areas and often contain permafrost ice. Being one of the components of the cryosphere, it is known that permafrost ice is sensitive to climatic changes over long time periods. Yet, the uppermost coarse blocky layer of rock glaciers acts as an isolating and therefore protective shield causing a buffered reaction to external temperature changes. The top blocky layer of rock glaciers (active layer) lies above the permafrost ice body and is subject to seasonal freezing and thawing processes. Considering the complexity, its thermal behavior is not fully understood yet. The present study aims to contribute to a better understanding of the thermal regime of the uppermost layer of relict compared to intact rock glaciers. The goal is to identify the main internal and external impact factors that influence the thermal regime of the upper coarse blocky layer of the two rock glacier types. Therefore, the ground surface- and ground temperature of different intact rock glaciers and one relict rock glacier were monitored for a specific period of time. The data were evaluated determining their correlation coefficients, applying cross-correlation methods and calculating the Rayleigh number. Considering geomorphological features of the rock glaciers, the temperature values were observed as function of time and depth and compared to the air temperature. The results suggest that the thermal regime of the top layer of both rock glacier types is influenced by the altitude, the corresponding air temperature, the grain size distribution and thus the porosity of the material, as well as by the microtopographic condition and the resulting exposition to solar radiation. The top layer of either rock glaciers is characterized by dampened and cooler temperature values compared to the air temperature. This is due to air convection, i.e. a vertical movement of cold air within the open voids of the blocky layers. The two rock glacier types differ in the interaction with the air temperature. The relict rock glacier is stronger affected by external temperature changes than the intact ones. The latter are shielded by a thicker and more continuous snow cover in winter given by their higher elevation. Additionally, the ice core of intact rock glaciers cools down the thermal regime of the active layer and induces a buffer effect, especially observed in summer, which suppresses the influence of the air temperature. Since rock glaciers represent a crucial hydrogeological component in Alpine regions it is important to observe their thermal behavior in order to understand their evolution in time.

Zusammenfassung

Blockgletscher gehören zu den häufigsten periglazialen Landschaftsformen hochalpiner Gebiete, die Permafrost-Eis beherbergen können. Als wichtiger Bestandteil der Kryosphäre reagiert Permafrost über lange Zeiträume sensibel auf klimatische Veränderungen. Jedoch antworten Blockgletscher auf externe Temperaturänderungen gedämpft, weil ihre oberste grobblockige Schicht als isolierendes Schutzschild fungiert. Diese oberste Blockschicht ist saisonalen Tau- und Frostprozessen ausgesetzt und liegt oberhalb der Permafrostgrenze. Das thermische Verhalten der Schicht ist wegen des komplexen Aufbaus noch nicht vollständig bekannt. Diese Studie vergleicht das thermische Regime der obersten Blockschicht von reliktischen mit intakten Blockgletschern. Es soll aufgezeigt werden, welche externen und internen Faktoren das Temperaturverhalten beeinflussen und wie sich die beiden Blockgletschertypen thermisch unterscheiden. Innerhalb eines bestimmten Zeitraums wurden dafür Oberflächen- und Bodentemperaturen an verschiedenen intakten und einem reliktischen Blockgletscher gemessen. Diese Temperaturdaten wurden analysiert, indem der Korrelationskoeffizienten berechnet, die Kreuzkorrelation angewandt und die Rayleigh-Nummer kalkuliert wurde. Die Temperaturdaten wurden als Funktion der Zeit und Tiefe untersucht und mit der jeweiligen Lufttemperatur verglichen. Dabei wurden auch geomorphologische Aspekte der Blockgletscher in die Analyse miteinbezogen. Ergebnisse zeigen, dass sich die Höhenlage und die entsprechende Lufttemperatur, die Korngröße und die korrespondierende Porosität sowie die mikrotopographischen Bedingungen und die sich daraus ergebende Exposition zur Sonneneinstrahlung direkt auf das Temperaturverhalten auswirken. Im Vergleich zu den Lufttemperaturen zeigen die Temperaturwerte der obersten Schicht beider Blockgletscher einen gedämpften Verlauf und relativ niedrige Werte. Das ist darauf zurückzuführen, dass Energie in der grobblockigen Schicht hauptsächlich über Luftzirkulation in Form von vertikaler Konvektion transportiert wird. Der Unterschied zwischen den beiden untersuchten Blockgletschertypen zeigt sich hauptsächlich in ihrer Wechselwirkung mit der Atmosphäre. Der reliktische Blockgletscher wird intensiver von äußeren Temperaturschwankungen beeinflusst, während der intakte Blockgletscher nur abgeschwächt darauf antwortet. Durch die höhere Lage erweist sich die dickere und kontinuierliche Schneedecke als Schutzschicht im Winter. Weiters kühlt der Eiskern der intakten Blockgletscher das thermale Regime der oberen Blockschicht auf und wirkt vor allem im Sommer abdämpfend, da er den Einfluss der Lufttemperatur unterdrückt. Da Blockgletscher eine wesentliche Rolle in der hochalpinen Hydrogeologie spielen, ist es entscheidend ihr thermisches Verhalten und dessen Entwicklung mit der Zeit zu verstehen.

Riassunto

I ghiacciai rocciosi ("rock glaciers") sono fra i fenomeni periglaciali più frequenti delle aree alpine e possono contenere ghiaccio interstiziale, il quale nel tempo è sensibile ai cambiamenti climatici. Tuttavia, lo strato superiore dei ghiacciai rocciosi è costituito principalmente da blocchi grossolani che fungono da isolante attenuando i cambiamenti di temperatura dell'aria esterna. Lo strato superiore al permafrost, o "strato attivo", è sottoposto stagionalmente a processi di congelamento e scongelamento. Data la sua complessità strutturale, il comportamento termico dello strato attivo non è ancora del tutto chiarito. Questo studio mira a raggiungere una migliore comprensione in merito al comportamento termico dello strato attivo, mettendo a confronto lo strato superiore di ghiacciai rocciosi attivi e ghiacciai rocciosi relitti. Per fare questo, è stata monitorata la temperatura dello strato superiore di diversi ghiacciai rocciosi attivi e inattivi per un certo periodo di tempo. L'analisi dei dati è stata effettuata calcolando l'indice di correlazione sulla base del metodo di correlazione incrociata e valutando il numero di Rayleigh. Prendendo in considerazione le caratteristiche geomorfologiche di ogni singolo ghiacciaio roccioso, è stata analizzata l'evoluzione termica nel tempo. Questa è stata poi messa a confronto con la temperatura esterna dell'aria. I risultati dimostrano che il regime termico dipende dalla temperatura esterna che a sua volta dipende principalmente dall'altitudine, dalla granulometria e dalla risultante porosità del materiale, cosi come da attributi microtopografici che a loro volta condizionano l'esposizione alla radiazione solare. Entrambi i ghiacciai rocciosi mostrano temperature medie più smorzate e generalmente più basse rispetto alla temperatura dell'aria. Questo è dovuto principalmente alla circolazione dell'aria (convezione) tra i vuoti presenti tra i blocchi che costituiscono lo strato superficiale attraverso flussi verticali. La differenza tra i due tipi di ghiacciai rocciosi si nota soprattutto nella loro interazione con l'atmosfera. Laddove il ghiacciaio roccioso relitto viene particolarmente influenzato da cambiamenti di temperatura esterna, il ghiacciaio roccioso attivo reagisce in modo più attenuato. L' effetto smorzante è dovuto al manto nevoso che ricopre il ghiacciaio roccioso attivo d'inverno. Il manto si presenta più compatto e massiccio sul ghiacciaio roccioso attivo, poiché quest' ultimo presenta un'altitudine maggiormente elevata. Il nucleo di ghiaccio presente nei ghiacciai rocciosi attivi, funge da ulteriore attenuante. Infatti, soprattutto in estate, il nucleo congelato dei ghiacciai rocciosi attivi raffredda lo strato attivo inducendo una sorta di effetto tampone che inibisce l'influenza della temperatura esterna. In quanto i ghiacciai rocciosi svolgono un ruolo essenziale nel sistema idrogeologico alpino, è importante comprendere il loro comportamento termico nel tempo.

1. Introduction

The cryosphere represents one of the most important parts of the Earth's climate system. Within this sphere the Earth's surface water exists in solid form (Kong and Wang 2017), influencing the planet's energy budget and water cycle. Since all components of the cryosphere, including glacier, permafrost, snow, ice sheets as well as river, lake and sea ice, react sensitively to temperature changes over long periods of time, this sphere embodies a crucial evidence of climate change (Intergovernmental Panel on Climate Change 2014). Glacier retreat and permafrost thaw are among the most important consequences of the current climate change (Brighenti et al. 2019). Given the consistent increase of temperature, permafrost areas will shrink, the southern boundary of permafrost in the northern hemisphere will move northward and the snow water equivalent as well as the volume of ground ice stored in permafrost will decrease significantly in future (Kong and Wang 2017). The progressive thawing of permafrost in Alpine areas may lead to a significant change in Alpine hydrology, geomorphological stability and stream ecosystems (Brighenti et al. 2019). It is therefore important to understand the thermal behavior of permafrost bodies and its reaction to external temperature changes. Due to different surface properties, the response of ice-rich permafrost to climate change differs significantly to the one from ice sheets. The coarse debris cover, typical for periglacial environments (Herz et al. 2003) and especially to be found in rock glaciers, acts as protecting shield and causes a slower reaction to temperature increase (Scherler et al. 2011). The coarse material on the surface hereby acts not only as thermal buffer, but can also cause a decrease of temperature within the permafrost body. The cooling effect of coarse grained surface layers has been observed in different studies all over the world (Hanson and Hoelzle 2004; Hinkel and Outcalt 1994; Guodong et al. 2007; Romanovsky et al. 2010). For two years Harris and Pederson (1998) monitored air and ground temperatures beneath coarse blocky materials comparing them to mineral soils. They observed that temperatures in blocky materials are 4-7 K cooler than in mineral soils. Therefore, it is possible to find permafrost conditions in block fields located even below the regional continuous permafrost limit. Using crushed rock embankments, permafrost tables can rise significantly (Wu et al. 2009) and thermal regimes can be controlled in order to avoid destabilization of permafrost grounds in sensible regions (Qingbai et al. 2007). The understanding of the processes leading to the cooling effects is still matter of many different researches. In general, the processes controlling thermal transport within coarse grained surface layers are conduction within blocks, convection within the open voids and thermal radiation (Wagner et al. 2019b). Conduction is mainly effective in between blocks. Hence, it is a limited process when it comes to coarse grained layers, since blocks are only connected by single points (Juliussen et al. 2008). Convection is a density driven transport of air (cold air is denser than warm air) and can be divided into vertical circulation (Balch effect) and lateral circulation (advection – Chimney effect, according to Harris and Pederson (1998). Thermal radiation includes shortwave (originated by

sun) and longwave radiation (reflected by rock) (Scherler et al. 2014) and is directly influenced by geomorphological conditions, e.g. slope and aspect (Nield and Bejan, 2019). Due to the complex structure of such bodies and the alteration of solid rock material and air filled voids, it is difficult to characterize the exact thermal behavior. Unlike fine grained sediments, in which the thermal behavior is mainly controlled by conduction and solely depending on petrophysical properties, in coarse grained sediments the amount of open voids in between the blocks permits atmospheric processes to influence the thermal regime (Herz et al. 2003). Depending on external conditions, for instance snow cover and exposition to the wind, specific processes can serve as temperature transport within the voids. Harris and Pederson (1998) summarized four of these possible processes, which are the Balch effect, the chimney effect, the summer evaporation/sublimation of water/ice in blocky debris and the continuous air exchange with the atmosphere. Lebeau and Konrad (2016) suggested that convection and thermal radiation are the most effective transport processes acting in dry coarse grained layers and causing respectively cooling or heating effects.

In Alpine areas, coarse grained layers are especially found in rock glaciers, which are a very common periglacial landform and can contain permafrost ice. Acting as significant groundwater storages, they represent a crucial hydrological component in Alpine regions (Pauritsch et al. 2017). It is important to distinguish between different rock glaciers depending on their evolutionary stage (Colucci et al. 2019). According to their degree of activity and content of ice volume, rock glaciers can be subdivided into intact (active and inactive) and relict rock glaciers (Barsch 1992). Haeberli (1991) and Barsch (1992) proposed the following classification: Active rock glaciers are characterized by the presence of ice, sufficient to cause internal deformation which induces creeps and movement. Inactive rock glaciers contain ice, but do not move anymore due to the ice melting, i.e. climatically inactive, or due to morphological obstacles, i.e. dynamically inactive (Colucci et al. 2019). Relict rock glaciers do not move anymore and it is assumed that internal ice is completely absent. Wagner et al. (2019b) compared the thermal regime of two relict rock glaciers with opposing aspects, being exposed to different wind and snow cover conditions. So far, knowledge related to the difference between the thermal behavior of intact and relict rock glaciers is very limited. Since it is believed, that due to climate change, more and more intact rock glaciers will progressively evolve into relict rock glaciers (Pauritsch et al. 2017), it is an essential issue to observe their thermal behavior for a better understanding of their evolution over time.

This study tries to give insights into the differences of the thermal behavior of the uppermost coarse blocky layer of intact and relict rock glaciers. At first, the thermal heterogeneity on the surface of four investigated rock glaciers (Schöneben, Bergli, Hochschober and Tuxer Hauptkamm) will be analyzed comparing their ground surface temperature data. Secondly, the internal heterogeneity of two specific

rock glaciers is investigated. Using datasets of the relict (Schöneben) and the intact (Bergli) rock glacier, the difference will be observed using ground temperatures and ground surface temperatures. Both parameters will be analyzed and compared as function of time (for a period of one year) and depth (to a maximum of 1 m depth). The Rayleigh number will be calculated in order to estimate the influence of free convection acting within the coarse grained material. Finally, the reaction of ground temperature and ground surface temperature to the changing air temperature will be investigated using statistical cross-correlation methods.

The final aim is to identify the differences of the thermal regime and determine the internal and external factors that lead to the diverse thermal behavior of intact compared to relict rock glaciers.

2. Study Areas

The investigated rock glaciers are situated in Austria within the Eastern Alps. The relict rock glacier Schöneben is located in Styria and the intact rock glaciers Bergli, Tuxer Hauptkamm and Hochschober, are distributed over the region of North and East Tyrol (Figure 1). According to the Alpine Permafrost Index Map (Boeckli et al. 2012), the intact rock glaciers are situated above the permafrost limit suggesting the presence of permafrost ice underneath their active layer. In contrast, permafrost ice is expected to be mainly absent in the relict rock glacier, since it is located underneath the limit proposed by Boeckli et al. (2012).

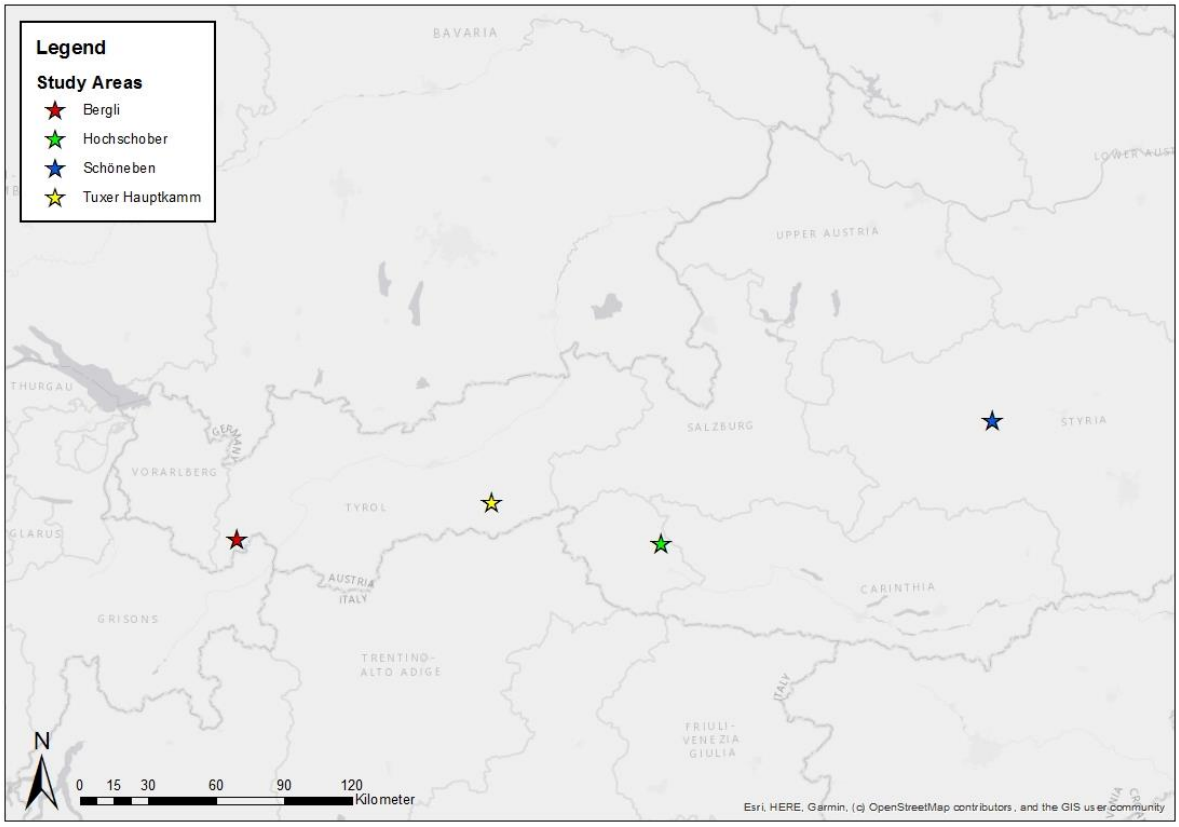

Figure 1 Overview of all study areas located in Styria (Schöneben rock glacier: blue star) and Tyrol (Bergli rock glacier: red star, Tuxer Hauptkamm: yellow star and Hochschober: green star), Austria, Eastern Alps (ESRI, HERE, Garmin, © OpenStreetMap contributors, and the GIS user community)

2.1. Rock Glacier Schöneben, Styria

The rock glacier Schöneben, SRG hereinafter (Kellerer-Pirklbauer et al. 2015b), is located in the Niedere Tauern, Styria (Austria). The catchment area has an expansion of 0,67 km^2, it distends to 2295 m a.s.l. and it is drained by a spring located directly at the front slope of SRG (Winkler et al. 2016b). The rock glacier is facing NE and is characterized by steep slopes at the front and its root and by a more gentle slope in the middle section (mean slope is 22,2°). It is a tongue shaped rock glacier (see Figure 2 and Figure 3) with a maximal length of 746 m, a maximal width of 244 m and an area of 0,11 km^2 (Wagner et al. 2019a). Geologically it lies within the “Seckauer Tauern” nappe as part of the “Silvretta-Seckau”

nappe System, the lowermost part of the Upper Austroalpine Unit. The nappe consists of a basement of Variscan metamorphic imprint and remnants of Permian to Triassic cover sediments. The lithology in this area is dominated by granitoidic-gneissic rocks (Pfingstl et al. 2015). The rock glacier is covered by vegetation such as pinus mugo, larch and pinus cembra (Kellerer-Pirklbauer et al. 2015a).

(a)

(b)

Figure 2 Rock glacier Schöneben shown in bird's eye view (a) and from a frontal perspective (b) in direction south-southeast (GoogleEarth image © 2019 Maxar Technologies)

The morphology is characterized by ridge and furrow topography as well as collapse structures and the surface consists of coarse grained to blocky debris. The size of the coarse material ranges from a few decimeters up to boulders of several meters in diameter (Wagner et al. 2019b). Permafrost is expected to be absent, since it is located underneath the permafrost limit which is modelled in the Alpine Permafrost Index Map (Boeckli et al. 2012). Mainly due to the morphological aspect and the mean water temperatures of the spring reaching more than 2,0° C, it is defined as relict rock glacier (Kellerer-

Pirklbauer et al. 2015a). Cold water temperature pulses were observed after relatively warm rainfall events (Winkler et al. 2016b) and could be explained by cooling effects acting within the rock glacier. Geophysical studies (Winkler et al. 2016b; Pauritsch et al. 2017) have shown that the upper layer, which is several meters thick, consists of coarse surface material. The underlying zone, being several tens of meters thick, is dominated by coarse grained to blocky material that also includes fine grained material. The main aquifer responsible for the baseflow of the spring is assumed to be the lowest with a 15m thick layer containing fine sand to silty material.

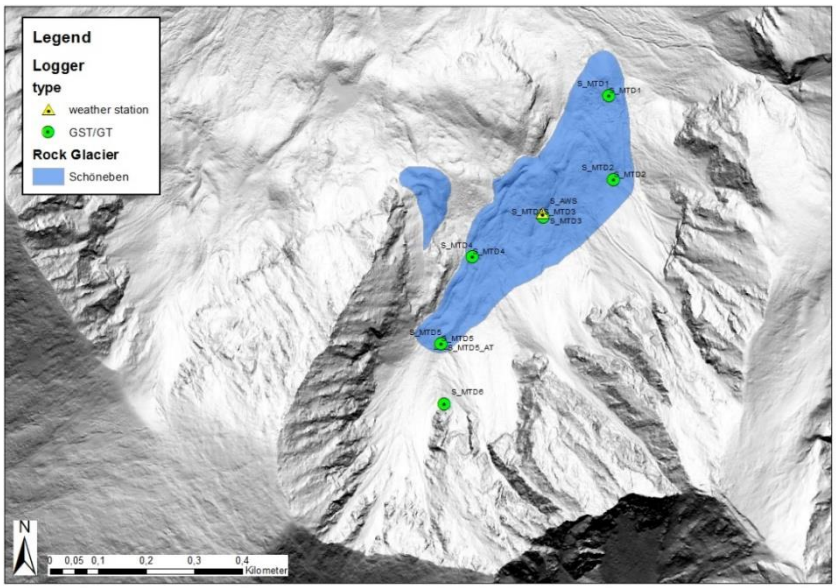

Figure 3 Rock glacier Schöneben; blue area shows the rock glacier and green dots indicate the location of the temperature loggers

2.2. Rock Glacier Bergli, Tyrol

The rock glacier Bergli (RGB hereinafter) is located in the southernmost part of the Silvretta Alps, a mountain range of the Central Eastern Alps in Tyrol. It's situated in the valley of Larein, south-east of Galtür within the cirque named "Innerer Bergli" facing NE (Pedevilla 2019). The area of the hydrological catchment covers 1,59 km^2 and underneath the front slope of the rock glacier four springs drain the groundwater. Due to the evident steep front (ca. 40°), it differs clearly from the surrounding periglacial moraines (see Figure 4). The maximal length is 1545 m, the maximal width 674 m, its root lies at 2668 m a.s.l. and its front slope at 2164 m a.s.l. (Wagner et al. 2019a).

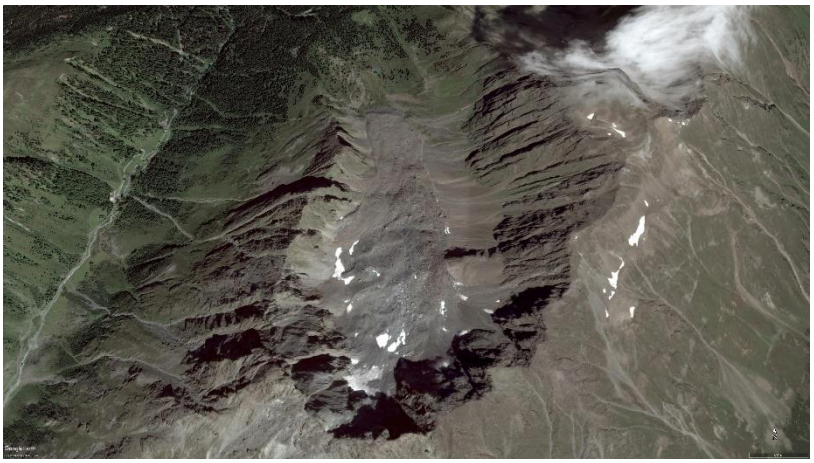

(a)

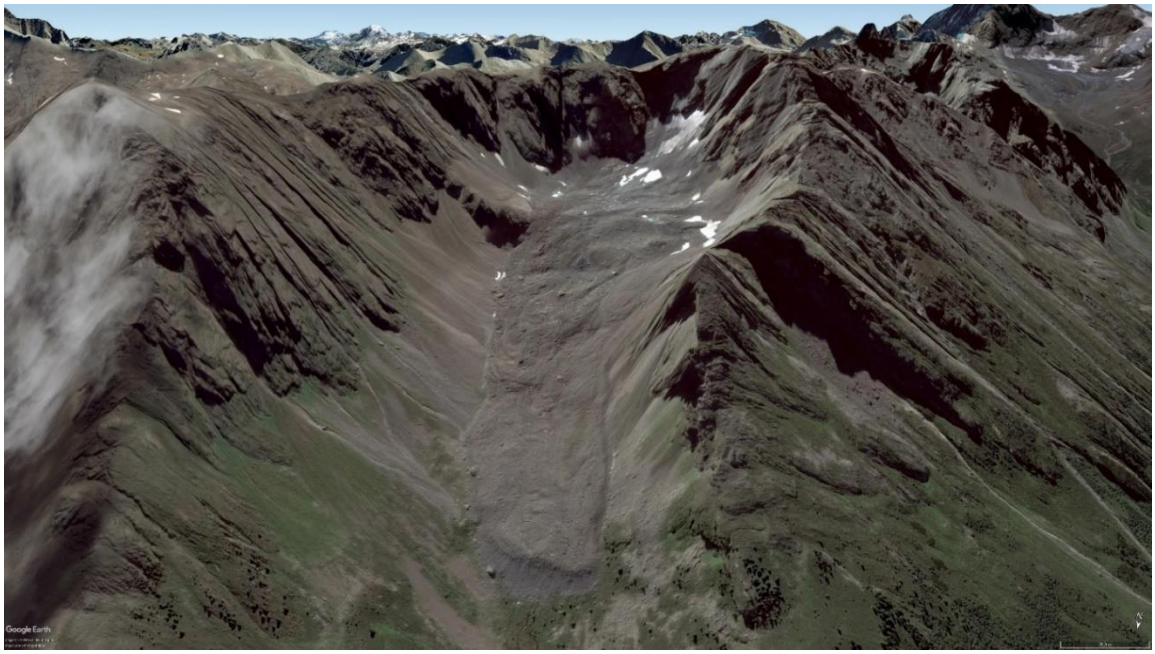

(b)

Figure 4 Rock glacier Bergli shown in bird's eye view (a) and from a frontal perspective (b) in direction south - Berglerloch (GoogleEarth image © 2019 Maxar Technologies)

The front part is divided into two tongue shaped bodies (Figure 5). Quartz-gneiss are dominating the lower part of the rock glacier as well as the eastern and western mountain ranges. Pegmatites are partly found in the eastern areas. In the upper area of the rock glacier amphibolite and migmatites are prevailing. The lowermost part of the rock glacier is partially covered by vegetation; therefore, it can be assumed, that the degree of activity is already low. Also, in the areas characterized by fine grained material, vegetation (e.g. larch) is found. The grain size of the surface ranges from fine grained, coarse grained (diameter up to 50 cm) to blocky (range of meters) material (Wagner et al. 2019a).

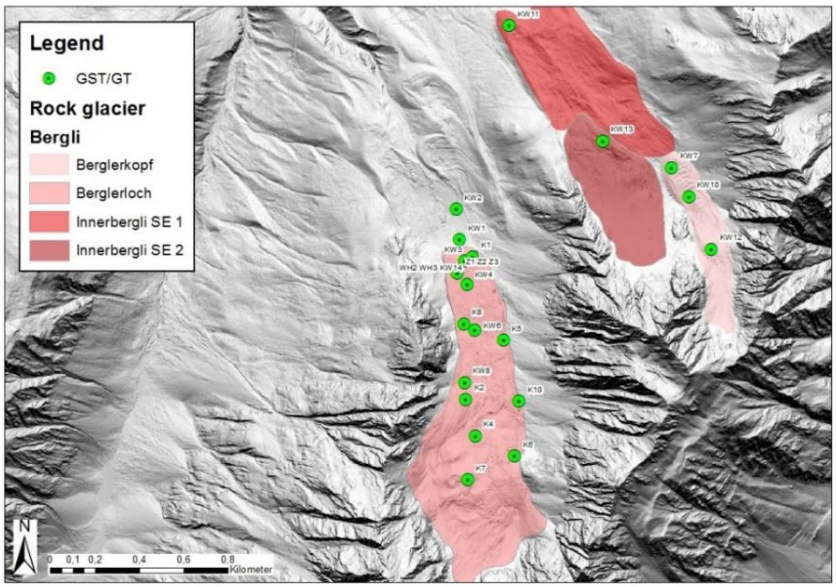

Figure 5 Rock glacier Bergli: red areas indicate the rock glacier and green dots show the positions of the temperature loggers

2.3. Rock Glaciers Hochschober, Tyrol

In the area of the "Hochschober", several different rock glaciers (RGH hereinafter) are situated. Most of these rock glaciers are located in the northern area of the Schober group, which is a sub-group of the Hohe Tauern mountains in the Central Eastern Alps, geologically characterized by the "Koralpe-Wölz" nappe system. The lithology is dominated by shists and paragneiss, whereat amphibolites and eclogites are sparely distributed (Klackl 2018). According to Wagner et al. (2019a) either relict or active rock glacier are found in this area (Figure 6).

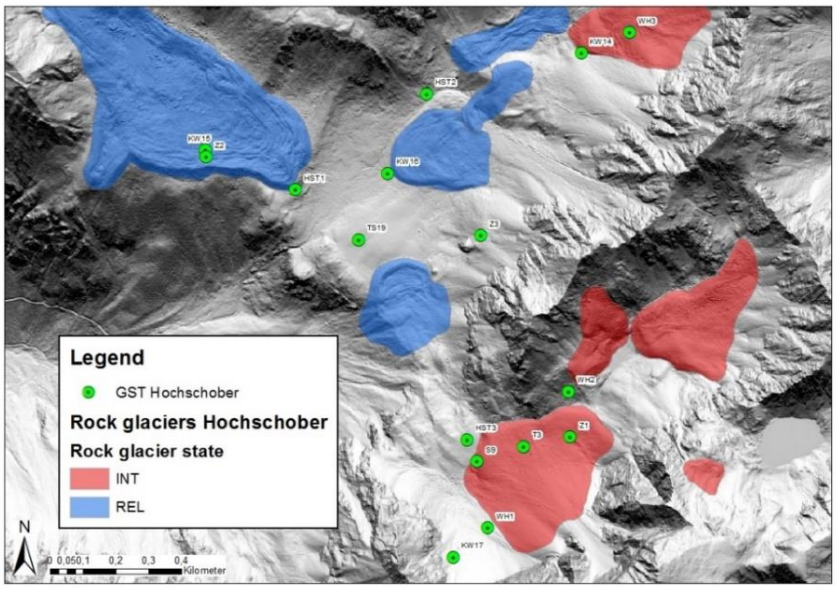

Figure 6 Rock glaciers at Hochschober: relict rock glaciers indicated as blue areas and intact rock glaciers as red areas; green dots show the location of the temperature loggers

2.4. Rock Glaciers Tuxer Hauptkamm, Tyrol

The study area of the Tuxer Hauptkamm is located in the Hohe Tauern Window (Wagner et al., 2019a). Three different rock glaciers were monitored in this region (Haberfeldkopf, Mittelschneidkar, Lange Wand Kar; hereinafter RGT1, RGT2 and RGT3 respectively). The smallest rock glacier, with an area of 0,3 km^2, is represented by RGT1 and its lithology is characterized by carbonate debris (Kogler 2018). The maximal length and the maximal width of RGT2 is 975 m and 327 m respectively and the front slope is situated at 2394 m a.s.l. The biggest and easternmost rock glacier is RGT3 (see Figure 7), being 1595 m long and 268 m wide, with the front slope at 2247 m a.s.l. (Wagner et al. 2019a). According to Kogler (2018), the geological background of these rock glaciers is characterized by karstified marble dominating in the lower parts ("Hochstegenmarmor") and gneissic rocks prevailing in their middle and upper range ("Zentralgneiss"). Springs underneath the rock glaciers are absent, indicating a complex karst aquifer system (Wagner et al. 2019a). According to Boeckli et al. (2012) permafrost can be expected in all rock glaciers. The surface of RGT2 and RGT3 is characterized by coarse blocky material, whereas RGT1 consists of significantly finer grained material (Kogler 2018).

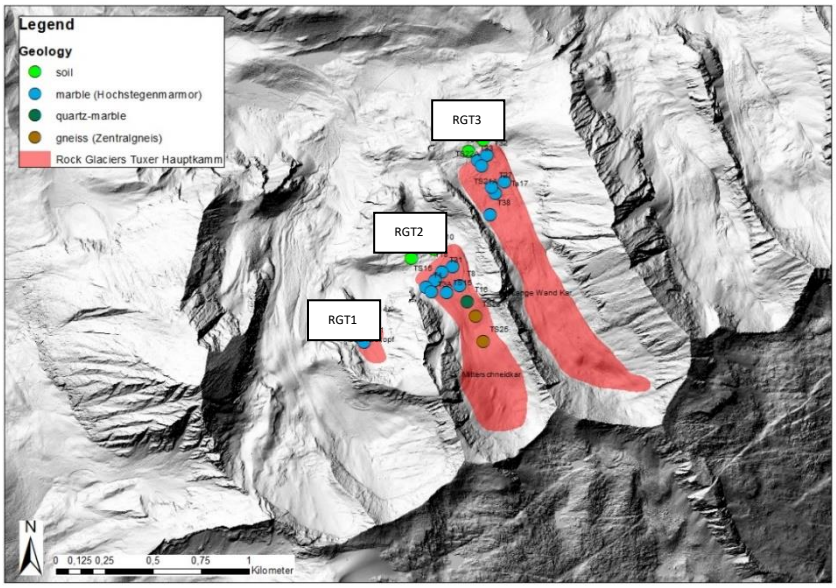

Figure 7 Rock glaciers at Tuxer Hauptkamm: red areas indicate the rock glaciers and the colored dots show the position of the loggers. The different colors correspond to the geology of the bedrock found in the specific areas (after Wagner et al. 2019b)

3. Methods

Based on the data listed in the next chapter, the following methods were applied in this study.

3.1. Field data

As listed in Table 1, the field data were provided by the Institute for Earth Science of the University of Graz and by the Department of Geology of the University of Innsbruck.

Table 1 General information of the loggers used in this study and most important geographical and geomorphological characteristics of the rock glaciers (after Wagner et al. 2019a). Ground surface temperature indicated as "GST"; ground middle temperature defined as "GMT" and ground temperature given as "GT"

rock glacier	n° of loggers	logger type	measuring period	data provided by	geography	aspect	altutide [m a.s.l]	geology	vegetation	graine size distribution
Schöneben (SRG)	5 + 5	GST + GT	11/2011 -present	Institute for Earth Science (University of Graz)	Niedere Tauern	NE	1814	gneiss	pinus mugo, larch, pinus cembra	coarse - blocky
Bergli (RGB)	29 + 2 + 2	GST + GMT + GT	10/2016 – 07/2018	Department of Geology (University of Innsbruck)	Silvretta Alps	N	2416	quartz-gneiss	scarce on fine-grained area - larch	fine - coarse - blocky
Hochschober (RGH)	14	GST	10/2016 – 06/2017	Department of Geology (University of Innsbruck)	Schober group	NW	2559	shists/ para gneiss	no vegetation	fine - coarse - blocky
Tuxer Hauptkamm (RGT)	23	GST	10/2016 – 06/2017	Department of Geology (University of Innsbruck)	Hohe Tauern window	NW	2498	marble/ marble quartz/ gneiss	no vegetation	fine - coarse - blocky

At the rock glacier Schöneben, five miniature temperature loggers with an accuracy of +/- 0,1 °C (at 0°C) and a resolution of +/- 0,01 °C (M-Log5W-SIMPLE; GeoPrecision GmbH) were used to measure ground surface temperature (GST) and ground temperature (GT) within the rock glacier. The loggers monitoring the ground surface temperature were installed underneath a shielding block which protected them from direct solar radiation. The loggers measuring the ground temperature were put on a wooden stick and placed into a pore space of the coarse blocky layer to a depth of one meter. The loggers have been monitoring the temperature since December 2011 to an hourly interval. They were installed along a longitudinal profile, distributed over the whole elevation of the rock glacier body. Furthermore, an automatic weather station (S-AWS) was installed on the rock glacier measuring air temperature (AT) and other climate parameters at site SMTD3 (see Figure 8 - a). Additionally, air temperature (type M-Log-5W-HUMIDITY; GeoPrecision GmbH) was measured 2 m above the ground

surface at site SMTD5 (see Figure 9). According to Wagner et al. (2019b) the temperature data of the two weather stations installed on the relict rock glacier correlate well. Therefore, the air temperature data of the weather station S-AWS (at SMTD3) was considered representative for the rock glacier and thus used for the calculations of this study.

(a) 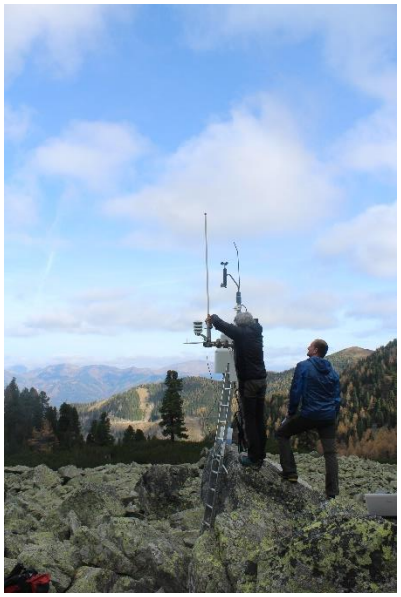  (b)

Figure 8 Automatic weather station (S-AWS) at site SMTD3 (a) and coarse blocky uppermost layer of the relict rock glacier Schöneben (b) – 25/10/2019

At RGB overall 29 temperature loggers with an accuracy of +/- 0,2 °C were installed (HOBO Water Temperature Pro v2 Data Logger, Onset Computer Corporation). As indicated in Figure 9, 11 of those were installed in October 2016 and measured ground surface temperature to a two hour interval until June 2017. 8 more temperature loggers were installed in October 2017 and monitored the ground surface temperature until July 2018. As shown in Figure 5 the data loggers are distributed in two different areas of RGB, providing an overview of the regional temperature setting. Furthermore, from August 2017 until July 2018, two temperature logger-profiles were stationed within coarse grained and fine grained sediment. Each profile was equipped with three loggers, which measured the temperature on the ground surface at 0,10 m depth, in the ground at 1,0 m depth and in between ground and surface at 0,50 m depth. The logger profiles were installed in the lower part of the rock glacier (see Figure 9).

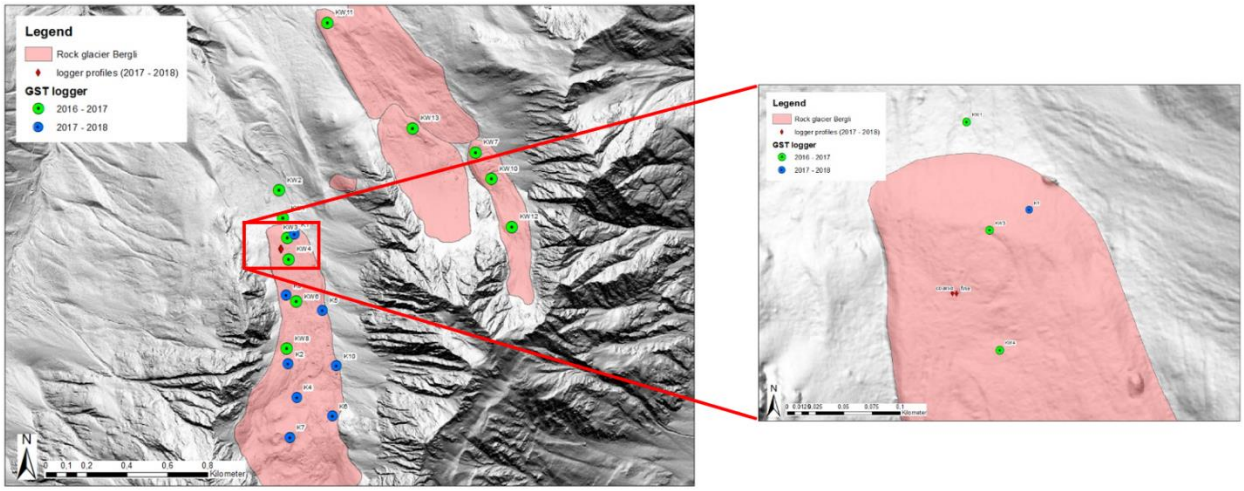

Figure 9 Exact position of the two logger profiles installed at RGB within fine and coarse grained material. Green dots indicate the position of the loggers that monitored GST from October 2016 until July 2017 and blue dots show position of the loggers that measured GST from September 2017 until August 2018

The air temperature monitored at the weather station Ischgl-Idalpe, situated 5 km from RGB at an elevation of 2308 m a.s.l. (Figure 10), was provided by ZAMG ("Zentralanstalt für Meteorologie und Geophysik"). Given the geomorphological settings, the latter data set was assumed to be the prevailing temperature for the specific area of RGB and was used for the further calculations in this study.

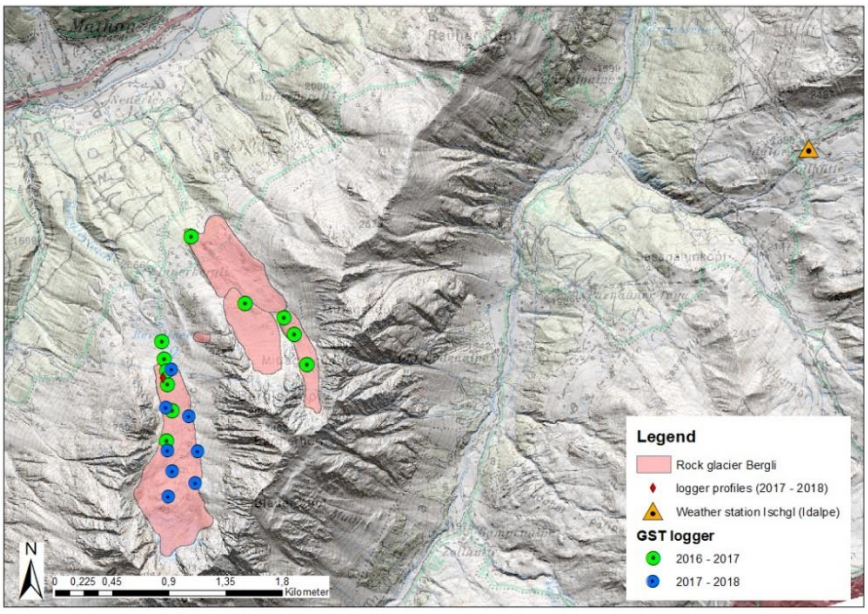

Figure 10 Rock glacier Bergli and the weather station (orange triangle) installed at Ischgl-Idalpe by ZAMG („Zentralanstalt für Meteorologie und Geophysik")

At RGH, 14 temperature loggers with an accuracy of +/- 0,2 °C (HOBO Water Temperature Pro v2 Data Logger, Onset Computer Corporation) were installed in October 2016 measuring the ground surface temperature until July 2017.

At the Tuxer Hauptkamm allover 23 temperature loggers with an accuracy of +/- 0,2 °C were installed (HOBO Water Temperature Pro v2 Data Logger, Onset Computer Corporation) monitoring the ground surface temperature from October 2016 until June 2017. Three of them were built in RGT1; 11 at RGT2 and 9 more at RGT3 (Figure 7).

3.2. Data processing

The overall collected data sets were revised using Rstudio as the programming language for the statistical calculations. The visualization of the results was computed by the program grapher. The geographic information systems ArcGIS was used for creating maps and calculating geostatistical characteristics of the studied areas.

3.2.1 Statistics

According to the total amount of data collected by the temperature loggers, a mutual time period was chosen to compare the data sets. For the general investigation of the superficial heterogeneity of the four rock glaciers (SRG, RGB, RGH and RGT) the period from October 2016 until July 2017 was observed. In order to interpret the ground surface temperature as function of time, the temperature values were summarized statistically by calculating their daily means. The correlation coefficient was computed to indicate the heterogeneity of temperature prevailing on the surface of the rock glaciers. According to Cohen (1988), the correlation coefficient, *r(x,y)*, indicates the strength of the relationship between two variables *(x, y)* and is calculated as shown in the following equation (1):

$$r(x,y) = \frac{\Sigma\,(x-\bar{x})(y-\bar{y})}{\sqrt{\Sigma(x-\bar{x})^2\,\Sigma(y-\bar{y})^2}} \qquad (1)$$

For the specific analysis of the internal heterogeneity of the two specific rock glaciers (SRG and RGB), values between October 2017 and July 2018 were examined in detail. The following statistical methods were additionally adopted to emphasize differences between the relict (SRG) and the intact rock (RGB) glacier: To get an overall view of the different data sets the daily, monthly and seasonal temperature means were calculated and analyzed as function of time. Temperature means were also observed as function of depth (to a maximum of one meter). Furthermore, the cross-correlation was used in order to understand how air temperature directly influences the ground surface and ground temperature within rock glaciers. This method aims to estimate the maximum amplitude and its corresponding lag value in hours based on equations given by Box and Jenkins (1976). The cross-correlation between air- and ground surface temperature as well as air- and ground temperature was calculated based on hourly data for each season. The seasons were defined according to the official calendar definitions and subdivided in autumn (23rd September to 21st December), winter (21st December to 21st March), spring (21st March to 21st June) and summer (21st June to 23rd September). The calculation of the cross-

correlation provides quantitative information about the strength of the correlation (amplitudes, given as R(k) max) and the temporally delayed response (propagation of signal, given as time lag in hours) (Mayaud et al. 2014). This offers an estimation about how fast and how intense temperature pulses from the atmosphere are propagated into the ground (Wagner et al. 2019b).

3.2.2 GIS-based analysis

The Topographic Position Index (TPI) was calculated in order to show geomorphological characteristics of the rock glaciers graphically (Wagner et al. 2019b). The Topographic Index is a numerical description of the microrelief on a relative scale. It indicates the difference between the elevation of each cell of a digital elevation model (DEM) and the mean elevation of a specified area surrounding this cell (Weiss 2000). According to Weiss (2000), positive Topographic Position Index values indicate regions that are higher than the average of the specified surrounding area and can therefore be described as ridges. Negative values represent regions that are lower than their surroundings and can therefore be assumed as valleys or cavities. TPI values close to zero show either flat regions or areas of constant slope. The TPI for this study was computed using a 1m DEM and its focal mean. Since the calculation of TPI is strongly depending on the scale used to define the surrounding area of the cell, three different calculations (see formula 2, 3 and 4) were computed and compared to each other in order to choose a surrounding area which leads to significant TPI values. The results obtained using the equation (3) showed the most indicative TPI values and are therefore presented in the following chapter.

$$TPI = dem - \ focalmean\ (dem, annulus, 6, 12) \quad (3)$$

$$TPI = dem - focalmean\ (dem, circle, 3) \quad (4)$$

$$TPI = dem - focalmean\ (dem, annulus, 1, 25) \quad (5)$$

Additionally, using high resolution digital elevation models, the potential mean of incoming solar radiation of the rock glaciers was calculated to give an estimate of the impact of short-wave radiation on the thermal regime.

3.2.3 Calculation of different parameters

The Rayleigh number (*Ra*) was determined using the equation (6) in order to quantitatively indicate possible free air convection. Pore air movement can be caused by free or forced convection. Temperature induced variations in air density can lead to free air convection, whereas pressure gradients in the air, caused by high wind speeds, generate forced convection (Juliussen and Humlum 2008). *Ra*, given by Goering (2003), indicates if free air convection is dominating the process of heat transport:

$$Ra = \frac{C\ \beta\ g\ K\ H\ \Delta T}{\vartheta\ \lambda} \quad (6)$$

Where C [kJ/(m³ K)], β [1/K] and ϑ [m²/s] constitute the volumetric heat capacity, the expansion coefficient and kinematic viscosity of the pore fluid (e.g. air), respectively, g is the gravitational acceleration, K [m²] the intrinsic permeability of the blocky debris layer, H [m] the thickness of the layer, ΔT [K] the temperature difference between the top and the bottom of the layer and λ [W/(m K)] the effective thermal conductivity of debris layer. *C, β, g and* ϑ are given constants, H is considered to be one meter and ΔT represents the difference between ground temperature and ground surface temperature. The effective thermal conductivity of the debris layer, λ, can be calculated using the following equations (7), described by Zehner and Schlunder (1970), as well as (8) and (9) adopted as simplifications of the latter:

$$\lambda = \lambda_f\left(1 - \sqrt{1-\rho} + \frac{2\sqrt{1-\rho}}{1-\xi B}\left[\frac{(1-\xi)B}{(1-\xi B)^2} ln\left(\frac{1}{\xi B}\right) - \left(\frac{B+1}{2}\right) - \frac{B-1}{1-\xi B}\right]\right) \quad (7)$$

where

$$B = C\left(\frac{1-\rho}{\rho}\right)^m \quad (8)$$

and

$$\xi = \frac{\lambda_f}{\lambda_s} \quad (9)$$

According to Zehner and Schlunder (1970) in rock glaciers, irregularly shaped particles can be assumed to present following values for C = 1,25 and m = 1,11. The thermal conductivity of air, λ_f, is 0,024 W/mK and λ_s (thermal conductivity of the rocks) was measured at a rock sample of SRG at the petrophysical laboratory of the Montanuniversität Leoben (unpublished data, Gegenhuber, 2016). Since the two rock glaciers are characterized by a similar lithological setting, λ_s is assumed to be the same for SRG and RGB. The intrinsic permeability, *Ki*, is calculated using the equation (10) and (11) (Johansen 1977):

$$Ki = \frac{\rho^3}{5S^2(1-\rho)^2} \quad (10)$$

where

$$S = \frac{6}{d_p} \quad (11)$$

The latter depends on the grain size of the investigated body and is therefore the only variable parameter. The porosity is hereby given by ρ [-], *S* [1/m] denots the specific surface area and d_p the equivalent diameter of the particles [m]. According to Nield and Bejan (2019), the porosity of coarse grained material of active layers is estimated to be 0,4 and the equivalent diameter of the particles is assumed to be the d_{10} percentile of the block sizes (0,35 m) measured at SRG (Winkler et al. 2016a). These values were considered to be valid for SRG and RGB within coarse grained material. For the logger at RGB installed in fine grained material the Rayleigh number was calculated combining different values for the porosity and the diameter of particles in order to estimate a possible threshold, which defines the transition between free convection- to conduction-dominated processes. Starting from a value given by the d_{10} percentile of the block sizes (0,05 m) measured at RGB (Pedevilla 2019), four different values of the equivalent diameter of the particles (d = 0,50 m; 0,10 m; 0,15 m and 0,20 m) were used in combination with three different estimated values for the porosity (ρ = 0,20; 0,25; 0,30). According to Nield and Bejan (2019) free convection is expected if the Rayleigh number exceeds the critical value of *40* (if the system is assumed to be closed, e.g. continuous snow cover), or *27* (if it is an open boundary system).

Furthermore, the thermal offset (TO) was computed subtracting the ground surface temperature from the ground temperature in order to estimate the temperature gradient prevailing within rock glaciers in time. Also, the surface offset (SO) was validated (ground surface temperature minus air temperature) to understand temperature gradients dominating between the ground surface and the atmosphere (Smith and Riseborough 2002).

3.3 Data limitation

The data sets provided for this study are limited in their temporal extension, their spatial distribution and the typological decision of measurements. Temperature data of RGB, RGH and RGT are limited for a relatively short period of time, which complicates the understanding of temperature trends over longer periods of time. The definition of representative data logger locations is challenging, but models such as the Topographic Position Index (Weiss 2000) and similar methods can preliminary offer decision criterions. The latter methods help to estimate microrelief-conditions of the rock glacier and facilitate the selection of significant and comparable measurement sites (Wagner et al., 2019b). Furthermore, the missing weather station at RGB complicates the understanding of the interaction between air and ground temperature. Additionally, the lack of a measuring site within fine grained material at SRG doesn't allow a complete comparison of the thermal behavior of the two bodies. For future studies, a better preliminary planning is suggested in order to obtain an overall dataset in which, the spatial and typological distribution of the loggers on different rock glaciers is as homogenous as possible.

4. Results

This chapter summarizes the most important results obtained by the above-mentioned methods.

4.1. Thermal heterogeneity on the surface of the rock glaciers

The superficial thermal heterogeneity of the investigated rock glaciers has been studied by observing and analyzing the ground surface temperature values monitored in the period between October 2016 and July 2017.

4.1.1 Temperature time series

Figure 11 shows the daily mean ground surface temperature evolution of all loggers for each rock glacier. The grey area indicates the range between the absolute maxima and minima of the daily mean ground surface temperature and the blue line demonstrates the corresponding mean over time. As listed in Table 2, the overall mean ground surface temperature (MGST) calculated for the period of time between October 2016 and July 2017 is 1,52°C for SRG. Between December 2016 and March 2017 the ground surface temperature fell constantly below 0°C at SRG. The MGST calculated for RGB is -1,41°C. The temperature on the surface was negative between October 2016 and May 2017. Additionally, in May 2017, a positive peak is evident at RGB (see Figure 11, a), which will be discussed in detail in the next chapter. At the Tuxer Hauptkamm the overall MGST is -1,89°C, where temperatures underrun 0°C from October 2016 even until June 2017. The MGST calculated for the rock glaciers at Hochschober is -2,09°C. Negative temperature values can be observed from October 2016 until the end of June 2017. The absolute lowest daily mean of the ground surface temperature computed for all rock glaciers has been monitored at RGT2 in January 2017 (-21°C) and the highest daily mean GST has been measured at RGT1 in June 2017 at the temperature logger T11 (+26°C).

Table 2 Summary of the calculated means and the daily minima and maxima of GST measured at the four rock glaciers (SRG, RGB, RGT and RGH) from October 2016 until July 2017 with their most important geomorphological characteristics

Rock glacier	Altitude [m a.s.l.] (mean)	slope [°] (mean)	aspect [°]	MGST [°C]	GSTmin [°C]	GSTmax [°C]
Schöneben	1814	20	60	**1,52**	-15,19	21,35
Bergli	2416	22	360	**-1,41**	-19,22	24,75
Hochschober	2499	21	300	**-1,89**	-16,47	18,8
Tuxer Hauptkamm	2559	25	300	**-2,09**	-21,62	26,16

The lowest average temperature was observed at the rock glaciers Hochschober (MGST = -2,09°C). In contrast, at SRG the highest average temperature was calculated, comprising also a shorter period of time in which temperatures underran 0°C at ground surface.

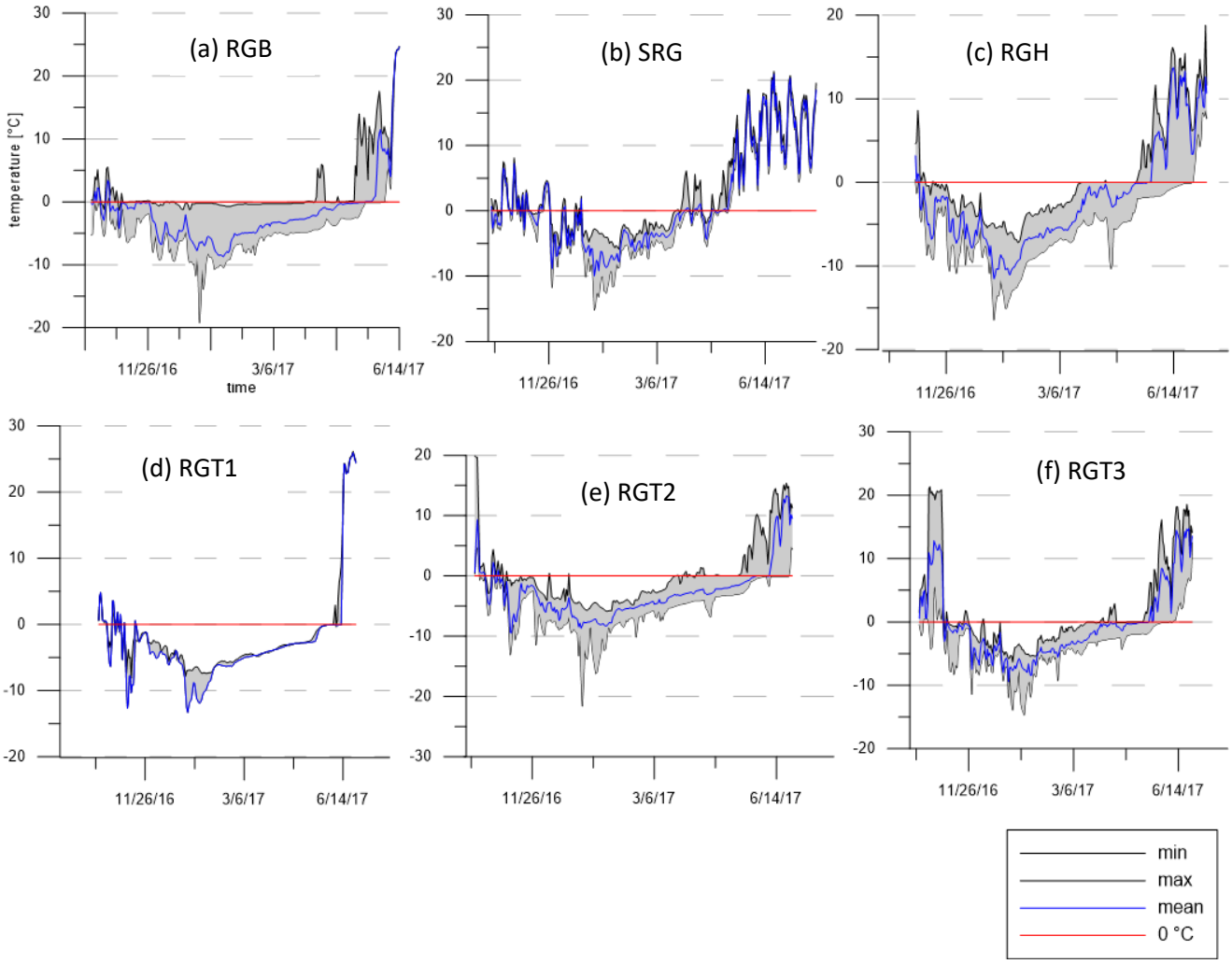

Figure 11 Daily mean of the ground surface temperature monitored from October 2016 until July 2017 at the four different rock glaciers (RGB - a, SRG - b, RGH - c and RGT – d, e and f) plotted as function of time; grey zone indicates the range of maxima and minima of daily means calculated for each logger and the blue line indicates the total mean

4.1.2 Correlation coefficient

Figure 12 indicates the cumulative histogram of the calculated correlation coefficient of the ground surface temperature for each rock glacier. The overall calculated correlation coefficients (*r*) are listed in Appendix 1. According to the results, three classes have been defined in order to significantly summarize the outcome. If values of *r* are bigger than 0,7, the correlation is estimated to be high. For *r* values between 0,5 and 0,7, the correlation is defined as medium. Values underneath 0,5 indicate a low correlation. The calculated correlation coefficients clearly show a homogenous distribution ($r > 0,8$) of the ground surface temperature at all investigated rock glaciers (see Figure 13) with the exception of RGB having few medium correlation coefficients ($0,5 < r < 0,8$) and RGT3 with some medium and few low correlation coefficients ($r < 0,4$).

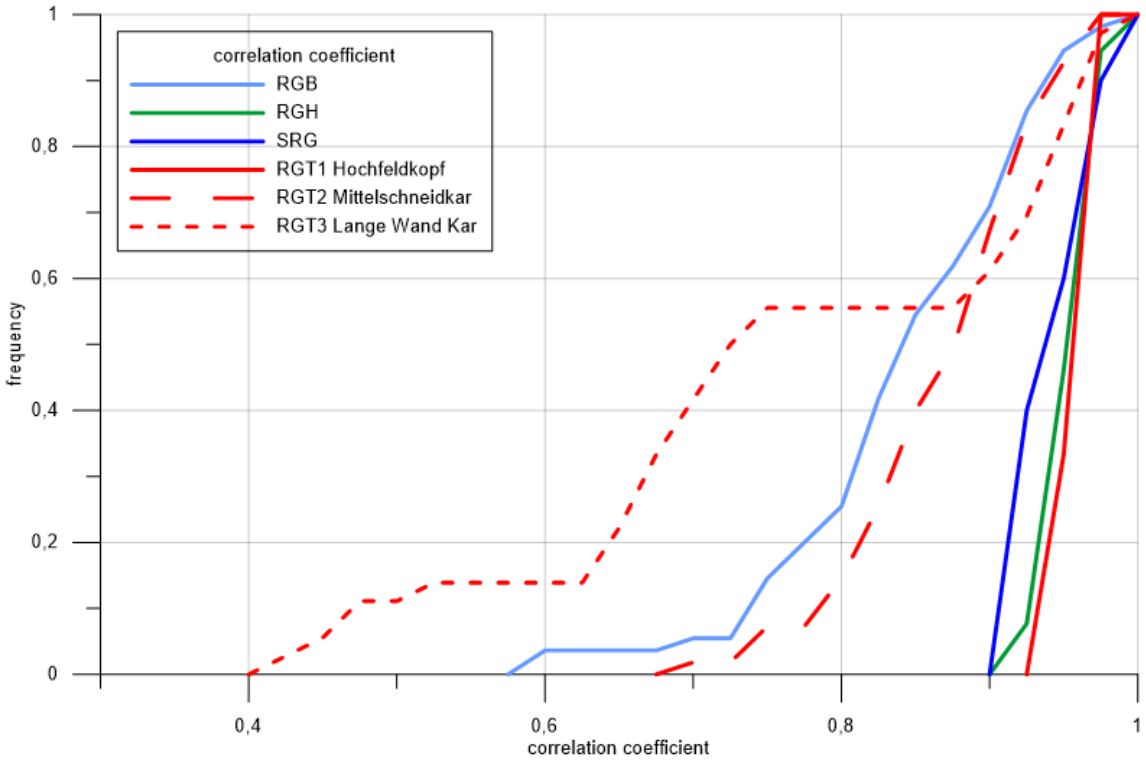

Figure 12 Cumulative histogram of the correlation coefficients calculated for GST of all rock glaciers.

At RGT3, the correlation coefficient calculated between the loggers T38 – TS32, T38 - T19, T38 – T9 is smaller than 0,5. As shown in Figure 7, T38 is installed in the uppermost and T32 in the lowermost region of the rock glacier. T19 and T9 are located underneath the rock glaciers within mineral soil (see Figure 7, after Wagner et al., 2019a). As shown in Figure 13 (a), T38 shows a significantly high daily ground surface temperature mean in October 2016 (up to 21°C). The average temperature recorded at T38 for the rest of the examined period is lower than the average temperature recorded by the loggers TS32, T19 and T9. TS32 shows a similar evolution of ground surface temperature as T38, yet the evident peak in October is lacking. Instead, at TS32 two negative peaks monitored in January and March 2017, are observed. At RGB especially the loggers KW1, KW2, KW11 and KW13 show lower correlation coefficients to each other ($5 < r < 0,8$) indicating less interrelationship between themselves (see Appendix 1). Figure 13 (b) indicates the temperature trend of KW2 and KW13 as example. KW2 is clearly showing less amplitudes in its temperature time series. As shown in Figure 5, KW1 and KW2 are installed underneath the rock glacier within the mineral soil. KW13, which shows an evident positive peak in spring, lies on the eastern part of the rock glacier.

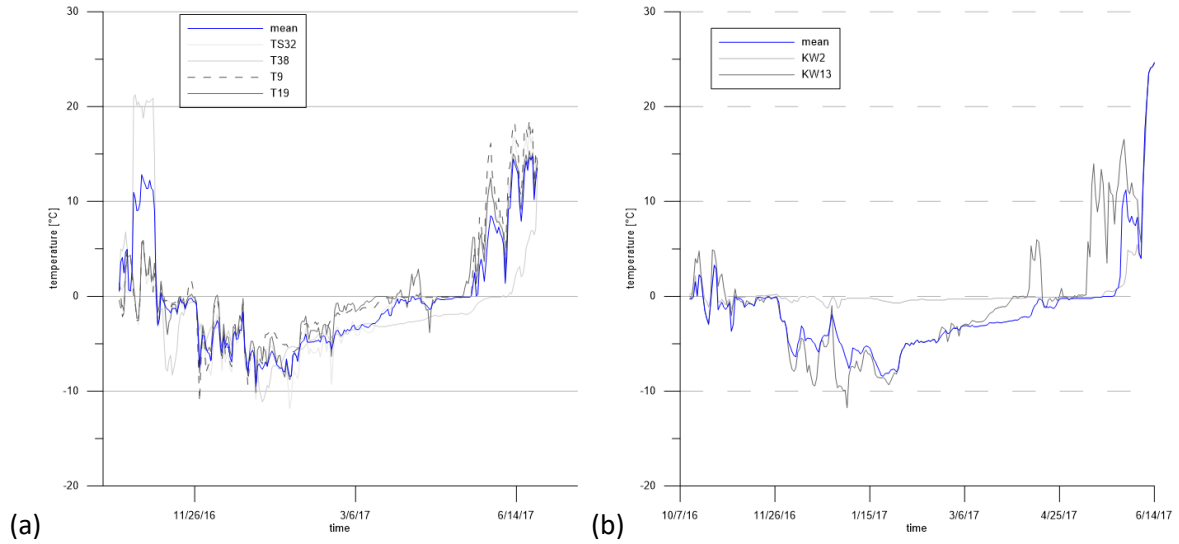

Figure 13 Graph (a) illustrates the daily means of GST recorded by the loggers with low correlation coefficients (T38, TS32, T19 and T9) at RGT3. The graph (b) demonstrates the daily mean of GST of two loggers (KW2 and KW13) with low correlation coefficients at RGB.

4.1.3 Topography Position Index

The geomorphological characteristics of the investigated regions are shown in Figure 14. The most significant result of the calculations for TPI is given by the difference between the original DEM (1m) and the average computed for the surrounding area, which is defined as annulus, that envelops the original cell with a radius from 6 to 12m. As seen in Figure 14 (a) and listed in detail in Table 3, the microrelief of SRG is the most homogenous one. Except for one logger (S-MTD4: TPI value close to zero), all loggers are situated in a position characterized by a positive TPI value (TPI > 0,2) and consequently located on a ridge. At RGB (Figure 14 – b) most of the loggers also lie on a ridge-like morphology. Six loggers are positioned on constant slopes or flat regions and only three of them are located in a small cavity. The loggers at RGH are installed in quiet variable microrelief positions (Figure 14 – c). Here, only four loggers show positive TPI values, while most of them show values close to zero. Consequently, most of the loggers are positioned in flat regions or areas with constant slope. Loggers at RGT (Figure 14 – d) show variable TPI values: two loggers at RGT1 are located in a cavity and one on a ridge. Except for logger T10, which is located in a cavity, all loggers at RGT2 are either situated on a flat area or on a ridge. TPI values at RGT3 show the highest heterogeneity of microrelief calculated for each logger.

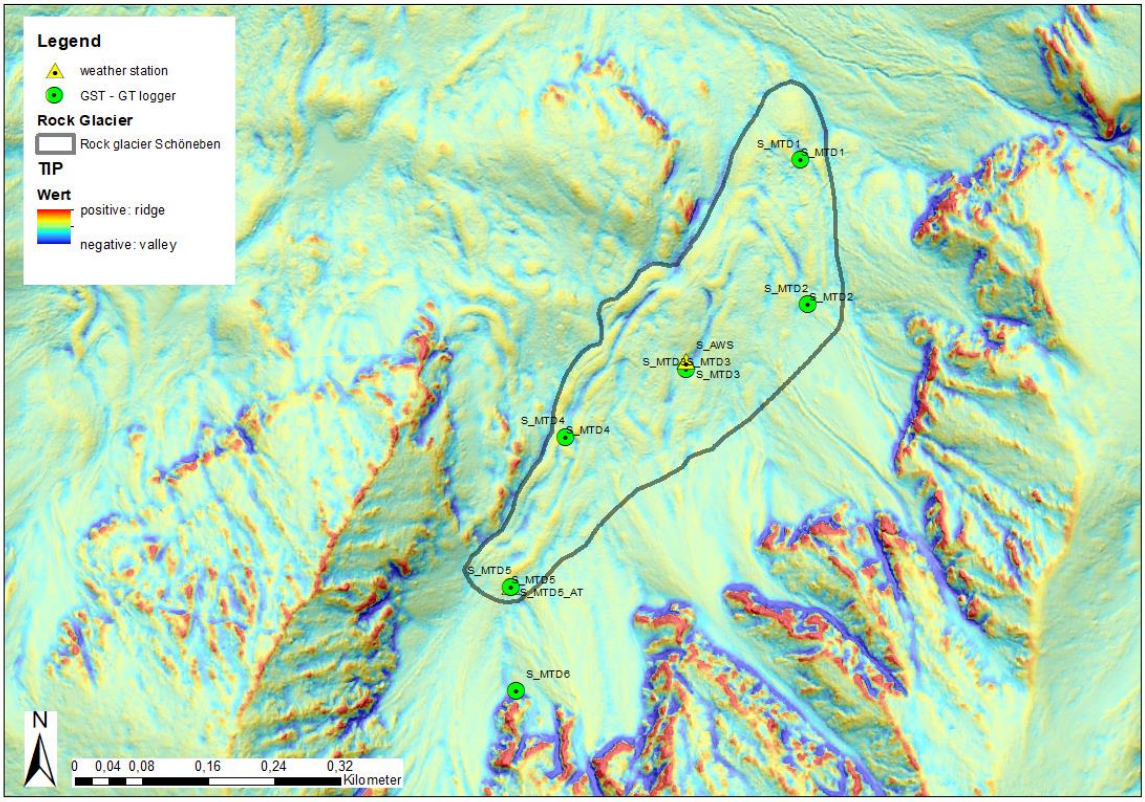
Legend
weather station
GST - GT logger
Rock Glacier
Rock glacier Schöneben
TIP
Wert
positive: ridge
negative: valley
S_MTD1
S_MTD1
S_MTD2
S_MTD2
S_AWS
S_MTD3
S_MTD3
S_MTD4
S_MTD4
S_MTD5
S_MTD5
S_MTD5_AT
S_MTD6
N
0 0,04 0,08 0,16 0,24 0,32
Kilometer

(a)

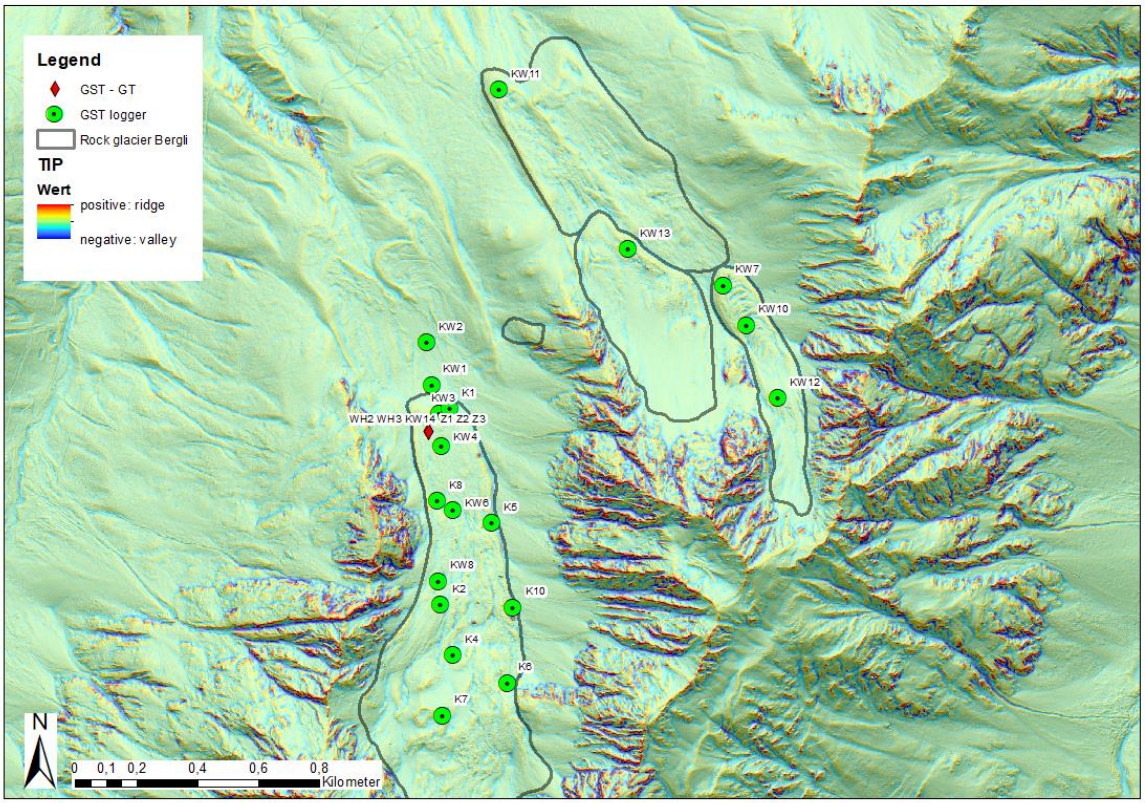
Legend
GST - GT
GST logger
Rock glacier Bergli
TIP
Wert
positive: ridge
negative: valley
KW11
KW13
KW7
KW10
KW2
KW1
KW3
K1
KW12
WH2 WH3 KW14 Z1 Z2 Z3
KW4
K8
KW6
K5
KW8
K2
K10
K4
K6
K7
N
0 0,1 0,2 0,4 0,6 0,8
Kilometer

(b)

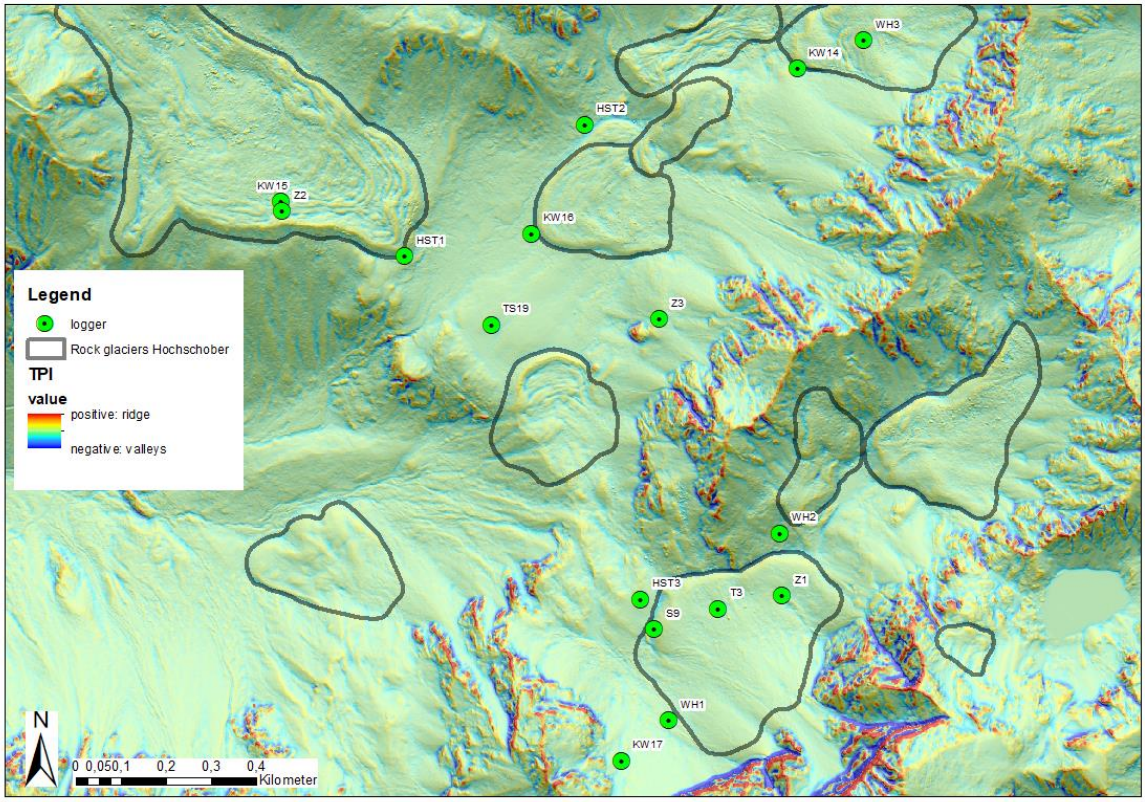

(c)

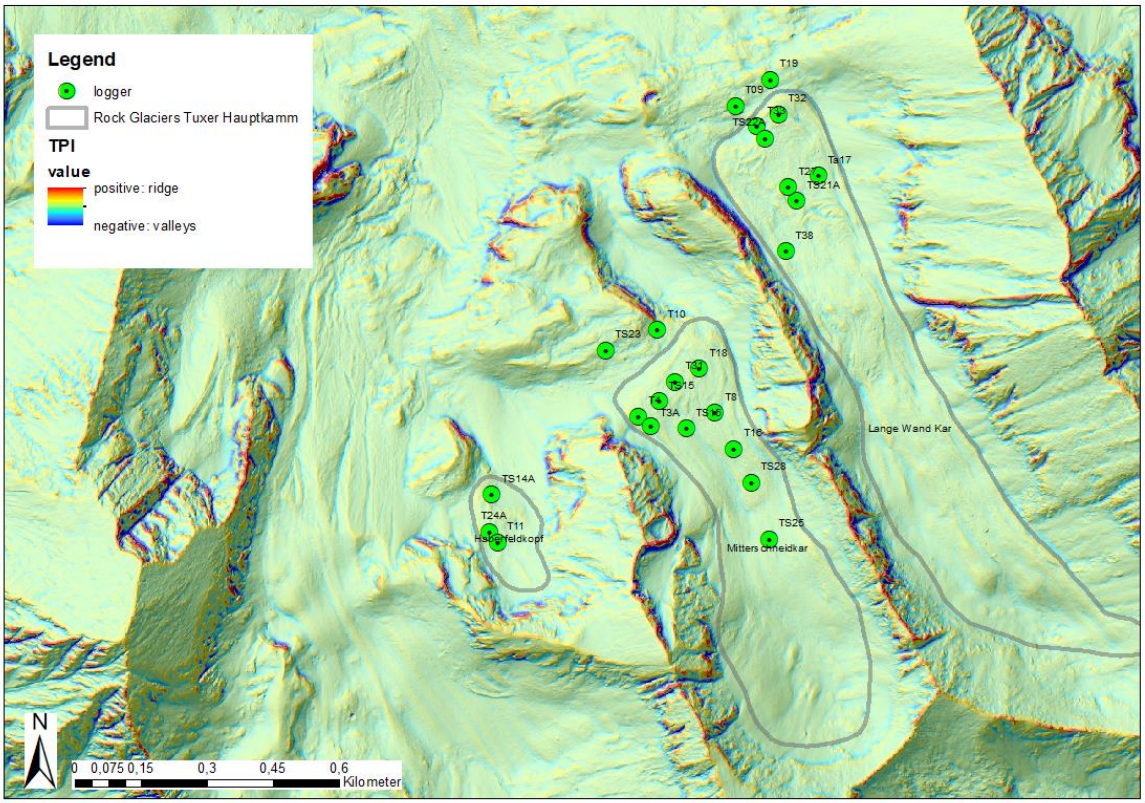

(d)

Figure 14 Topographic Position Index of all four rock glaciers (SRG - a, RGB - b, RGH - c and RGT - d), after Weiss (2000), computed using 50m DEM and its focal mean using following formula: tpi = dem – focalmean(dem, annulus, 6, 12); red regions indicate positive TPI (ridges) and blue regions indicate negative TPI (valleys).

Table 3 Calculated TPI values for all the loggers installed at each rock glacier: green values show flat areas or regions with constant slope; red values are characterized by ridge-like morphology and blue values indicate valleys or cavities

LOGGER	TPI	LOGGER	TPI	TPI value	morphology
Bergli		**Schöneben**		> 0,2	ridge
KW2	0,05	S-MTD1	0,45	-0,2 < TPI < 0,2	flat/constant
KW1	-0,51	S-MTD2	0,78	< -0,2	valley
KW4	0,76	S-MTD3	0,62		
KW6	0,21	S-MTD4	-0,11		
KW8	-0,98	S-MTD5	0,39		
KW7	-0,01	**Tuxer Hauptkamm**			
KW10	1,94	**RGT3**			
KW12	0,80	T19	-0,62		
KW13	0,18	T09	-0,20		
KW11	0,27	TS33	0,86		
KW3	0,65	TS32	0,48		
K1	0,04	TS22A	-0,40		
K5	0,91	TS21A	-0,33		
K10	-1,75	T27	-0,12		
K6	0,13	Ta17	0,13		
K4	0,01	T38	0,18		
K2	1,21	**RGT2**			
K8	0,24	TS23	0,73		
K7	1,77	T10	-0,62		
coarse	0,51	T18	-0,01		
fine	0,51	T31	0,28		
Hochschober		TS15	-0,07		
HST1	-0,70	T4	0,48		
HST2	-0,45	T3A	1,18		
HST3	0,33	TS15	0,95		
HST4	-0,17	T8	0,12		
HST5	0,06	TS25	0,67		
HST6	-1,64	TS28	0,20		
HST7	-0,03	T16	0,47		
HST8	1,11	**RGT1**			
HST9	-0,72	TS14A	-0,21		
HST10	-0,08	T24A	0,31		
HST11	0,13	T11	-0,89		
HST12	-0,12				
HST13	0,82				
HST14	0,19				
HST15	-0,58				
HST17	0,50				

4.2. Thermal heterogeneity within the uppermost coarse blocky layer of the two specific rock glaciers Schöneben and Bergli

The results of the specific comparison between the relict (SRG) and the intact (RGB) rock glaciers are shown in the following graphs and figures.

4.2.1 Temperature time series

Figure 15 represents the evolution of the ground surface temperature monitored at RGB and SRG in the period between October 2017 and July 2018. MGST is calculated to be -0,48°C at RGB and +1,75°C at SRG (see Table 4). Hence, MGST measured in the year 2017 - 2018 show higher values for RGB and lower values for SRG compared to the year before (see chapter above). The mean air temperature measured at Ischgl-Idalpe weather station is 0,89°C and the one directly monitored at SRG is +2,33°C. It is thereby seen that the mean air temperature monitored at both weather stations is higher than the mean ground surface temperature observed at the corresponding rock glaciers. At RGB one logger shows particularly low temperatures with a significant negative peak at the end of February 2018. In the period between April and May 2018 the temperature monitored at RGB shows constant values close to 0°C. During the phase transition from ice to water, especially in spring, the temperature stays constant, due to the release of latent heat. Only when the ice and snow is completely melted, temperature values can rise again. This process, called the "zero curtain effect", is observed in periglacial environments and shows that freezing and thawing processes are acting.

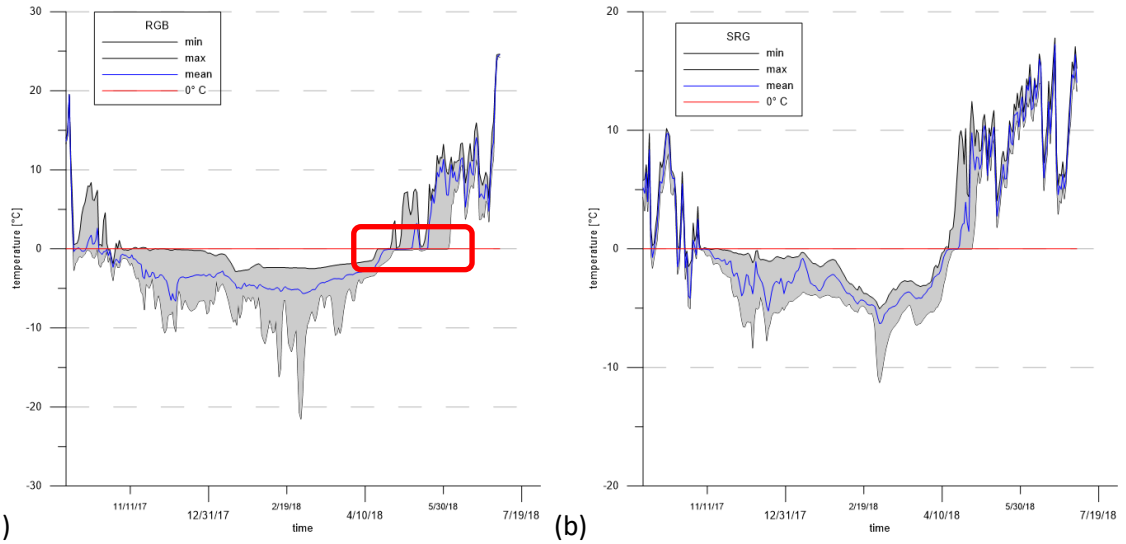

Figure 15 Temperature evolution of the ground surface temperature monitored at RGB (a) and SRG (b) from October 2017 until July 2018. The grey zone indicates the range of maxima and minima of daily means calculated for each logger, the blue line indicates the total mean. The red rectangle in figure (a) shows the zero curtain effect acting especially in spring, when the temperature remains constant because of the release of latent heat during the transition process from ice to water

Figure 16 and Figure 17 show the evolution of the daily mean of the ground surface -, and ground temperature monitored at SRG and RGB as function of time. The temperature within coarse grained material at RGB shows the following behavior (see Figure 16 - a): From October 2017 until May 2018, the ground temperature is higher than the ground surface temperature. During the rest of the examined period, the temperature on surface is warmer than in the ground. Unlike on the surface, the ground temperature is reacting more buffered (smaller amplitudes) to temperature changes. The fine grained material at RGB shows a relatively parallel evolution of the ground surface and ground temperature in time. Compared to the ground temperature, the surface shows lower values from October until May 2018 and higher values from June until July 2018. Similar to the coarse grained material, the ground temperature is reacting more buffered to temperature changes. The ground surface is always warming up relatively slow (see flat positive gradients in Figure 16 - a) and cooling down relatively fast (see steep negative gradients). It is generally evident, that in fine grained material, temperature is dampened in winter but very reactive (high amplitudes) in summer and spring. In coarse grained material, ground temperature is constantly dampened, but the ground surface temperature always shows rather high amplitudes throughout the whole year. Amplitudes of the ground surface temperature in fine grained material appear to be higher than in coarse grained material. From April 2018 until June 2018 the zero curtain effect is visible in fine grained material, whereas only April shows the latter effect within coarse grained material. The most evident difference between the two loggers is seen in spring (see Figure 16 – b), when the zero curtain effect is acting longer in fine grained than in coarse grained material. Figure 17 shows the ground surface temperature and the ground temperature evolution for the loggers installed at SRG, which clearly show the same trends. The temperature on the surface is always higher than in the ground from September until October 2017 as well as from April until July 2018. In contrast, temperatures in the ground are higher during winter time (from October 2017 until April 2018). In general, ground temperature reacts more buffered than ground surface temperature, which amplitudes are relatively high.

(a)

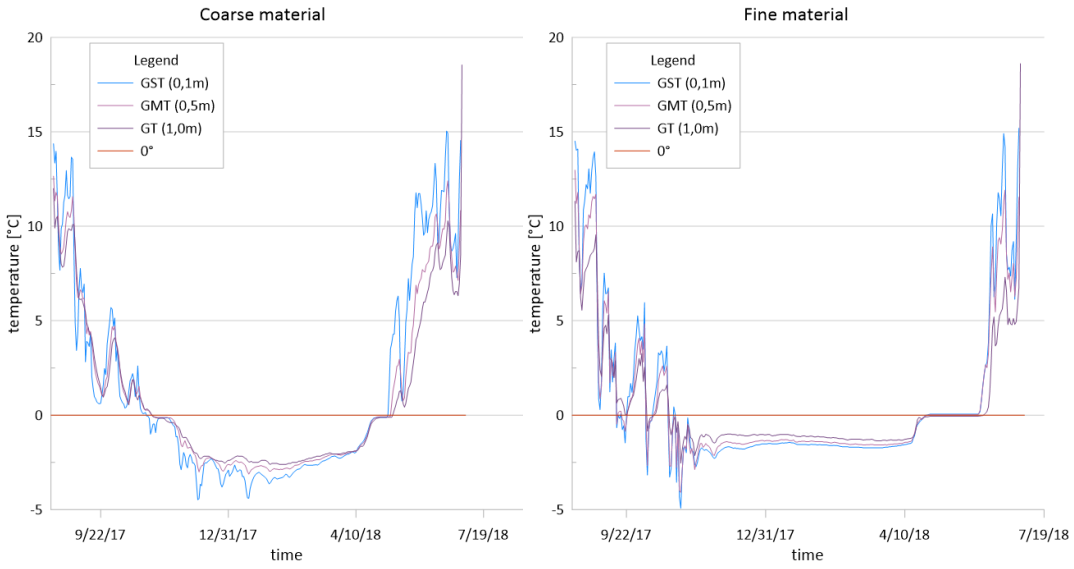

(b)

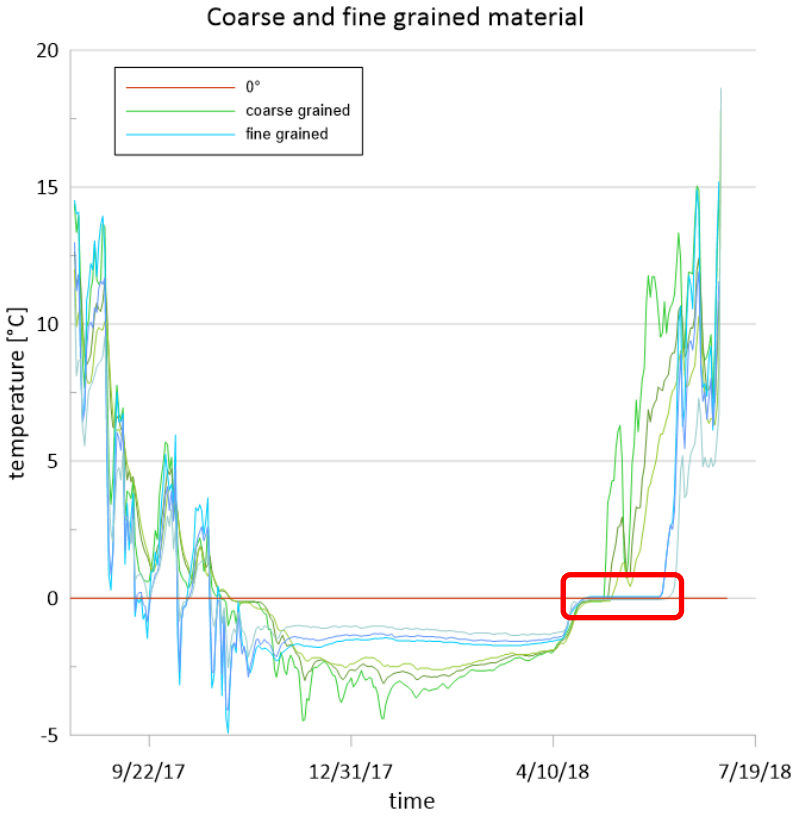

Figure 16 The daily mean of temperature as function of time of the two logger profiles installed in coarse grained and fine grained material at RGB (a). The temperature was monitored in three different depths: 0,10m (GST), 0,50m (GMT) and 1,00m (GT) between September 2017 and July 2018. The figure (b) shows the daily mean of the temperature of both logger profiles within a single graph evidencing the difference in spring, when the zero curtain effect (red rectangle) is acting longer within fine grained material

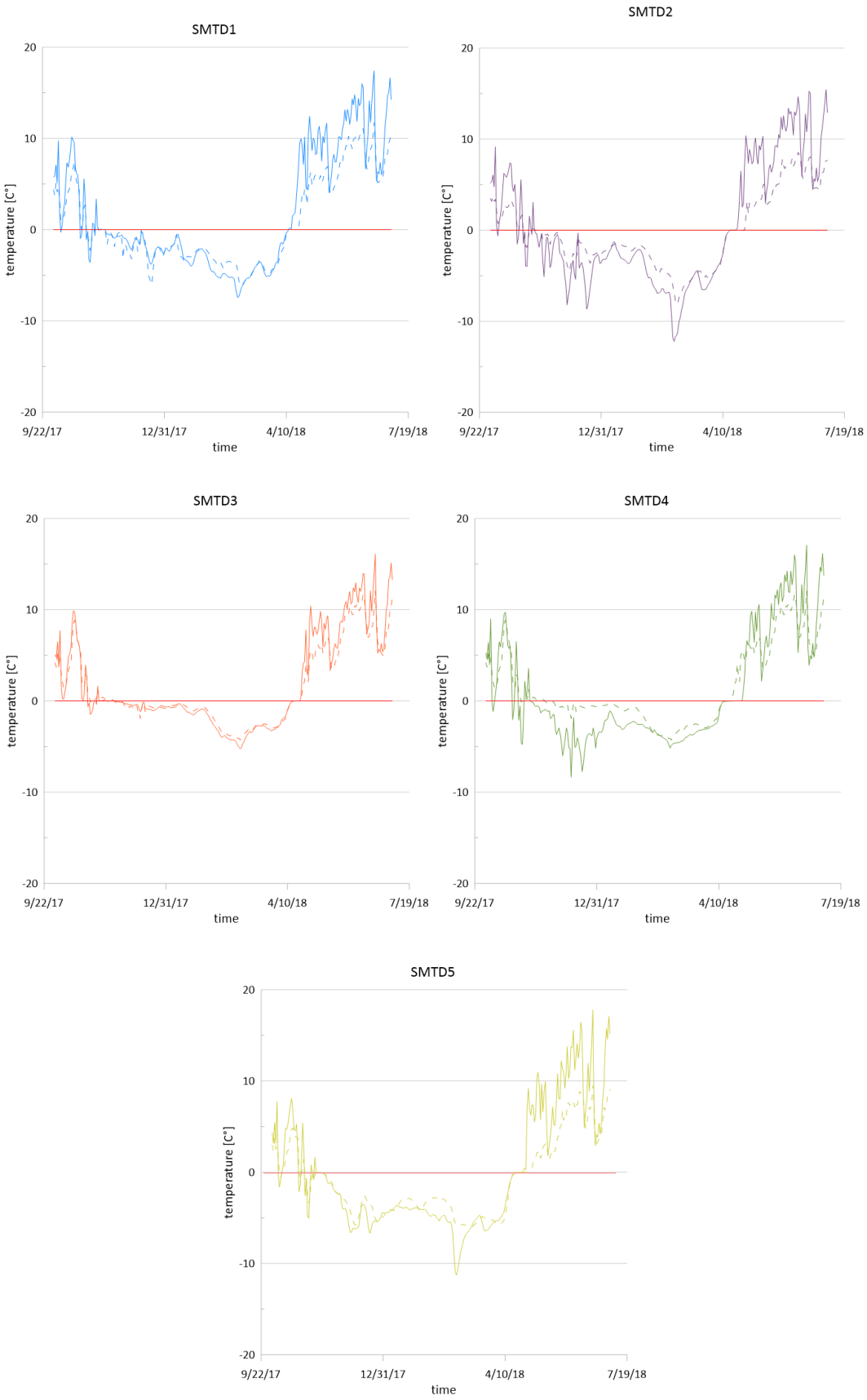

Figure 17 The daily mean of the ground surface and ground temperature as function of time recorded by the loggers at SRG. The temperature was measured at 0,10 m (GST; solid line) and 1,00 m (GT; dashed line) between September 2017 and July 2018

4.2.2 Temperature as function of depth

As listed in Table 4, the temperature means measured in fine grained material are lower than the ones calculated for the coarse grained material. Both logger profiles show that the temperature is decreasing in depth. Also at SRG, the average temperature in the ground is lower than on the surface.

Table 4 Maxima (GSTmax), minima (GSTmin) and total means (MGST) of the daily means recorded at RGB in fine and coarse grained material and at SRG between September 2017 and July 2018 compared to their altitude.

RGB	altitude	MGST	GSTmin	GSTmax	MGMT	GMTmin	GMTmax	MGT	Gtmin	Gtmax
fine	2102	0,52	-4,93	14,91	0,52	-4,09	12,97	0,35	-2,54	11,33
coarse	2102	0,96	-4,48	15,04	0,97	-3,12	12,41	0,74	-2,61	10,53
total mean		0,74			0,75			0,55		
K1	2056	0,34	-8,84	15,02	-	-	-	-	-	-
K2	2423	-0,46	-8,8	15,95						
K4	2458	-1,00	-9,68	13,05						
K10	2349	-2,52	-21,53	14,19						
K8	2295	-0,27	-8,54	16,11						
K7	2524	-0,99	-6,21	13,45						
K6	2457	-1,06	-6,07	11,41						
K5	2268	-0,33	-4,11	14,45						
total mean		-0,48								
SRG	altitude	MGST	GSTmin	GSTmax				MGT	Gtmin	Gtmax
SMTD1	1767	1,77	-7,44	17,41	-	-	-	0,70	-2,54	11,73
SMTD2	1807	0,28	-12,21	15,43				-0,24	-8,12	8,54
SMTD3	1823	1,84	-5,23	16,1				1,47	-4,28	12,05
SMTD4	1847	4,89	-8,36	17,08				0,30	-4,44	9,38
SMTD5	1909	-0,06	-11,27	17,79				-0,84	-11,27	17,79
total mean		1,75						0,28		

Monthly means calculated for the ground surface- and ground temperature are demonstrated in Figure 18 and Figure 19. Figure 18 shows the following trends for the loggers installed within fine grained material at RGB: from August until October 2017 the temperature in the ground is lower than on the surface. From November 2017 until April 2018 the trend tips and the ground temperature gets higher than the ground surface temperature. In May the surface temperature and ground temperature are rather similar and from June until July 2018 the ground temperature gets lower than the ground surface temperature again. In coarse grained material a similar, but yet shifted trend can be seen: in August 2017 the temperature in the ground is lower than on the surface. The tipping already starts in September. From September 2017 until March 2017 the ground temperature is higher than the surface

temperature. From April 2018 until July 2018 the ground temperature is lower than the surface temperature again.

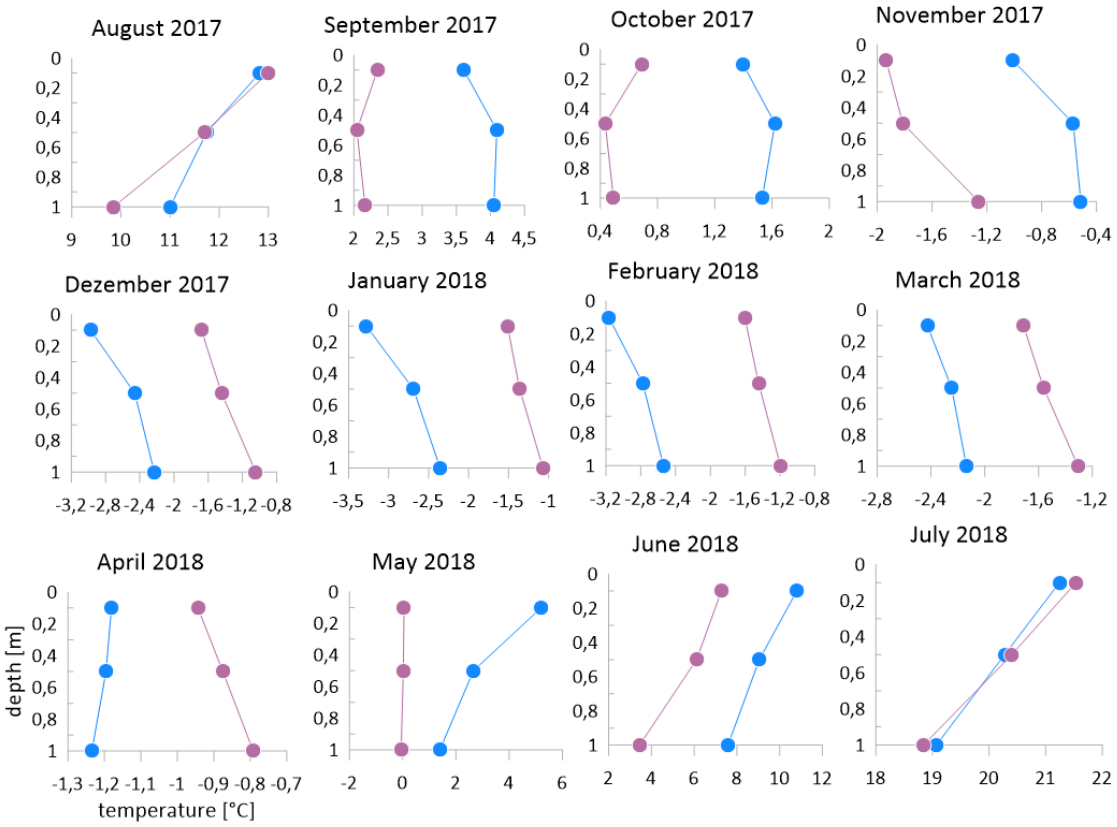

Figure 18 Monthly mean of GST (0,10 m), GMT (0,50 m) and GT (1,0 m) monitored at RGB within coarse material (blue line) and fine material (violet line) as function of depth in the period between August 2017 and July 2018

Similar trends can be noticed in Figure 19 for the loggers installed at SRG. Except for SMTD3 and SMTD5, all loggers show the following temperature evolution: In October 2017 the temperature in the ground is lower than on the surface. From November 2017 until March 2018 the ground temperature is higher than the ground surface temperature and from April until July 2018 temperatures tips again and gets lower in the ground. The logger SMTD3 shows a rather similar temperature in the ground and on the surface from October until December 2017. From December 2017 until March 2018 the ground temperature is higher than the ground surface temperature. In April 2017 the temperature tips again and gets lower in the ground. Logger SMTD5 shows lower temperature in the ground compared to the surface in October 2017. In November 2017 the surface temperature is similar to the ground temperature. From December 2017 until March 2018 the ground temperature is higher than the surface temperature and in April the temperature flips again.

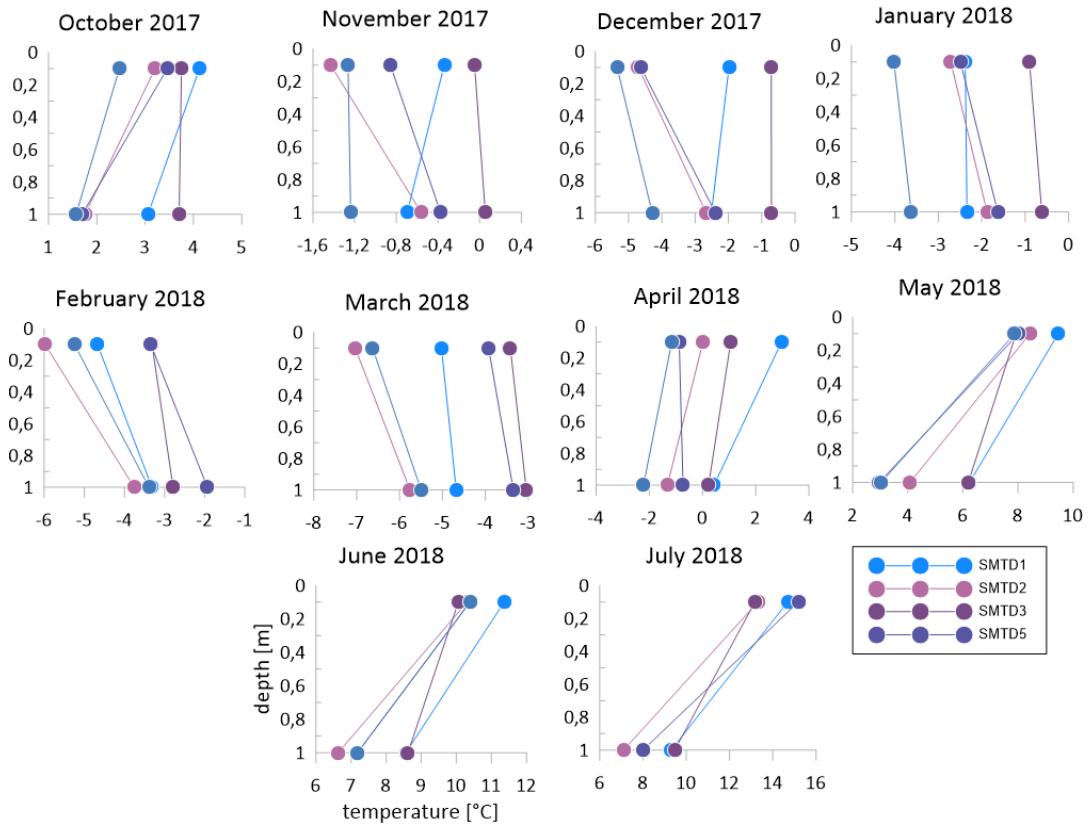

Figure 19 Monthly mean of GST (0,10 m) and GT (1,0 m) monitored in all loggers at SRG as function of depth in the period between October 2017 and July 2018. Due to a lack of a continuous data set in September 2017 and August 2018, only the months from October 2017 until July 2018 are shown in the graph.

Results shown in Figure 18 and Figure 19 were calculated using monthly means, yet daily mean temperature values can show a significant variability. To demonstrate the range of data measured within one month, the minima and maxima of the daily means were plotted with the corresponding monthly mean (see the example in Figure 20). In Appendix 2 the range of all loggers for each month is presented. One can clearly see, that at RGB the range decreases from December until February (see Figure 20 – a). In contrast, at SRG the daily temperature mean values constantly have a rather big range. Figure 21 and Figure 22 outline the monthly means within one graph showing the evolution of temperature in the period of time between August 2017 and July 2018. Both graphs clearly show the above-mentioned trends and flipping in temperature changes within one year. Unlike the total daily means, the monthly means of the coarse grained material show lower values compared to fine grained material, especially in winter (see Figure 21: January, February and March 2018). The lowest monthly means in fine grained material are observed in November 2017. In coarse grained material the lowest monthly means are recorded in January and March 2018. Figure 22 shows a similar trend in time for loggers at SRG. The coldest temperature is always measured in March 2018.

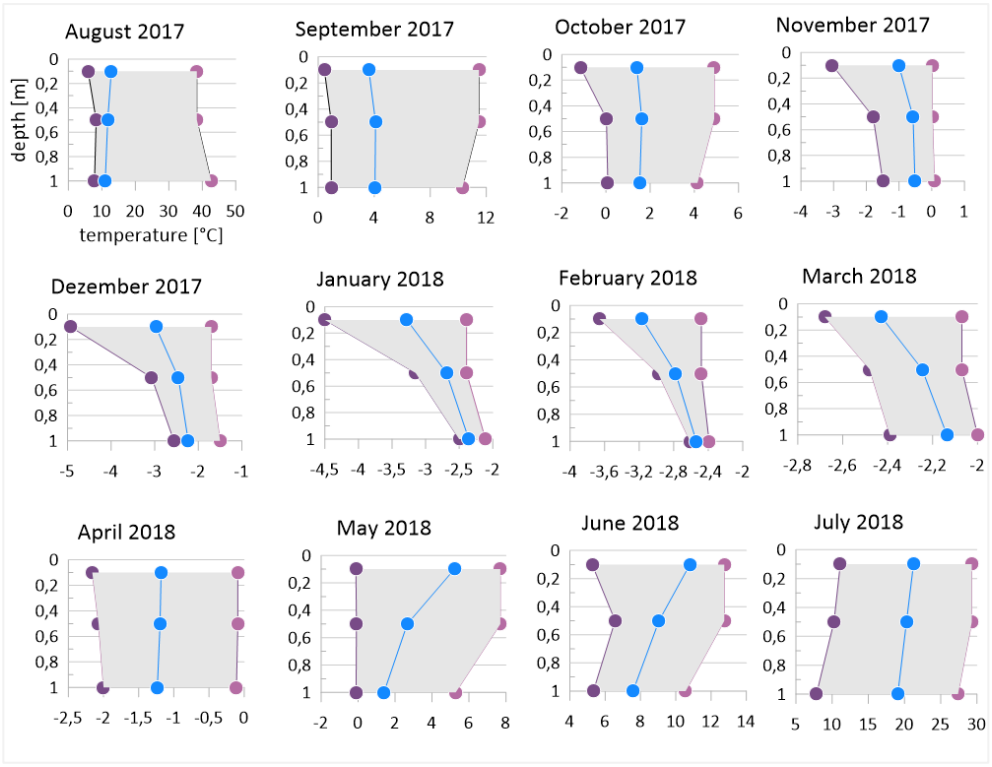

(a)

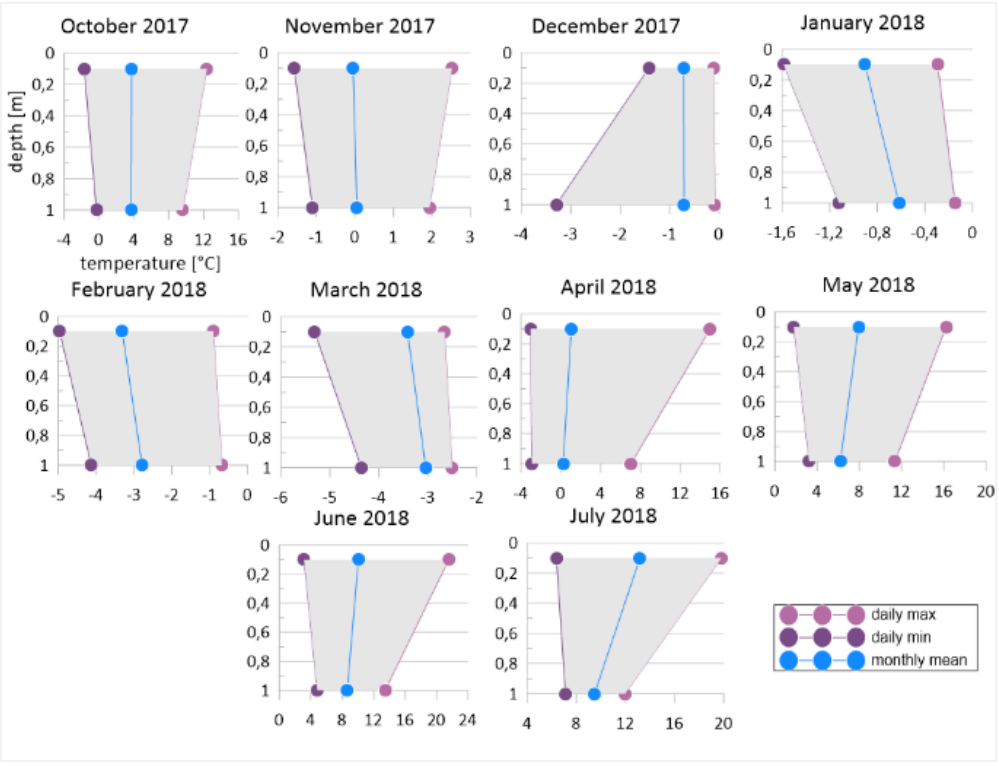

(b)

Figure 20 Minima and maxima of the daily temperature means recorded by the logger in coarse grained material on RGB (a) and by SMTD3 on SRG (b) shown as representative examples for the variability of the daily temperature within one month

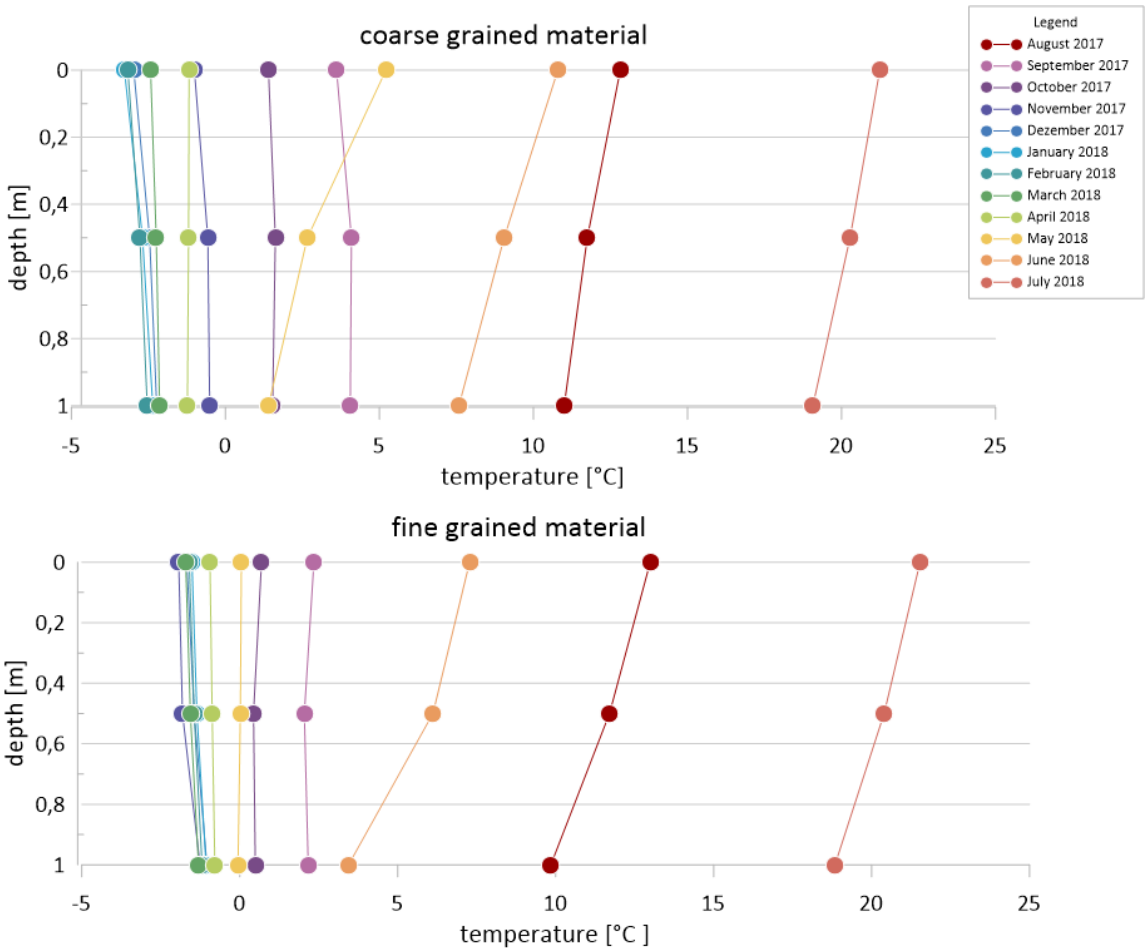

Figure 21 Evolution of temperature as function of depth within one year at RGB

In general, on both rock glaciers a similar thermal behavior can be observed in depth. The ground temperature means are lower than the temperature means on the surface of both rock glacier types. Also, the ground temperature values are higher in winter and lower in summer. Even though the tipping of temperature values in the ground happen in different months, the general trend is similar in all loggers. The striking difference, which is demonstrated in Figure 21 and Figure 22, is that the coldest monthly means are monitored at SRG. At RGB the monthly means stay above -5°C in winter, while in some winter months at SRG the monthly means underrun -5°C.

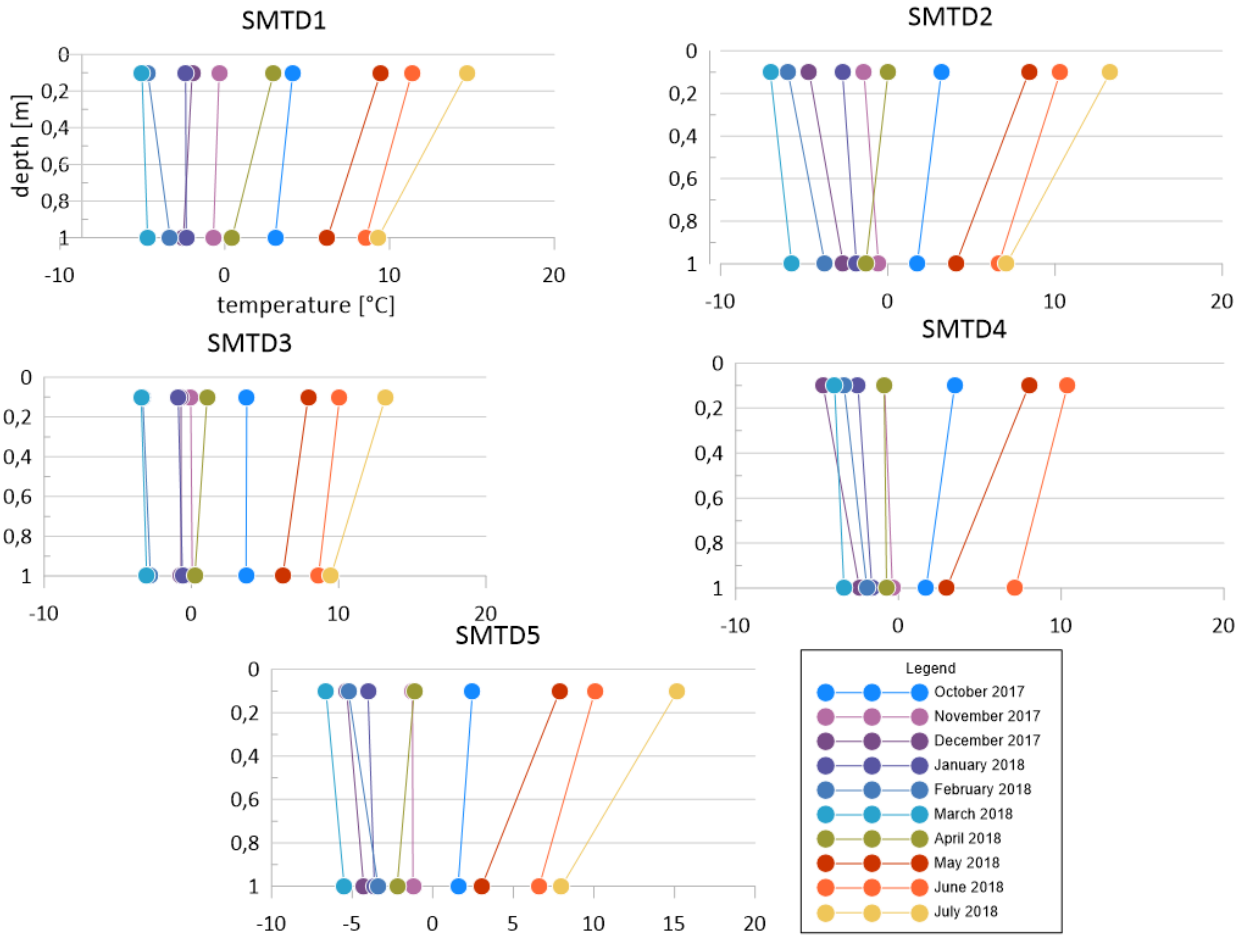

Figure 22 Evolution of temperature as function of depth within one year at SRG

4.2.3 Rayleigh number and thermal offset

Figure 23 demonstrates the Rayleigh number (Ra) and the thermal offset calculated for the loggers installed at RGB. By combining the different values of porosity and the equivalent diameter of the particles, different values of Ra were calculated for the fine grained material. For the first calculation shown in Figure 23 (a), *d* is assumed to be 0,05m and *p* is estimated to be 0,2. For the second calculation (Figure 23 – b), two different values were used (*d* = 0,15m and *p* = 0,2). The input values for the calculation of Ra within the coarse grained material at RGB (Figure 23 – c) are the same as used for the calculation of Ra at SRG listed in the chapter before. Rayleigh numbers for the lower limit case within fine grained material are constantly lower than the critical value. The second case shows that Rayleigh numbers exceed the critical value in some cases, if the thermal offset is bigger than 2,5°C. The third case, representing coarse grained material, shows relatively high Rayleigh numbers. The highest Ra was monitored in October. During winter (from November 2017 until March 2018), Ra values constantly exceed the critical value. As shown in Figure 24, the exceeding of Ra is always correlated to a minimum value of thermal offset (TO > 0,04).

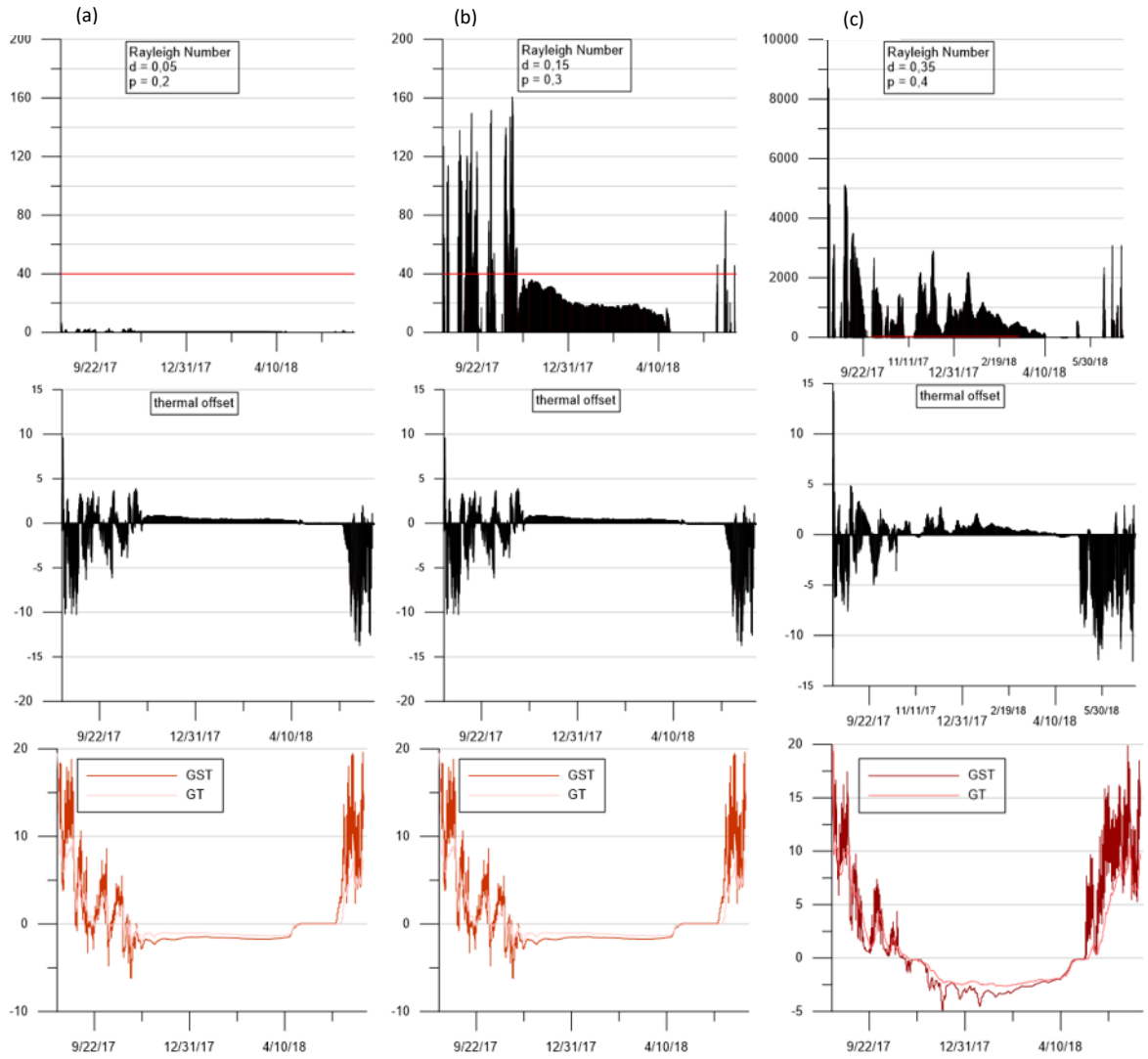

Figure 23 Rayleigh number, thermal offset (GT - GST) and temperature evolution over time based on hourly data for the loggers installed in fine grained material (a and b) and coarse grained material (c) at RGB. Ad fine grained material (graph a and b): Results of the overall lowest calculated Ra with input values d = 0,05m and p = 0,2 (a) and the highest calculated Ra with the input values d = 0,15m and p = 0,3 (b) are demonstrated as examples. The red line indicates the critical value. Ad coarse grained material (c): results are calculated with the same estimated values as SRG (d = 0,35m and p = 4)

Figure 25 shows the calculated Rayleigh numbers and the thermal offset of all loggers at SRG. SMTD1 shows the highest peak in October 2016 and between December 2017 and January 2017, Ra values constantly exceed the critical value. The highest value for Ra in SMTD2 is observed in December 2017. Similar to SMTD1, Ra continuously exceeds the critical value between December and February. The highest Ra value at SMTD3 is recorded in November 2017. Here a constant Ra value bigger than 40 is given from December 2017 and March 2018. SMTD4 shows the highest values in December 2017 and a continuous exceeding of the critical value is observed from January until February 2018. The highest peak detected at SMTD5 occurred in February 2018, where no constant exceeding of the critical value, but a rather constant fluctuation of Ra could be observed. The overall highest Ra value is computed for SMTD4 (Ra > 9000). It can be observed, that free air convection is suggested when the thermal offset is bigger than 0,04 in all loggers at SRG.

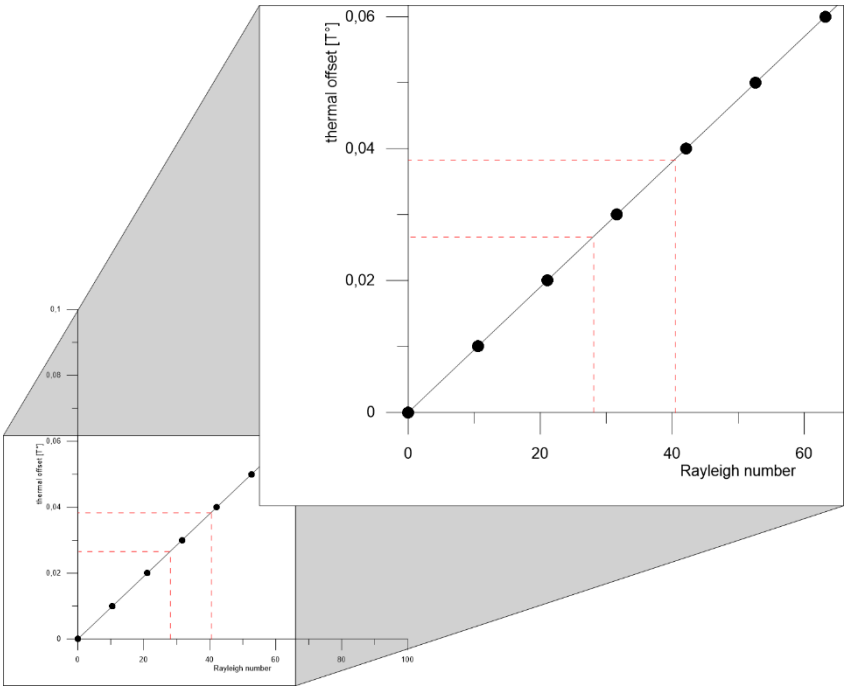

Figure 24 Thermal offset plotted as function of Rayleigh number with the results calculated for the loggers monitored within the coarse grained material at RGB. Graph shows the linear correlation of the two parameters. The Rayleigh number start exceeding the critical value of 27, when the thermal offset equals 0,027 and the critical value of 40, when the thermal offset equals 0,04.

In general, on both rock glaciers within coarse grained material Rayleigh numbers are constantly higher than the critical value in winter. The highest peaks are mostly observed in autumn. For both rock glaciers the Rayleigh number is directly correlated to the thermal offset (see correlation plotted in Figure 24), hence to the temperature gradient between the ground temperature and the ground surface temperature. The difference between the two rock glacier types can be observed in the time interval, in which Ra exceeds the critical value. Ra values at SRG surpass the critical value for a shorter period of time compared to RGB.

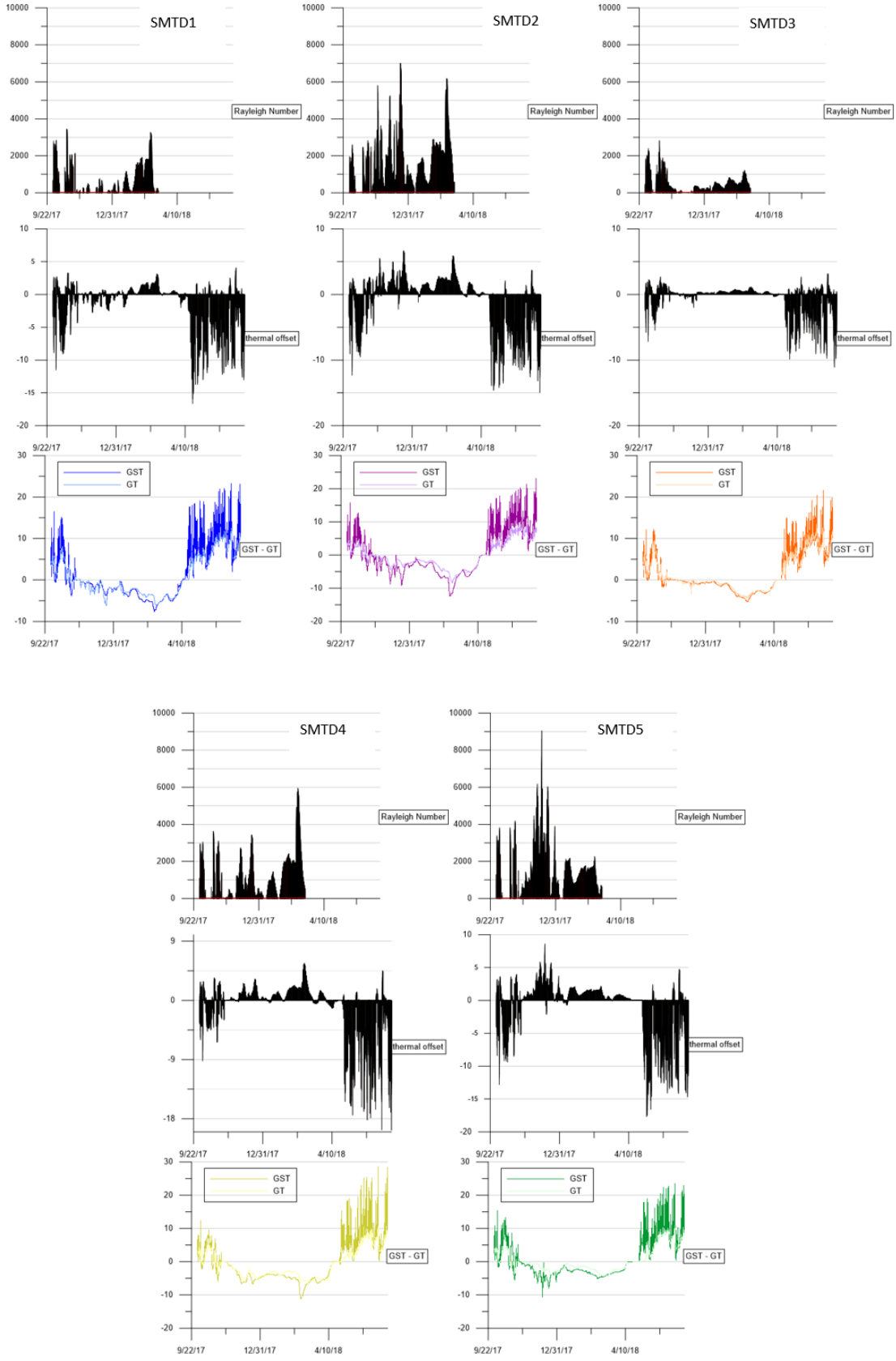

Figure 25 Rayleigh number, thermal offset (GT - GST) and temperature evolution over time based on hourly data for all loggers at SRG. Results are calculated with the same estimated values as RGB (d = 0,35m and p = 4)

4.2.4 Cross-Correlation and surface offset

At RGB no weather station has been installed. Therefore, temperature data of a nearby weather station positioned at similar geomorphologic conditions (Ischgl-Idalpe) were used for the calculations of the surface offset and the cross-correlation. Despite the similar altitudes and geomorphological settings, the data set can only be regarded as a rough estimation of the prevailing climatic conditions, due to the rather big distance to RGB. Therefore, the results of the surface offset and cross-correlation need to be interpreted with caution. Figure 26 shows the daily mean temperature evolution of the air temperature, ground surface (GST)- and ground temperature (GMT and GT) of both locations installed at RGB. One can clearly notice, that the air temperature is characterized by higher amplitudes, whereas temperatures in the rock glacier tend to be more buffered, especially in winter.

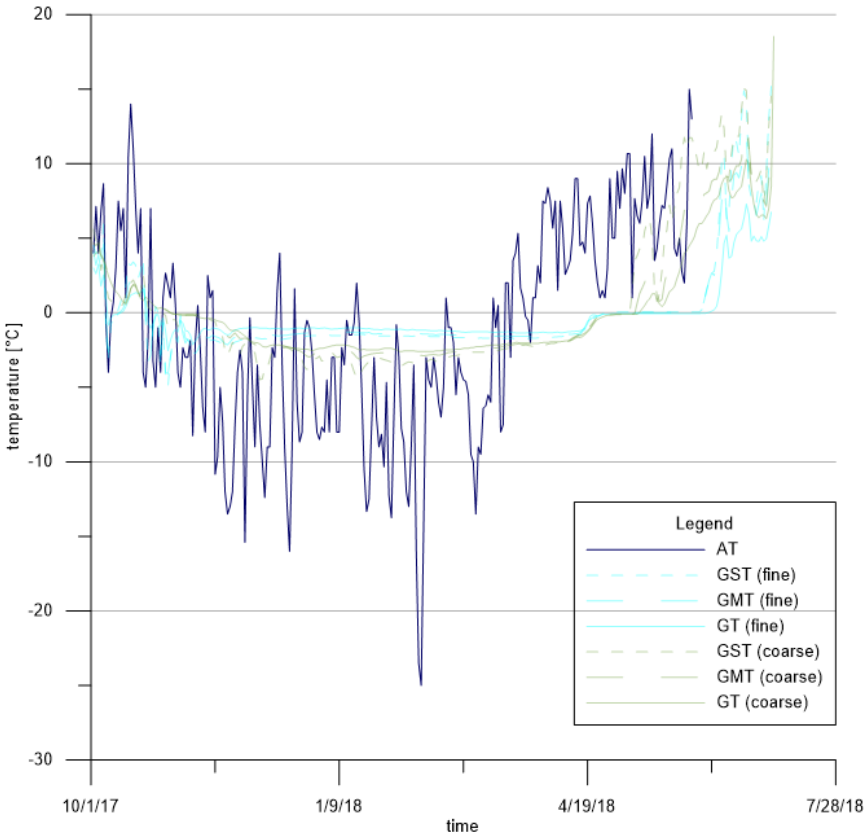

Figure 26 The daily means of GST, GMT and GT measured in fine and coarse grained material at RGB compared to the daily means of the air temperature (AT) monitored at the weather station Ischgl-Idalpe (ZAMG)

Figure 27 (a) presents the calculated surface offset (GST- AT) in fine and coarse grained material. From October 2017 until March 2018, the surface offset mostly shows positive values with some exceptions. In April, the coarse grained material clearly shows negative values, but from May until July 2018 the surface offset turns positive again. Also in fine grained material, the surface offset shows mostly positive values until April 2018, when they become negative. In July the values start becoming positive again. In February an extreme positive peak is evident in both loggers (SO > 20°C). The difference

between the two loggers is evident in Figure 27 (b) especially in spring. The surface offset in spring, becomes positive earlier in coarse grained material than in fine grained material.

(a)

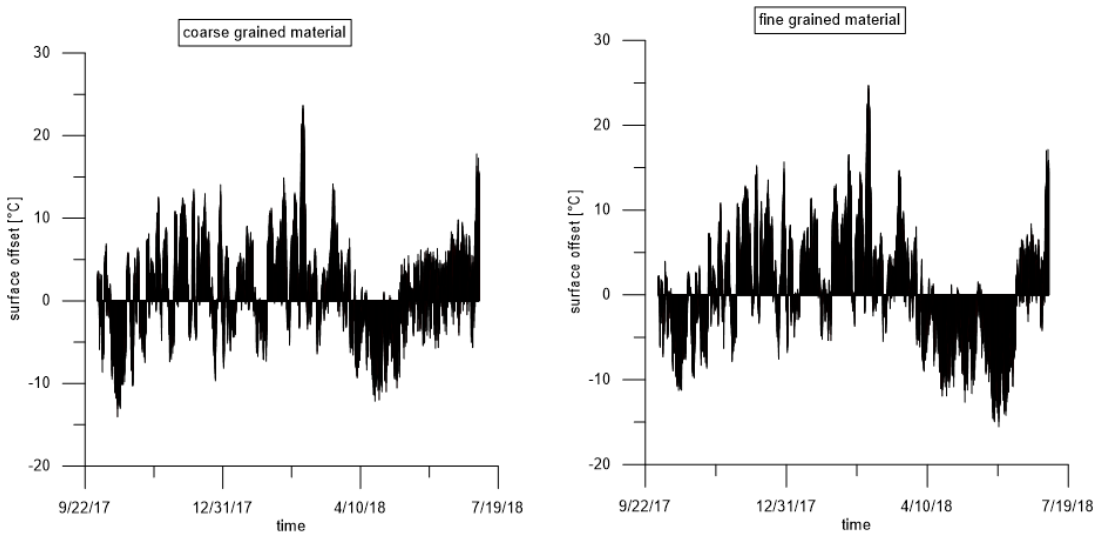

(b)

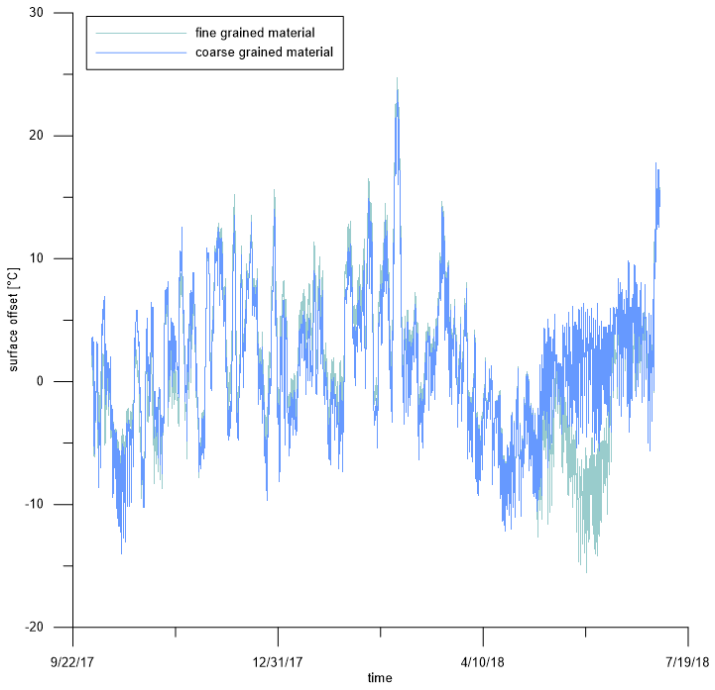

Figure 27 Surface offset (GST-AT) calculated for the fine and coarse grained material (a) at RGB using the daily temperatures monitored at Ischgl-Idalpe weather station (ZAMG). The graphs above (a) illustrate the surface offset of the coarse and fine grained material separately. The graph below (b) shows the surface offset of both loggers in one single graph demonstrating the differences evident especially in spring.

The cross-correlation is computed for all loggers dividing the data into four seasons (autumn, winter, spring and summer) in order to estimate the maximum R(k) and its time lag for a specific period of time. The overall results are given in Appendix 3.

Figure 28 shows the results obtained by the cross-correlation calculated for the loggers installed in fine and coarse grained material at RGB during each season. In autumn fine and coarse grained material shows a rather similar behavior: the values of the time lag increase with increasing depth, whereat temperatures in fine grained material appear to react faster (< 20h) than in coarse grained material. R(k) values in fine grained material are higher (> 0,5) than in coarse grained material (0,5). Also in spring, the ground surface temperature shows relatively low time lags. In contrast during winter time, R(k) shows lower values in fine grained (0,1) than in coarse grained material (0,5). In summer the time lags show the highest values (140h) of time lags. R(k)max values are relatively low, whereat values decrease with increasing depth. In summer and winter the ground within the coarse and fine material appears to be completely decoupled from the atmosphere.

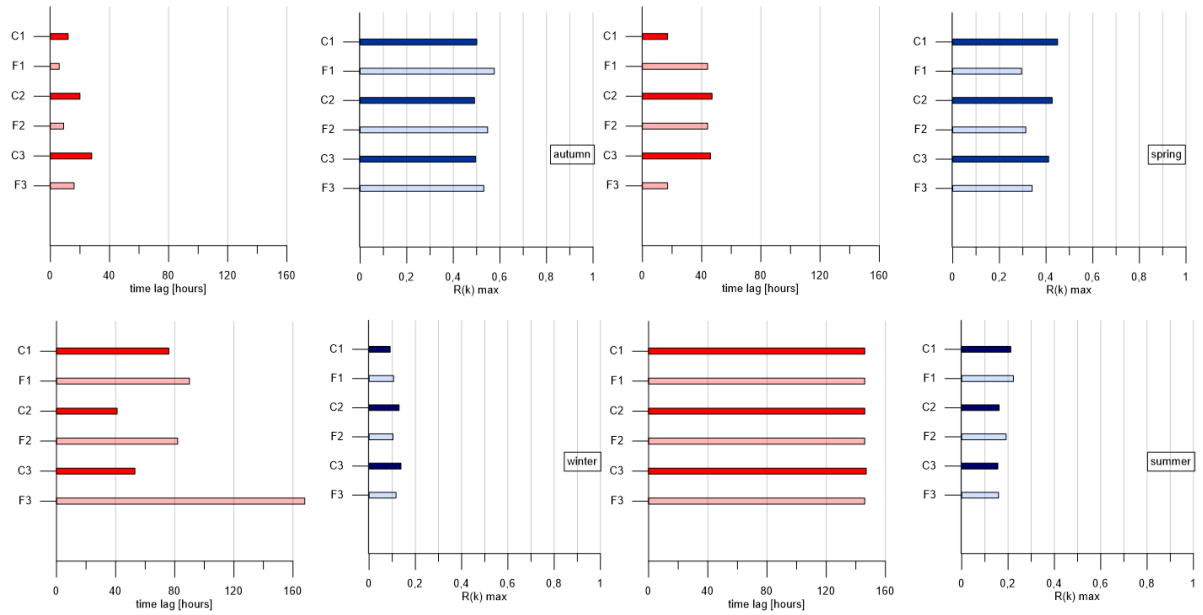

Figure 28 Time lags and maximum R(k) computed for both logger profiles installed at RGB using cross-correlation methods. Results are shown for the temperature data measured on the ground surface ("C1" – coarse; "F1" – fine), in the ground ("C3" – coarse; "F3" – fine) and in between the ground and the surface at 0,50 m depth ("C2" - coarse; "F2" – fine)

In Figure 29, the ground surface- and ground temperature of SRG are compared to the air temperature directly measured at the weather station of the rock glacier. It is evident that the air temperature shows much higher amplitudes, whereas the temperature in the ground and on the ground surface of the rock glacier always shows a more buffered temperature evolution.

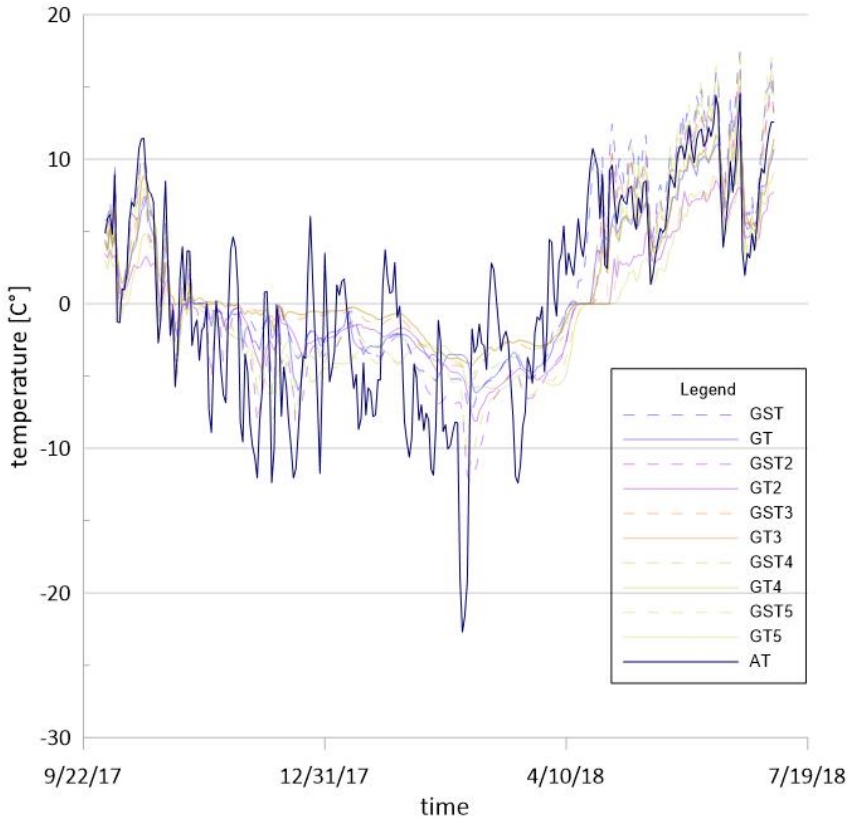

Figure 29 Daily means of GST and GT at SRG compared to the daily means of the air temperature (AT) measured directly at SRG as function of time

Figure 30 (a) presents the calculated surface offset (GST – AT) for each logger at SRG. The highest surface offset is monitored in SMTD4. It is evident that the SO of SMTD1 starts being positive earlier in spring compared to the other loggers (see Figure 30 - b). Similar to RGB, all loggers of the relict rock glacier show the highest peak of SO in February 2018.

(a)

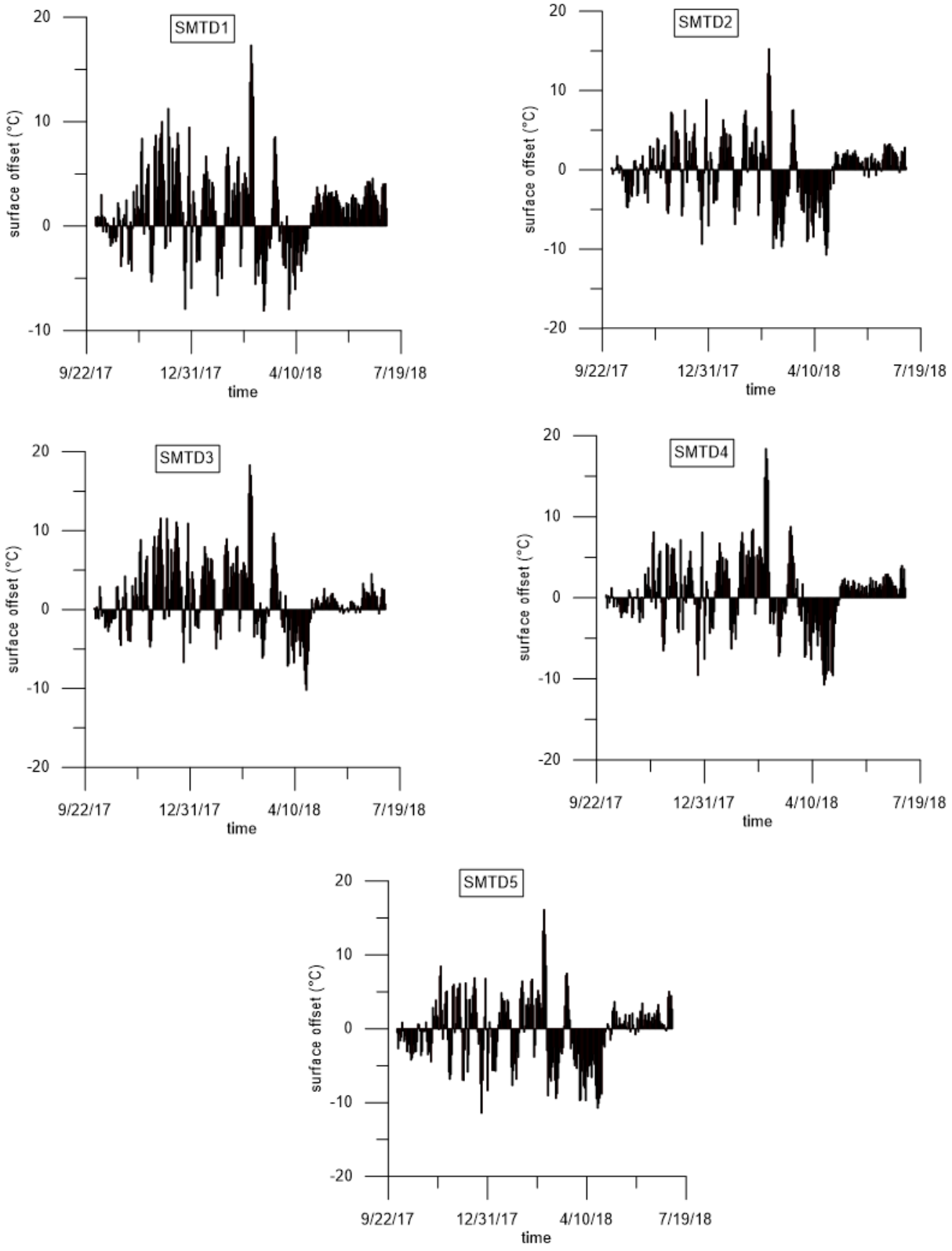
SMTD1
SMTD2
SMTD3
SMTD4
SMTD5
surface offset (°C)
20
10
0
-10
-20
9/22/17
12/31/17
4/10/18
7/19/18
time

(b)

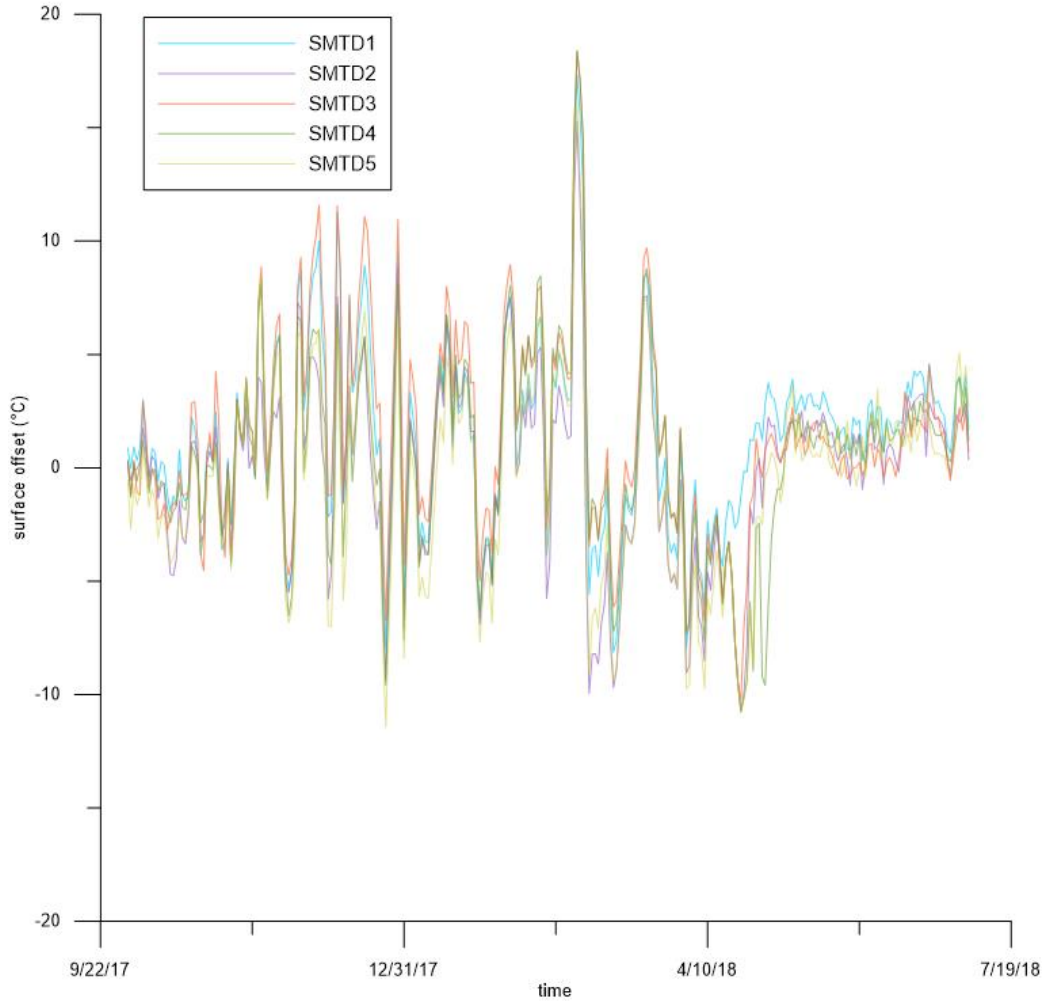

Figure 30 Graphs (a) show the calculated surface offset for each logger installed at SRG. Graph (b) demonstrates the surface offsets of all loggers installed at SRG in one single graph.

Figure 31 shows the time lags and the corresponding maximum R(k) for all the loggers installed at SRG. The cross-correlation shows that in autumn the ground surface temperature always reacts faster than the ground temperature. The slowest reaction in autumn is computed for the ground temperature at SMTD4 (20h). Yet, the same logger shows the fastest reaction of ground surface temperature (2h). The highest R(k) is computed for the ground surface temperature at SMTD2 (0,88). In winter the time lags are significantly higher, showing a maximum time lag of the ground temperatures at SMTD4 and SMTD5 (168h). In general, also in winter ground surface temperature react faster than ground temperature. Yet, the maximum R(k) shows significantly low values. The ground surface temperature of SMTD2 shows a maximum R(k) of 0,59, which corresponds to the highest maximum R(k) calculated in winter. The R(k) values of the ground surface temperature are always higher than the ground temperature in this period. Spring and summer are characterized by low time lags and rather high R(k) values. In spring the ground surface temperature always shows lower time lags than the ground

temperature. SMTD4 and SMTD5 even show a time lag of zero for ground surface temperature. The highest R(k) is given for the ground surface temperature of SMTD1. In summer, SMTD3 and SMTD4 show a time lag of zero for the temperature on the surface. The R(k) values are higher than in spring showing maximum values of 0,94 at SMTD4. In general, the ground surface temperature shows lower time lag values than the ground temperatures.

The intact and the relict rock glacier show less fluctuations of the temperature than the air temperature. Both rock glaciers show an evident negative peak of temperature in February 2018. The latter negative peak corresponds to the positive peak of the surface offset observed at each logger. The values of the surface offset in summer are mostly positive, in spring mostly negative and during winter positive with some exceptions. The cross-correlation for both rock glacier shows a similar interaction in winter, spring and autumn. Time lags at both rock glaciers are higher in winter and lower in spring and autumn. The difference between the two rock glaciers is evident only in summer, when the relict rock glacier indicates high correlation and the intact rock glaciers no correlation to the atmosphere.

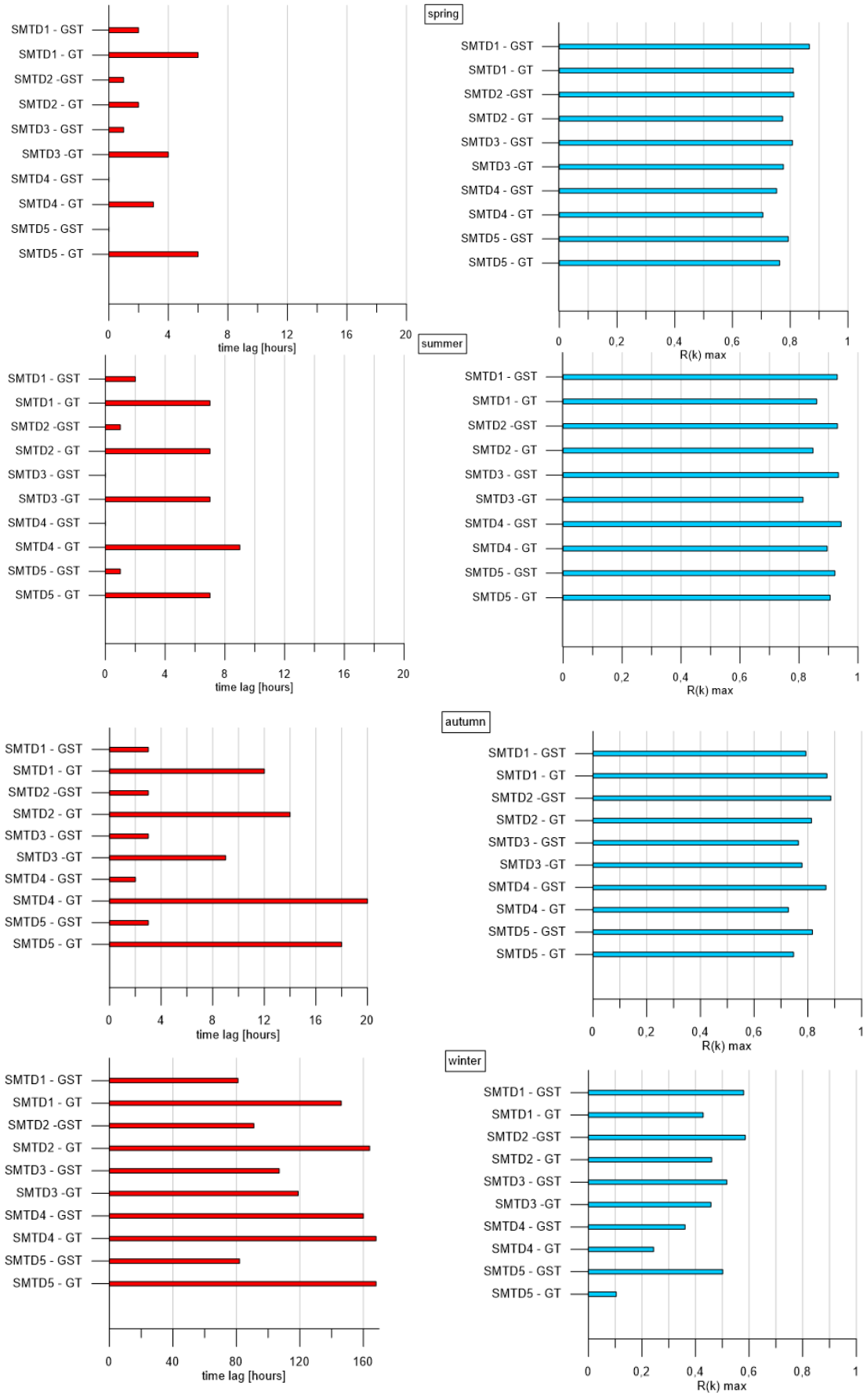

Figure 31 Time lags and maximum R(k) of the cross-correlation computed for the loggers installed at SRG for each season

5. Discussion and interpretation

This study tries to achieve a better understanding of the thermal behavior of the top layer of relict rock glaciers compared to intact rock glaciers. In the following chapter an evaluation and interpretation of the above-mentioned results is made.

5.1. Thermal heterogeneity on the surface of rock glaciers – characteristics and influencing factors

The negative MGST calculated for all intact rock glaciers (i.e. RGB, RGH and RGT) indicates the possible presence of permafrost. The positive MGST at SRG suggests that permafrost is absent in the relict rock glacier as shown by Boeckli et al. (2012). The lowest average temperature values have been detected at RGH and the highest at SRG. Comparing the results to Table 2, it can be noticed that RGH is located at the highest - and SRG at the lowest elevation. According to Kuhn et al. (2013) the air temperature gradient observed in Alpine regions is relatively homogenous with an average of -0,6°C per 100m. Similar to air temperature, the ground surface temperature appears to decrease with increasing elevation as shown in Figure 32.

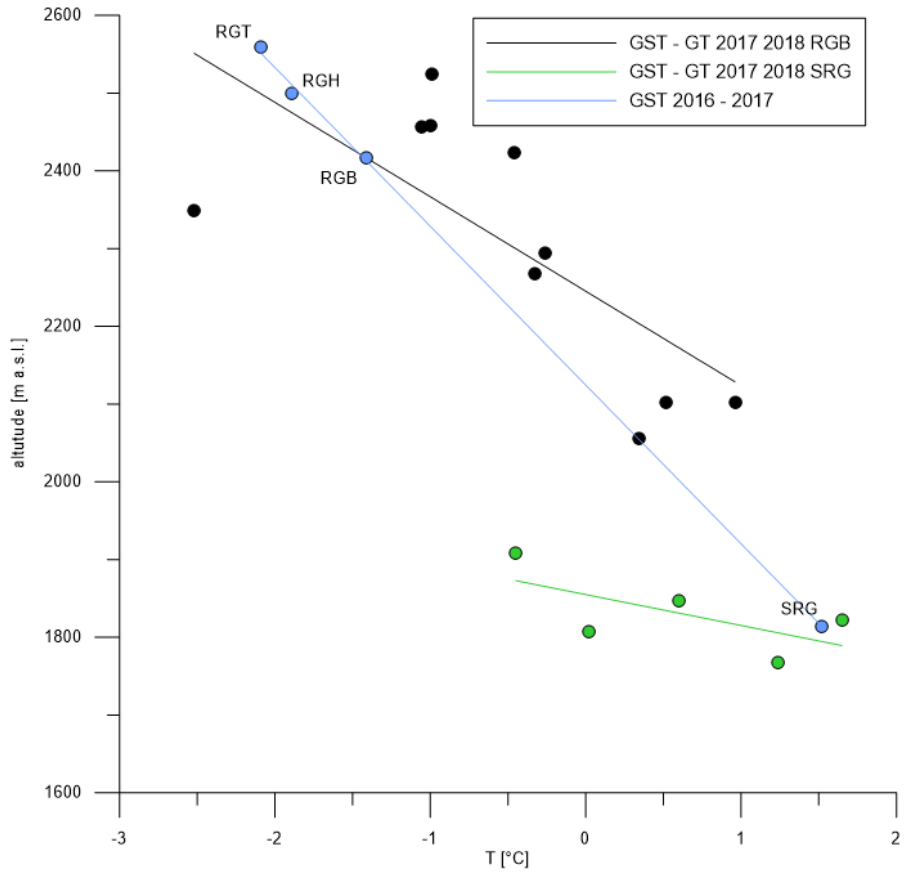

Figure 32 Mean ground surface temperatures compared to the altitude of the position of the loggers installed at SRG (green line; dots indicate each logger) and at RGB (black line; dots indicate each logger) from October 2017 until July 2018. The blue line shows the correlation between the altitude and GST monitored at SRG, RGB, RGH and RGT from October 2016 until July 2017 (dots indicate mean of all loggers).

As shown in Figure 11 maxima, minima and mean GST monitored between October 2016 and July 2017 at SRG, RGB, RGH and RGT mostly show a parallel temperature evolution over time. Only one logger (KW13) at RGB clearly shows some positive peaks in April and May 2017 (see Figure 33), which are not corresponding to the overall temperature evolution.

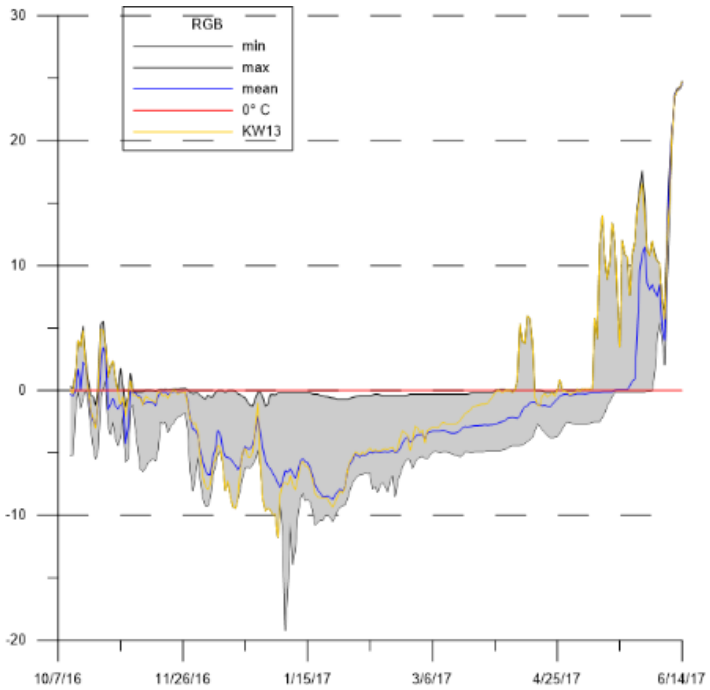

Figure 33 Minima, maxima and total mean daily temperature means of GST monitored at RGB with the highlighted outlier indicated by the yellow line (logger KW13) with its evident positive peaks in April and May 2017

The logger KW13 is installed in the medium range of the rock glacier (see Figure 34). Therefore, the temperature anomaly cannot be related to the elevation-depending change of temperature illustrated in Figure 32. The microrelief (see Figure 34 - a) reveals that KW13 is the only logger at RGB situated on a slope facing SW. Therefore, this logger is exposed to more solar radiation (Figure 34 - b). This leads to an earlier and faster snow melt, hence more and earlier exposure to shortwave radiation causing the positive temperature anomaly.

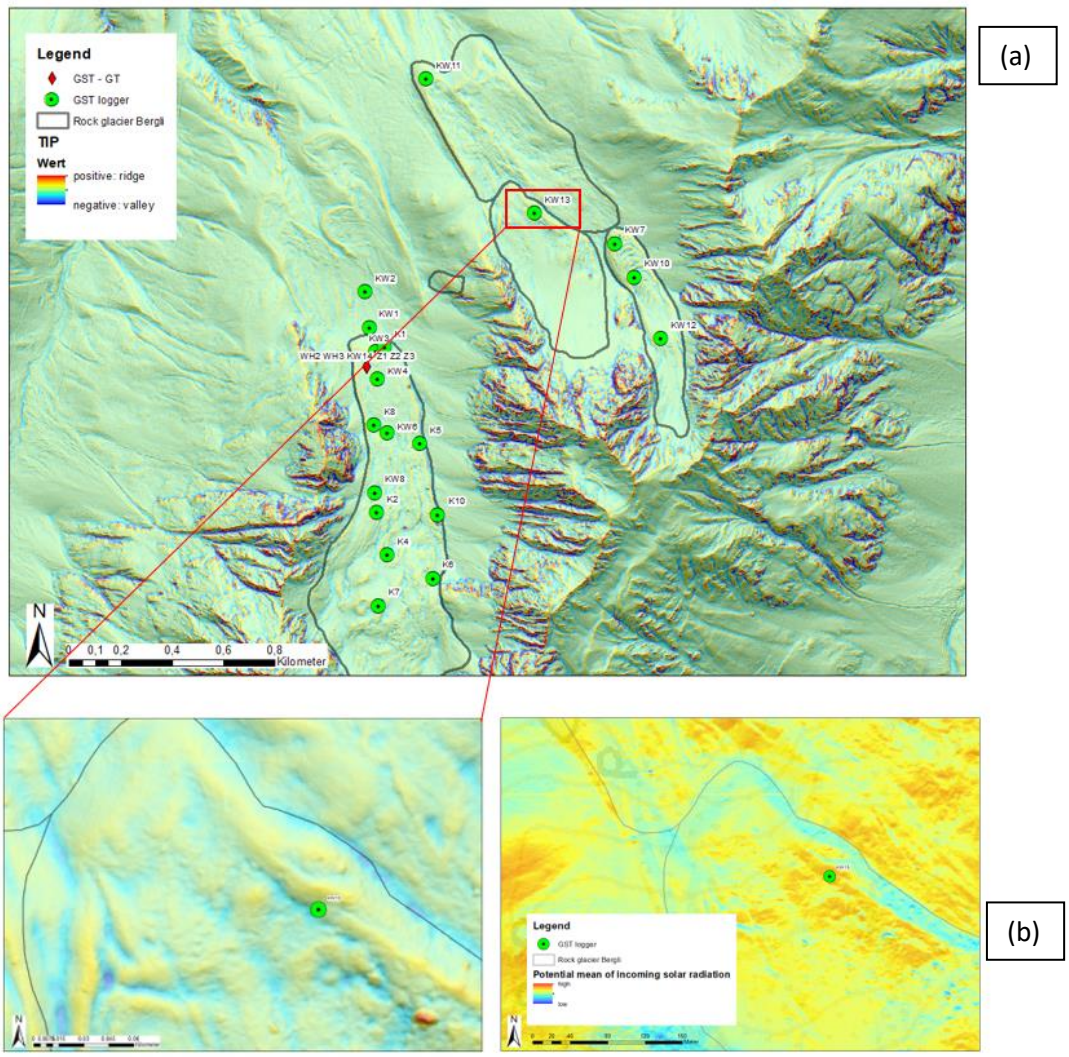

Figure 34 TPI values shown in graph (a) and its zoomed image, illustrate that KW13 is the only logger at RGB located on a slope facing SW. Graph (b) indicates the potential mean of incoming solar radiation which, in the area of the logger KW13, is rather high.

Also during the measuring period between October 2017 and July 2018 one logger (K10) at RGB clearly stands out due to its specific ground surface temperature values (see Figure 35). K10 shows rather cold temperature values with pronounced amplitudes in winter and relatively high temperatures in spring. The logger mostly defines the minimum daily mean observed in winter and the maximum daily mean calculated in summer. The TPI map of K10 (see Figure 35) shows that it lies on the western side of the eastern ridge of the rock glacier. Due to its specific position, it is suggested that this area is exposed to more shortwave radiation provided by the sun as well as longwave radiation reflected by the slope on its eastern side. Consequently, the snow cover might be patchy and can lead to more interaction between the air and ground surface temperature. This could result in extreme low temperatures and

high amplitudes during winter time. The relatively early and evident change to warm temperatures in spring can also be explained by pronounced influence of short- and longwave radiation.

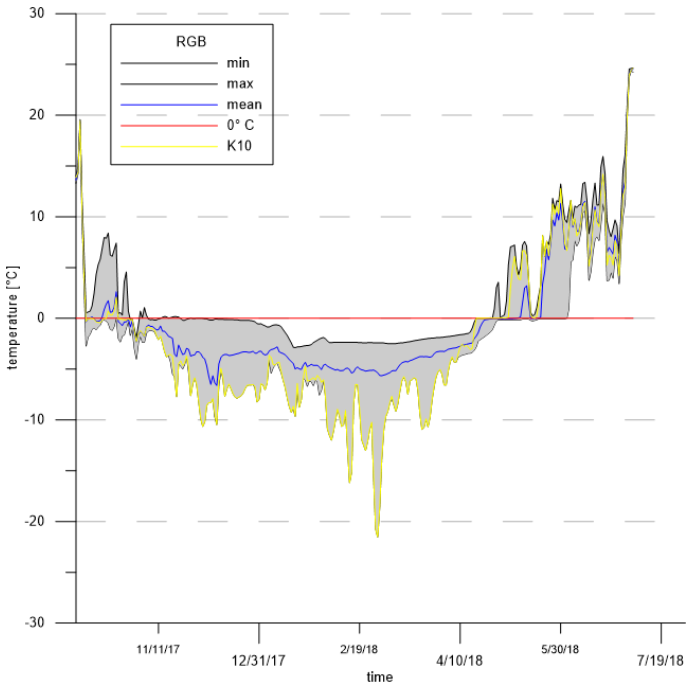

Figure 35 Maxima, minima and total mean of the daily temperature means of GST recorded at RGB: yellow line points out logger K10 with the lowest temperatures monitored on the rock glacier and the negative peak detected in February 2018

On a large scale, the temperatures of the ground surface are decreasing with increasing elevation showing a similar behavior to air temperature. Yet, some exceptions (e.g. logger KW13 and K10 at RGB) are observed. These can be attributed to individual conditions of the microrelief leading to specific microclimatic characteristics (e.g. enhanced exposure to solar energy). Shortwave, as well as long wave radiation might thereby have a decisive impact on the heating up processes of parts of the rock glacier (Lebeau and Konrad 2016).

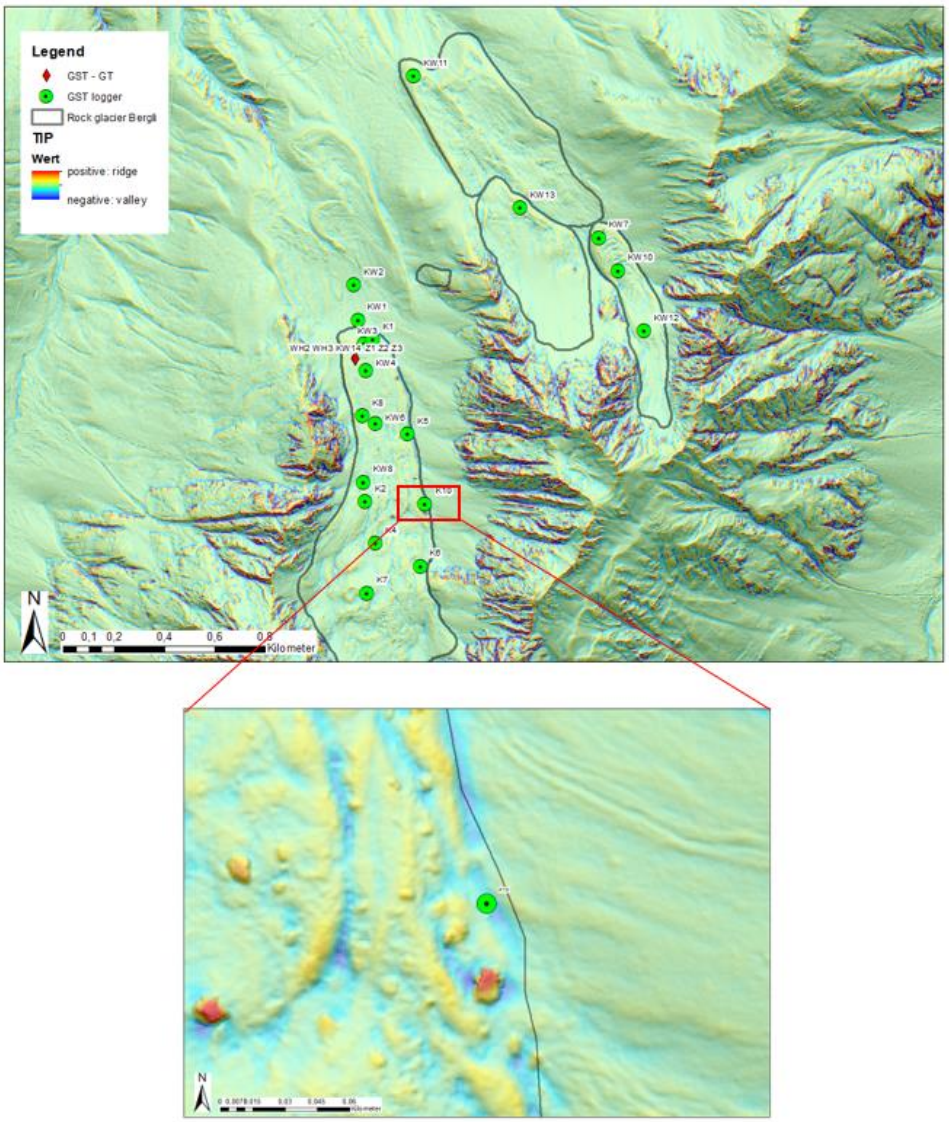

Figure 36 Microrelief of the logger K10 at RGB

The low correlation coefficient calculated for four loggers at RGT (TS32, T38, T19 and T9) indicate a heterogenous temperature distribution of the surface of the rock glacier. The TPI values listed in Table 3 suggest that T38 is situated in a rather flat area or a region of constant slope, TS32 on a ridge and T19/T9 in a small cavity. Due to its microrelief and geomorphologic position, T38 is possibly exposed to more solar energy. Consequently, the snow cover period might start later in this area leading to a positive temperature anomaly in autumn. Unlike T38, TS32 is situated on a ridge and could therefore be exposed to more wind leading to a rather patchy snow cover too. The lack of a continuous and thick snow cover in this area might permit air temperature to descend into the active layer of the intact rock glacier causing relatively low temperatures in winter. As seen in Figure 7, the geology of the bedrock underneath RGT2 is evidently heterogenous, ranging from gneissic rocks (“Zentralgneiss”) in the middle range, to marble (“Hochstegenmarmor”) in the lower parts and mineral soil right under the rock glacier. The lithology of the blocks that compose the active layer of RGT2 is also mainly dominated

by gneissic rocks and marble (Kogler 2018). According to Siegesmund and Dürrast (2011) the thermal conductivity of marble ranges from 1,59 to 4,00 W/mK and the conductivity of gneissic rocks varies from 0,94 to 4,86 W/mK. Even though the thermal conductivity of the rock types can differ, the correlation coefficient showed a rather homogenous ground surface temperature (correlation coefficients for RGT2: r > 0,7). Thus, it can be assumed that geology is not playing a significant role in the distribution of surface temperature at rock glaciers. Since rock glaciers are characterized by coarse grained material with a high porosity (Scherler et al. 2014) and open space voids (Jones et al. 2019), the contact between single blocks is rather rare and this can limit the potential conductivity between rocks (Wagner et al. 2019b). The ground surface temperature is thus not influenced by geology. T19 and T9, which are both located underneath RGT3 and installed within mineral soil, show warmer temperatures and a more buffered temperature evolution, especially in winter. This phenomenon has been observed at other researches (Harris and Pederson 1998). Due to the fine grained material given in this area, the ground surface temperature shows less reaction to temperature changes in the atmosphere. Unlike in coarse grained material, in which air filled voids allow processes from the outside influencing the intern thermal setting, the interaction within fine grained material is dampened due to its dense consistence and lower porosity. Similar to RGT3, temperature values of the logger KW2, installed at RGB within the mineral soil, behaves in a rather dampened way over time. As seen in Figure 13, KW2 shows smaller amplitudes indicating a pronounced buffering effect of the soil. KW11 is situated on the lowermost part of the western rock glacier tongue (see Figure 5). The position within the rock glacier complex and the relation to all the other loggers can be the explanation for the relatively different thermal behavior of this area. The logger KW13 has already been discussed previously. Its specific geomorphologic position leads to an individual thermal behavior which doesn't correspond to the overall behavior of the ground surface temperature measured at RGB.

The study of the correlation coefficients has proven, that the microrelief leads to specific microclimatic conditions, influencing the grade of impact of solar energy as well as wind forced processes (e.g. thinner and patchy snow cover). Nevertheless, Figure 37 shows that the correlation is not only depending on the TPI values and thus the microtopography. Only SRG, RGB and RGT3 indicate that the difference of TPI values (ΔTPI) is indirectly correlated to the correlation coefficients. Hence a big correlation coefficient is given when the difference of the TPI values is small. The other rock glaciers do not show this negative correlation. Hence, the microtopography is not the only parameter influencing the thermal regime of the rock glacier's surface. The thermal heterogeneity on the surface of rock glaciers is suggested to be influenced by an interaction of several factors, such as the grain size distribution with its corresponding porosity, the altitude and the microtopographic condition of the specific area.

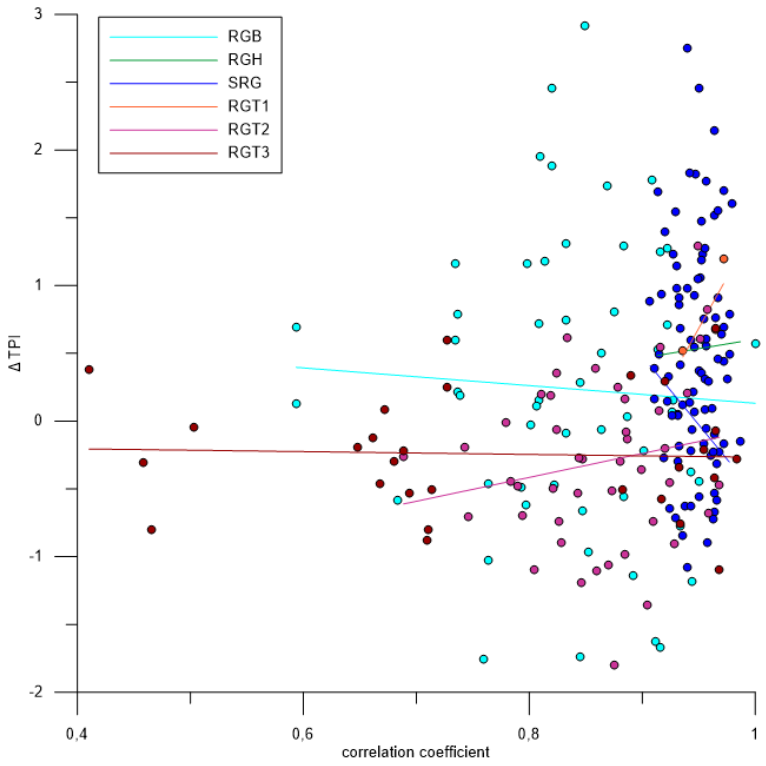

Figure 37 Correlation coefficient calculated between each logger of the rock glaciers plotted against the corresponding difference of TPI values. Dots show each logger pair of the rock glaciers and lines show the linear fit calculated for the overall results. It is shown that the correlation coefficient is negatively correlated to the ΔTPI at SRG, RGB and RGT3.

5.2. Thermal heterogeneity within the uppermost coarse blocky layer of rock glaciers – characteristics and influencing factors

The detailed investigation of the two different rock glaciers (SRG and RGB) has led to results that present the following characteristics for each rock glacier type and reveal different influencing factors that impact their thermal regime.

5.2.1 Temperature behavior in time

The overall evaluation of the ground surface- and ground temperature of the logger installed in fine grained material (Figure 16) at RGB indicate trends, which are not corresponding to the existing results studied for instance by Harris and Pederson (1998). Indeed, mean temperature of GST, GMT and GT measured in fine grained material are lower than in coarse grained material (see Table 4). The mean temperature values calculated in fine grained material are lowered by the prolonged zero curtain effect observed in spring (see Figure 16 - b). In this period, the coarse grained material is more affected by the solar radiation due to the bigger reaction surface (Baehr and Kabalec 2017). The elevated exposure to shortwave radiation leads to an earlier heating up of the blocks which on its side causes temperature values to rise relatively fast. In contrast, the temperature in fine grained material remains constant for a longer period of time. The melting process of ice and snow on the fine grained material

is suggested to be slower because more energy needs to be used in order to allow the phase transition. The loggers are installed in the lowermost part of the rock glacier within the active layer, which lies above the permafrost table and is subject to seasonal freezing and thawing processes. These freezing and thawing processes impact coarse and fine grained material in different ways. The fine grained material might temporarily be saturated and thermal processes can be influenced by pore water convection (Lebeau and Konrad 2016) caused by the infiltration of water especially in warm seasons and periods with more rainfalls. This explains the relatively high amplitudes of the ground surface- and ground temperature trends during spring and summer time in fine grained material. Though, apart from the specific period in spring, the temperature in the coarse grained material are lower than in fine grained material, especially in winter. Indeed, the water freezes to a constant temperature and can therefore explain the rather constant temperature trend within fine material (at -3°C) during winter time (see Figure 16). Consequently, the thermal regime within fine grained material is suggested to be influenced by pore water convection given by the infiltration of water in summer (high fluctuation of temperature) and by the evolution of the permafrost table and the snow cover in winter (constant low temperature). In coarse grained material, the temperature in summer shows less fluctuations than the temperature in fine grained material. The buffered temperature in the ground can be explained by the dampening effect of the coarse blocky layer. The lower temperature prevailing in the ground is the result of the air convection acting within voids in between the coarse material (Wagner 2019b). In summer, the colder and heavier air is trapped in the voids of the coarse material and no exchange of air between the surface and the ground is given. Therefore, the temperature in coarse grained material is characterized by less amplitudes and a more constant thermal regime in summer. In winter, the temperature values in coarse grained material are colder than in fine grained material. The open voids permit colder air to descend into the active layer and circulate through the material lowering the temperature values. In spring, the temperature tends to be warmer compared to fine grained material. As explained before, it is suggested that the snow cover on blocky layers is patchy and not as continuous as on fine grained material. Therefore, solar radiation heats up the blocks earlier with the result of higher temperatures. Hence, the thermal regime in coarse grained material is mainly influenced by the intra-layer thermal processes, the descending of cool air in colder seasons, as well as partially by the solar radiation heating up the surface of the blocks. The loggers at SRG installed in different depths show a rather homogenous and clear trend: The ground surface temperature tends to be warmer in summer and colder in winter reflecting the atmospheric temperature changes. The ground temperature reacts more buffered to these changes and shows the exact opposite behavior than the ground surface temperatures. Similar to the loggers at RGB, the cold air gets trapped within the open voids of the coarse blocky layer outlasting warmer seasons in depth. In spring the temperature especially on the surface turns positive rather fast. This is due to the solar radiation that

heats up the blocks after the snow has melted. Here, the thermal regime appears to be affected solely by intra-layer processes and the communication with the atmosphere (Wagner et al. 2019b).

In general, the logger at RGB installed within coarse grained material shows a similar temperature evolution as the loggers installed at SRG. Due to the elevated impact of solar radiation, the spring shows rather high temperature values. The rest of the months are characterized by dampened temperature behavior. The thermal regime within the fine grained material of RGB appears to be completely different, due to the high fluctuations seen in summer and the rather constant temperature observed in winter. These results show clearly that the thermal regime of the coarse material of the upper layer of both rock glaciers is mainly influenced by intra-layer processes and partially by solar radiation, especially in spring. The fine grained material, in contrast, is influenced by external temperature changes and the alternation of thawing and freezing processes. The difference is due to the diverse grain size distribution that leads to different physical properties of the material.

5.2.2 Temperature behavior in depth

The trends of temperature in depth shown in Figure 18 and Figure 19, clearly show that generally ground temperature is lower in warmer seasons and higher in colder seasons. Consequently, ground surface temperatures are higher in warmer seasons and lower in colder seasons. Thus, temperatures on the surface tend to reflect the atmospheric conditions. The temperature in the ground is dampened and shows a delayed response to any external temperature change. Usually, in soils the heat is transferred through vibrations of molecules which touch other molecules. This process is called conduction. The soil's ability to transfer temperature into the depth is strongly depending on the porosity and the water content. Air is a poor thermal conductor. Due to air pockets present in soils, the heat is transferred slowly to the ground (Koorevaar et al. 1983). This delayed response increases with depth (see Figure 38, after Stull, 1988). Comparing the trends recorded at RGB to Figure 38, it can be noticed that the evolution observed within one year is similar to the evolution expected in soils during one day according to Stull (1988). Nevertheless, a clear deviation in the timing of tipping is noticeable especially in coarse grained material.

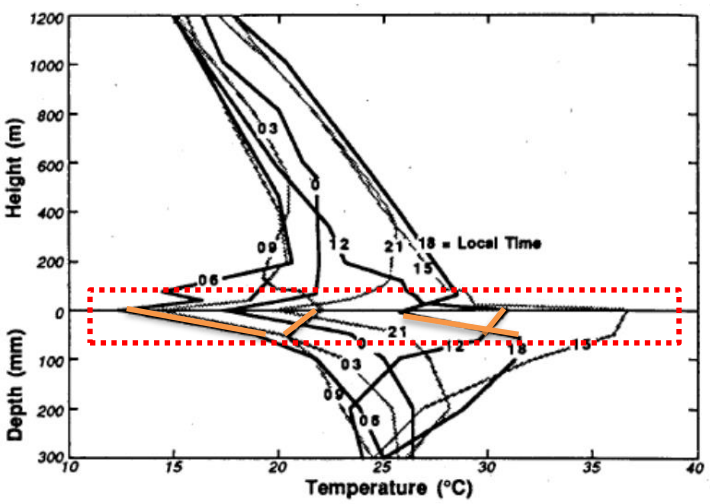

Figure 38 Temperature trend measured in the atmosphere and propagated into the depth (Stull 1988) during one day. Red rectangle indicates the zone which is relevant for this study. Hourly trends underlined as orange lines are suggested to represent seasonal trends during one year: 12:00 – August, 18:00 – November, 03:00 – February, 09:00 – May

Temperatures in fine grained material behave similar to the evolution trends shown in Figure 38, except from the thermal regime in May. It can be therefore deduced that the main force controlling thermal regime in this fine grained material is conduction. Yet, as already mentioned, the deviation observed in May, might be caused by rarely controlling convection processes given by the pore water in the possibly saturated area. In contrast, the coarse grained material shows a more evident deviation and shifts of temperature tipping compared to Figure 38. Here, the period in which ground temperature is higher than ground surface temperature starts earlier (September), whereas in April the ground temperature is showing lower values than the ground surface temperature. The deviation suggests that in coarse grained material convection is acting as the main thermal transport rather than conduction. Hence, the reactions and tipping of temperature happen faster and more efficiently than in fine grained material, where conduction plays the most important role. Still, the trend of the tipping temperatures (summer: GT < GST and winter: GT> GST) can be observed in each case. The ground is hence always reacting slower to the temperature changes in comparison to the surface. The loggers at SRG show similar deviations to Figure 38. The shifted tipping of temperature, which here already starts in April, can likewise be explained by the convection controlled thermal processes acting in coarse grained material rather than by the conduction as observed in fine grained material. The following events observed in the loggers installed at RGB (within coarse grained material) and SRG, can be seen as general evolution: In summer the air temperature is warm and because of the density differences of warm and cold air, no interaction between the ground surface and the ground temperature is expected. The ground temperature is colder because within the coarse grained material, an exchange of cold air dropping to depth happens in the cooler seasons before summer. Hence, cold air is trapped in the ground, while higher temperatures are prevailing on the surface. In

autumn, the temperature of the atmosphere above the surface decreases, influencing the ground surface temperature of the rock glacier, as it responses faster to the air temperature. Temperature affects directly the air density, which induces a temperature gradient between GT an GST and causes in further consequence air convection within the voids of the coarse grained material. From winter until spring, temperatures in both ground surface- and ground temperature, tend to get constantly lower, whereat the ground temperature is relatively warmer compared to the surface. This is mainly caused by the delayed and buffered reaction of GT to the external air temperature pulses. In spring, when the snow has melted, solar radiation warms up the surface again. The ground surface is affected by solar radiation, reacts faster to temperature changes and warms up. The cold air saved from the winter months drops down because of its higher density and keeps trapped in the depth as the permafrost ice body represents a cold boundary below the active layer. Therefore, the ground temperature gets lower during the summer months. Comparing this behavior with the trend shown in Figure 38, the main difference can be seen in the timing of tipping of the temperature gradients. This shift in time is explained by the convection acting in coarse grained material, which transports energy faster than conduction (Baehr and Kabalec 2017).

The differences observed between the relict and the intact (coarse grained) rock glaciers are seen in the timing of the definitive tipping of the thermal regime in autumn. Compared to the relict rock glacier which mostly changes its thermal regime in December, the intact rock glacier changes its thermal regime earlier (in the month of September). This is due to the elevation differences which causes a generally colder air temperature and the present permafrost ice body underneath the active layer. Air temperatures at RGB start becoming lower earlier causing a faster change of the thermal regime within the coarse blocky layer. In spring, both rock glaciers behave in a rather similar way changing their thermal regime mostly in April. The snow melting dynamics are directly coupled to solar radiation. This indicates, that in both cases, solar radiation plays an important role in the thermal regime of blocky layers.

5.3. Main heat transport

As seen in Figure 23 at RGB, in fine grained material, Ra values only exceed the critical value if the equivalent diameter of the particles is 0,15 m, the porosity 0,2 and if the thermal offset (GT – GST) is bigger than 2,5 °C. Consequently, given these parameters, convection might act in fine grained material. In the other presented case, Ra values never exceed the critical value, hence no air convection is acting. Since the analyze of the grain size distribution conducted in a 400x400 raster (Pedevilla 2019) at RGB showed d_{10} equals 0,05 m, it is rather suggested that in this examined fine grained material no air convection is acting. Within fine grained material, the main energy transport is therefore suggested to be conduction between grains. In the coarse grained material, Rayleigh

numbers always exceed the critical value when thermal offsets are bigger than 0,04 (see Figure 24). Consequently, free air convection is suggested to act. From April until July 2018 no free air convection is expected, since the thermal offset is negative. In this period the ground temperature is lower than the ground surface temperature and due to the density differences of air, no interaction between GST and GT is given. Mainly in winter, Ra values are higher than the critical value suggesting free air convection to be a main driver in thermal processes. Comparing these values to the temperature trends discussed before, one can notice that in this period the ground temperature is always higher than the ground surface temperature. Given this positive thermal offset, density gradients, caused by the difference of temperature, are created. These lead to air forced convection. The highest peak of Ra always correlates directly to the highest peak of thermal offset, showing that free air convection is acting when the temperature gradient between the surface and the ground reaches values bigger than 0,04. This case is given in September, when at RGB, the temperature outside tends to get colder but the snow has not covered the rock glacier yet. Similar to the logger in coarse grained material at RGB, all loggers at SRG tend to show Ra values higher than the critical value especially in winter time. Yet, here Ra exceeds the critical value in a significantly shorter period of time and the highest peak is later reached. This is due to the lower elevation that comprise higher air temperatures. SMTD5 is the only logger showing its highest peak in February 2018. Being the logger situated at the highest elevation, snow might cover this area earlier, even before the temperature in the atmosphere might decrease significantly and lead to air forced convection. Since the snow covers the area earlier in autumn, the thermal offset is not big enough to induce density driven air convection. Only in spring, when snow melts again, the ground surface temperature can be influenced by cold air temperature and Ra numbers show a possible air forced convection. Yet, the Ra shows relative low values compared to the other loggers.

In either relict and intact rock glaciers, air convection can be expected (within coarse grained material) when the air temperature is relatively low. Due to its higher density, colder air descends into open voids replacing the warm air within coarse material. This vertical movement of air can be described as Balch-effect (Harris and Pederson 1998). In intact rock glaciers, the air driven convection is mainly expected in the active layer (Delaloye and Lambiel 2005) and is therefore affected by seasonal changes. Air convection during snow free periods in summer time is only restricted in single events, when air temperature temporarily drops. The highest peaks of Ra, consequently the highest probability of vertical air forced convection, are recorded when the air temperature starts to get colder (e.g. autumn), but no snow cover is already present (Zhang 2005). The difference between the two rock glaciers is the actual period, in which the critical value of Ra is exceeded. Within the intact rock glacier, the critical value is surpassed for a longer interval. Therefore, temperature is transported by air

convection for a longer period of time. According to Guodong et al. (2007) conduction as thermal transporter appears to be absent in coarse grained material. In contrast, in the fine grained material at RGB, no convection is acting. The main process of heat transport in this material is conduction between grains.

5.4. Reaction to changes of the air temperature

The response of the rock glaciers to external temperature changes was calculated using cross-correlation methods. Temperatures measured in rock glaciers generally show a more dampened evolution over time in comparison to the air temperature (see Figure 26 and Figure 29). The dampened response is quantitatively shown as R(k) value (always smaller than 1,0) as well as the time lags and is evident in all loggers at SRG and RGB. According to Scherer (2012), this happens because of its coarse grained shield which protects the rock glacier from temperature changes leading to a slower reaction of the system. As suggested in the previous chapter, the ground surface temperature mostly shows lower time lags and thus reacts faster to temperature changes than the ground temperature. Furthermore, the dampening effect depends on the snow cover evolution. The cover is thereby acting as an additional buffer and lowers the interaction between the air temperature and the ground surface temperature. Cross-correlation calculated for the loggers at RGB shows the following behavior: only autumn and spring are characterized by relative high R(k) values and rather low time lags suggesting an interaction between the air temperature and the coarse layer. Autumn shows the highest correlation between the air and the ground at RGB indicating that this period is less snow covered than spring. Hence, temperature changes in the air are propagated into the active layer in this period. In winter and summer, cross-correlation shows almost no interaction between air and ground. The latter result indicates, that the loggers are thermally decoupled from the atmosphere in this period. Hanson and Hoelzle (2004) observed, that the correlation between the active layer and the atmosphere become weaker starting from a daily mean air temperature of 6°C. Juliussen and Humlum (2008) also detected an insulating effect of the active layer in summer. The active layer and its underlying permafrost ice-table are hereby acting as protecting features. This leads to a decoupled thermal regime prevailing within the active layer in summer. Not only the logger placed within the coarse grained material, but also the logger installed within fine grained material, shows nearly no thermal connectivity between the atmosphere and the ground in summer. This might be explained by the above-mentioned fact, that in summer thawing processes affect the thermal setting in this specific zone of the rock glacier. Infiltrated water can act and influence the thermal regime within fine grained material significantly (Lebeau and Konrad 2016). Consequently, it is evident that temperature in the ground of fine grained material is also completely decoupled from the atmosphere in summer and that possible pore water convection influences the thermal regime. In winter, time lags and R(k) values in

both loggers suggest no communication between air and ground, because the snow cover is acting as an insulating roof.

The results of cross-correlation (see Figure 31) for each season at SRG shows the following trend: in summer, the values of R(k) are rather high and time lags are relatively low indicating a significant and fast interaction between air and ground. In spring, this interaction appears to be even faster, but with a more dampened reaction given by the R(k) values. Winter is characterized by rather low R(k) maxima and high time lags demonstrating a low interaction rate between air and ground. As explained before, the absence of interaction between ground and air temperatures can be interpreted as a result of the insulating effect of the snow cover in winter. Consequently, in winter, temperature changes in the air are not transmitted into the relict rock glacier. In periods which are mostly snow free (summer, spring and autumn), the interaction between the air temperature, the ground surface temperature and the ground temperature is clearly seen in these results. In general, at SRG, the ground temperature always shows more buffered, hence slower reaction to air temperature changes, compared to the ground surface temperature. Also, R(k) values of the ground temperature are lower than the values of the ground surface temperature, demonstrating the buffering effect of the coarse grained material. These results correspond to the results demonstrated in Wagner et al. (2019b).

In general, at RGB higher time lags and lower R(k) are computed. This might be explained by two facts: RGB is positioned at a higher elevation comprising lower average temperature and thus longer snow covered periods. Additionally, the snow cover in this region is suggested to be thicker than at SRG. Since the snow cover is acting as insulator, the latter effect is increasing with increasing thickness. A thicker snow cover therefore leads to a more dampened behavior in ground, hence slower reaction (time lags) and less efficient interaction (R(k) max - value) between air and ground temperature. Additionally, permafrost ice is present in RGB, impacting on the thermal regime as well. One should consider, that the air temperature used for the cross-calculation at RGB is not directly measured on the rock glacier as it is at SRG. This might cause a general correlation error which cannot precisely be detected, nor eliminated. In general, the main difference resulting from the cross-correlation method is that the relict rock glacier shows less correlation only during winter, when snow covers the rock glacier and is acting as insulator. In contrast, at RGB, a decoupled thermal regime can be observed in winter and in summer. Impulses from the atmosphere only reach the ground when the air temperature is relatively cold and no snow covers the rock glacier (autumn and spring). This can be explained by the permafrost-ice present in the intact rock glacier but absent in the relict rock glacier. The permafrost table keeps temperatures in the ground at RGB continuously rather cold. This prevents the relative warm air temperature in summer from being transported within the active layer. The ground appears to be decoupled from atmosphere in summer, because temperature differences (i.e. density

differences) are big enough only in this period. In autumn and spring the air temperature gets colder changing the density gradients and allowing air to be transported again. Hence, at the intact rock glacier the thermal regime in summer is not affected by atmospheric processes, but solely by the ice-core evolution and partially by solar radiation. In colder seasons, the cooler air can descend into the open voids as long as snow is not covering the active layer. At SRG permafrost is not suggested to exist (Boeckli et al. 2012). Therefore, the temperature gradient in summer is not as big, allowing external temperature changes to influence the rock glacier's thermal regime.

The range of the daily means within one month (Figure 20) indicates that the intact rock glacier, which shows smaller variability, is thermally more homogenous than the relict rock glacier. As seen in Figure 21 and Figure 22, in winter, the monthly means of the relict rock glacier are lower than the monthly means of the intact rock glacier. Despite the elevation differences and the expected lower temperatures prevailing at RGB, the relict rock glacier appears to be characterized by colder temperatures in winter. The potential mean of incoming solar radiation at SRG is summed up to 785,5 kWH/m^2 and at RGB to 8.373,4 kWH/m^2. The relict rock glacier is therefore heated up less by solar radiation than the intact rock glacier. This might be the reason why the relict rock glacier shows a lower starting temperature at the beginning of winter. Nevertheless, at RGB the snow cover in winter is suggested to be more continuous and thicker, hence in winter RGB is more isolated than SRG. Additionally, the ice-core present at the intact rock glacier causes a rather constant temperature in winter. Therefore, the temperature measured in the intact rock glacier tends to stay on a rather constant value, without falling below -4°C (Figure 21) in winter. In contrast, on the relict rock glacier, the snow cover is suggested to be thinner and less continuous. Consequently, the thermal regime within SRG is once more proven to be more influenced by the colder air temperature in winter generating values below -5°C (see Figure 22). Due to the thinner snow cover at SRG, warm air can possibly escape through holes in the snow cover leading to a further decrease of temperature within the relict rock glacier.

The prevailing temperature gradient between the air and the studied rock glaciers is indicated by the surface offset. The evolution of the surface offset calculated for the relict and the intact rock glaciers show a rather similar trend: As shown in Figure 26 and Figure 29, all loggers at RGB and SRG demonstrate their highest peak of surface offset around February 2018. The air temperature in this period reaches its minimum (AT = -21°C at SRG and AT = -24°C at RGB) and is therefore responsible for the positive surface offset peak at both rock glaciers. Positive surface offsets indicate a relative high ground surface temperature or relative low air temperature. This is caused by the presence of a snow cover which leads to an insulation effect (Wagner et al. 2019b). Due to the insulation, the ground surface temperature is not influenced by the air temperature and therefore remains rather high. All

loggers show negative surface offset values in spring. This effect might also be explained by the snow cover evolution. In spring the rock glaciers are partially still covered by snow, while temperatures in the air start becoming higher. The difference observed in the loggers of RGB is seen in spring (see Figure 27 - b). Here, the SO of the coarse grained material becomes positive earlier in comparison to the fine grained material. This is due to the faster heating up of the blocks, caused by the bigger reaction surface. The faster heating up of the blocks induces an earlier melting of snow, allowing solar radiation to rise the surface temperature values. It is hereby seen, that the grain size of the material has an impact on the influence capacity of the solar radiation. On the relict rock glacier the logger SMTD1 is showing an individual SO behavior in summer. AT SMTD1 the SO starts becoming positive earlier, indicating that snow is melting faster in this position. This can be explained due to the position of this logger. It lies on the lowest part of the rock glacier and is therefore exposed to warmer temperatures compared to the other loggers. The period of summer is mainly characterized by a positive surface offset. In this snow free period, the solar energy is directly radiating onto the rocks causing a higher temperature in comparison to the air temperature. Hence, the snow cover and accordingly the exposition to the solar radiation is once more proven to be a main factor controlling the thermal regime. It indicates and underlines the importance of the snow cover evolution which can act as insulator (Zhang 2005). In absence of a continuous snow cover, the solar energy causes a heating up effect of the rocks (Lebeau and Konrad 2016). The latter heating up effect on its side, is depending on the grain size distribution of the affected material.

Generally, the relict rock glacier is suggested to be more influenced by temperature changes of the air compared to the intact rock glacier. The intact rock glacier interacts with the air temperature only in autumn. The only external impact factor which appears to effectively influence the intact rock glacier's thermal regime is the shortwave radiation originated by the sun.

6. Conclusion and Outlook

The analysis of temperature data monitored on the surface of the four investigated rock glaciers lead to the conclusion that the superficial thermal regime is not influenced by geology. The main factors controlling the temperature are rather the altitude, as well as the grain size distribution and the micro-morphological settings. The altitude is a parameter that generally affects the temperature values on a large scale. The grain size distribution and its corresponding porosity control the modality of heat transfer acting within the layer as well as the impact intensity of solar radiation. The microrelief induces specific microclimatic conditions such as exposure to solar radiation and wind, which on their side have a great effect on the snow cover development. The temperatures on the surface in coarse grained material are characterized by higher amplitudes and lower temperature values compared to fine

grained material and show a more effective interaction between the ground and the atmosphere. This is due to its open voids which allow atmospheric processes to influence the thermal regime.

The detailed investigation of the internal thermal regime of the relict (SRG) and one intact rock glacier (RGB) showed a more buffered evolution over time compared to the air temperature. This proves the protecting effect of the uppermost coarse blocky layer in both rock glaciers. Additionally, temperatures in both rock glaciers are in average colder than in the atmosphere. The cooling effect in the relict rock glacier is controlled by intra-layer processes and the interaction with the atmosphere (especially in snow free and cold periods). This intra-layer processes permit colder air to be trapped in the coarse material. The cooling effect in intact rock glaciers, in contrast, is influenced by permafrost thawing and freezing of the active layer, the air driven convection acting within the active layer, as well as partially by atmospheric processes. The latter effect is suggested to be more pronounced in the relict rock glacier in winter and in the intact rock glacier in summer. The patchy and thinner snow cover, as well as the weaker solar radiation impact at the relict rock glacier, explains the relatively low temperatures in winter. Thawing and freezing processes and the presence of permafrost-ice are the reasons for the relatively low temperatures at the intact rock glacier in summer.

The absolute warmest and absolute coldest daily means are observed at the relict rock glacier. It is thereby shown, that the intact rock glacier is characterized by a more homogeneous thermal regime which reacts less to external temperature changes than the relict rock glacier. In the intact rock glacier, atmospheric temperature changes are propagated into the ground only in autumn and spring, when snow is not continuously covering the layer and the difference between the air and ground temperature is not as big as in summer. The intact rock glacier appears to be completely decoupled from atmospheric processes in winter due to its snow cover and in summer due to the present ice-core underneath the active layer causing a temperature gradient that doesn't allow an exchange. Both conditions lead to a partially closed system, in which the thermal regime is evolving as a result of the ice-core- and snow cover evolution, as well as of the intra-layer air induced convection, independently from external temperature changes. The relict rock glacier reacts to external temperature changes as long as snow is not covering the landform. Thus, it is more influenced by the communication with the atmosphere, as well as the intra-layer processes and it can be suggested that it behaves mainly as an open system. Nevertheless, in both cases the evolution of snow cover and the exposure to solar radiation are significant for the evolution of the thermal regime proving the crucial importance of micro-morphological settings leading to specific microclimatic conditions.

The main temperature transport acting within both rock glaciers is suggested to be the vertical convection, defined as Balch effect. The latter is mainly acting in autumn and winter, when air

temperature is lower than the temperature in the ground. The temperature differences induce a density driven movement of air within the layer. Only in fine grained material no convection is assumed, because the porosity and the grain size distribution do not allow the presence of open voids permitting the transport of air. Instead, conduction is suggested to be the main driver within fine grained material.

This study emerges limited results and permits only restricted interpretation. But it is suggested that rock glaciers tend to outlast climate changes longer than glaciers due to its pronounced dampened thermal behavior. The latter buffered behavior is especially seen in the intact rock glacier. Thanks to the ice-core protected by the coarse grained layer, intact rock glaciers are suggested to be more climatically resilient than relict rock glacier. Once the ice-core has disappeared from underneath the active layer, the rock glacier is interacting more actively with the atmosphere. The latter increase of communication with the atmosphere can enhance the cooling effect in winter. Given that precipitations in future will more and more fall as rain instead of snow, the lack of continuous snow cover might additionally lower temperature values in winter within the uppermost coarse blocky layer. This increased cooling effect might not be compensated by the increasing solar radiation, as it is controlled by convection and captured in the depth of the rock glacier. As long as winters are characterized by low temperature values, cold temperature values in relict rock glaciers can be expected to survive thanks to the free air convection. Due to the observed thermal behavior it might be possible, that rock glaciers do not directly evolve from intact to relict rock glacier, but show a more complex thermal evolution over time.

For future studies it is suggested to use high resolution snow cover models which show the precise extent and thickness of the snow cover present in the studied areas in order to quantitively calculate the influence of the snow cover on the thermal regime. Also, a new offset between air temperature and ground temperature within the active layer of intact rock glaciers can be introduced. The latter might give an estimation of the temperature difference that is needed, between the ground and the air, to block their interaction. Additionally, a longer time period could be analyzed in order to understand the evolution of temperature over several years. Loggers could additionally be installed at comparable microtopographic positions and within similar materials allowing a better confrontation. Temperature loggers at greater depth might contribute to an even wider understanding of the thermal regime within rock glaciers. It might be then possible to estimate how long rock glaciers remain intact and when they start becoming relict by losing their ice-core. It is of crucial importance to understand the lifetime of rock glaciers and their transformation in order to estimate future changes in hydrogeological settings such as groundwater storage, as well as in geomorphological processes like mass movements in Alpine areas.

References

Baehr, H. D.; Kabalec, S. (2017): Thermodynamik. Grundlagen und technische Anwendungen. 16., aktualisierte Aufl. 2017 (Lehrbuch).

Barsch, D. (1992): Permafrost creep and rockglaciers. In: *Permafrost Periglac. Process.* 3 (3), p. 175–188. DOI: 10.1002/ppp.3430030303.

Boeckli, L.; Brenning, A.; Gruber, S.; Noetzli, J. (2012): Permafrost distribution in the European Alps: calculation and evaluation of an index map and summury statistics. In: *The Cryosphere* (6), p. 807–820.

Box, G.E.P.; Jenkins, G. M. (1976): Time series analysis forescasting and control. San Francisco, Calif.: Holden-Day.

Brighenti, S.; Tolottu, M.; Bruno, M. C.; Wharton, G.; Pusch, M. T.; Bertoldi, W. (2019): Ecosystem shifts in Alpine streams under glacier retreat and rock glacier thaw: A review. In: *Science of the Total Environment* (675), p. 542–559.

Cohen, J. (1988): Statistical power analysis for the behavioral sciences. 2nd ed. Hillsdale, N.J: L. Erlbaum Associates.

Colucci, R. R.; Forte, E.; Žebre, M.; Maset, E.; Zanettini, C.; Guglielmin, M. (2019): Is that a relict rock glacier? In: *Geomorphology* 330, p. 177–189. DOI: 10.1016/j.geomorph.2019.02.002.

Delaloye, R.; Lambiel, C. (2005): Evidence of winter ascending air circulation throughout talus slopes and rock glaciers situated in the lower belt of alpine discontinuous permafrost (Swiss Alps). In: *Norsk Geografisk Tidsskrift - Norwegian Journal of Geography* 59 (2), p. 194–203. DOI: 10.1080/00291950510020673.

Goering, D. J. (2003): Thermal response of air convection embankments to ambient temperature fluctuations. In: *Permafrost, Phillips, Springman & Arenson*, p. 291–296.

Guodong, C.; Yuanming, L.; Zhizhong, S.; Fan, J. (2007): The 'thermal semi-conductor' effect of crushed rocks. In: *Permafrost Periglac. Process.* 18 (2), p. 151–160. DOI: 10.1002/ppp.575.

Haeberli, W. (1991): Creep of mountain permafrost. Internal structure and flow of alpine rock glaciers. Zurich: Eidgenossischen Technischen Hochschule.

Hanson, S.; Hoelzle, M. (2004): The thermal regime of the active layer at the Murtèl rock glacier based on data from 2002. In: *Permafrost Periglac. Process.* 15 (3), p. 273–282. DOI: 10.1002/ppp.499.

Harris, S. A.; Pederson, D. E. (1998): Thermal Regimes Beneath Coarse Blocky Materials. In: *Permafrost and Periglacial Processes* (9), p. 107–120.

Herz, T.; King, L.; Gubler, H. (2003): Microclimate within coarse debris of talus slopes in the alpine periglacial belt and its effect on permafrost. In: *Permafrost, Phillips, Springman & Arenson*, p. 383–387.

Hinkel, K. M.; Outcalt, S. I. (1994): Identification of Heat-Transfer Processes during Soil Cooling, Freezing and Thaw in Central Alaska. In: *Permafrost and Periglacial Processes* (5), p. 217–235.

Intergovernmental Panel on Climate Change (2014): Observations: Cryosphere. In: Intergovernmental Panel on Climate Change (Hg.): Climate Change 2013 - The Physical Science Basis. Cambridge: Cambridge University Press, p. 317–382.

Johansen, O. (1977): Thermal Conductivity. USA: Hanover.

Jones, D. B.; Harrison, S.; Anderson, K.; Whalley, W. B. (2019): Rock glaciers and mountain hydrology: A review. In: *Earth-Science Reviews* 193, p. 66–90. DOI: 10.1016/j.earscirev.2019.04.001.

Juliussen, H.; Humlum, O. (2008): Thermal regime of openwork block fields on the mountains Elgåhogna and Sølen, central-eastern Norway. In: *Permafrost Periglac. Process.* 19 (1), p. 1–18. DOI: 10.1002/ppp.607.

Juliussen, H.; Humlum, O.; Kristensen, L.; Christiansen H. H. (2008): Thermal Processes in the Active Layer of the Larsbreen Rock Glaciers, Central Spitsbergen, Svalbard, 2008, p. 877–882.

Kellerer-Pirklbauer, A.; Bartsch, A.; Gitschthaler, C.; Reisenhofer, S.; Weyss, G.; Riedl, W.; Avian, M. (2015a): permAT – Long-term monitoring of permafrost and periglacial processes and its role for natural hazard prevention: Possible strategies for Austria (in German).

Kellerer-Pirklbauer, A.; Pauritsch, M.; Winkler, G. (2015b): Widespread occurrence of ephemeral funnel hoarfrost and related air ventilation in coarse-grained sediments of a relict rock glacier in the seckauer tauern range, austria. In: *Geografiska Annaler: Series A, Physical Geography* 97 (3), p. 453–471. DOI: 10.1111/geoa.12087.

Klackl, D. (2018): Quartärgeologie und Hydrogeologie mit Schwerpunkt Blockgletscher in der Umgebung der Hochschoberhütte, Schobergruppe (Osttirol). Unpublished Master Thesis.

Kogler, T. (2018): Quartärgeologie und Permafrost (Blockgletscher) am Tuxer Hauptkamm (Zillertaler Alpen, Tirol, Österreich). Unpublished Master Thesis.

Kong, Y.; Wang, C. H. (2017): Responses and changes in the permafrost and snow water equivalent in the Northern Hemisphere under a scenario of 1.5 °C warming. In: *Advances in Climate Change Research* 8 (4), p. 235–244. DOI: 10.1016/j.accre.2017.07.002.

Koorevaar, P.;Menelik, G.; Dirksen, C. (1983). Elements of Soil Physics, 13. Elsvier (Development in Soil Science), p. 193-207

Kuhn, M.; Dreiseitl, E.; Emprechtinger, M. (2013): Temperatur und Niederschlag an der Wetterstatin Obergurgl, 1953 - 2011. Kapitel 1. In: *Koch, E.-M., Erschbamer, B. (Hrsg.) Klima, Wetter, Gletscher im Wandel. Alpine Forschungsstelle Obergurgl – Band 3, p. 11-30. Innsbruck University Press.*, 2013.

Lebeau, M.; Konrad, J-M. (2016): Non-Darcy flow and thermal radiation in convective embankment modeling. In: *Computers and Geotechnics* 73, p. 91–99. DOI: 10.1016/j.compgeo.2015.11.016.

Mayaud, C.; Wagner, T.; Benischke, R.; Birk, S. (2014): Single event time series analysis in a binary karst catchment evaluated using a groundwater model (Lurbach system, Austria). In: *Journal of hydrology* 511 (100), p. 628–639. DOI: 10.1016/j.jhydrol.2014.02.024.

Nield, D. A.; Bejan. A. (2019): CONVECTION IN POROUS MEDIA. Fifth Edition. DOI: 10.1007/978-3-319-49562-0

Pauritsch, M.; Wagner, T.; Winkler, G.; Birk, S. (2017): Investigating groundwater flow components in an Alpine relict rock glacier (Austria) using a numerical model. In: *Hydrogeol J* 25 (2), p. 371–383. DOI: 10.1007/s10040-016-1484-x.

Pedevilla, T. (2019): Geological Mapping and Investigations of the permafrost and hydrogeology in the area of Inneres Bergli, Lareintal, Tyrol. Hydrogeologische Untersuchung an Blockgletschern im Lareintal. Unpublished Master Thesis.

Pfingstl, S.; Kurz, W.; Schuster, R.; Hauzenberger, C. (2015): Geochronological constraints on the exhumation of the Austroalpine Seckau Nappe (Eastern Alps). In: *AJES* 108 (1), p. 172–185. DOI: 10.17738/ajes.2015.0011.

Qingbai, W.; Shiyun, Z.; Wei, M.; Luxin, Z. (2007): Qinghai-Xizang Railroad Construction in Permafrost Regions. In: *J. Cold Reg. Eng.* 21 (2), p. 60–67. DOI: 10.1061/(ASCE)0887-381X(2007)21:2(60).

Romanovsky, V. E.; Drozdov, D. S.; Oberman, N. G.; Malkova, G. V.; Kholodov, A. L.; Marchenko, S. S. et al. (2010): Thermal state of permafrost in Russia. In: *Permafrost Periglac. Process.* 21 (2), p. 136–155. DOI: 10.1002/ppp.683.

Scherler, D.; Bookhagen, B.; Strecker, M. R. (2011): Spatially variable response of Himalayan glaciers to climate change affected by debris cover. In: *Nature Geosci* 4 (3), p. 156–159. DOI: 10.1038/ngeo1068.

Scherler, M.; Schneider, S.; Hoelzle, M.; Hauck, C. (2014): A two-sided approach to estimate heat transfer processes within the active layer of the Murtèl–Corvatsch rock glacier. In: *Earth Surf. Dynam.* 2 (1), p. 141–154. DOI: 10.5194/esurf-2-141-2014.

Siegesmund, S.; Dürrast, H. (2011): Physical and Mechanical Properties of Rocks. In: S. Siegesmund (Hg.): Stone in architecture. Properties, durability, Bd. 9. 4. ed. Berlin, Heidelberg: SPRINGER, p. 97–225.

Smith, M. W.; Riseborough, D. W. (2002): Climate and the limits of permafrost: a zonal analysis. In: *Permafrost and Periglac. Process.* 13 (1), p. 1–15. DOI: 10.1002/ppp.410.

Stull, R. B. (1988): An Introduction to Boundary Layer Meteorology. Dordrecht: Springer Netherlands (Atmospheric Sciences Library, 1383-8601, 13).

Wagner, T.; Kainz, S.; Wedenig, M.; Pleschberger, R.; Krainer, K. (2019a): Wasserwirtschaftliche Aspekte von Blockgletschern in Kristallingebieten der Ostalpen. Speicherverhalten, Abflussdynamik und Hydrochemie mit Schwerpunkt Schwermetallbelastung (RGHeavyMetal). Endbericht. Unter Mitarbeit von Simon Kainz, Michael Wedenig, Roswitha Pleschberger, Karl Krainer, Andreas Kellerer-Pirklbauer, Markus Ribis et al.

Wagner, T.; Pauritsch, M.; Mayaud, C.; Kellerer-Pirklbauer, A.; Thalheim, F.; Winkler, G. (2019b): Controlling factors of microclimate in blocky surface layers of two nearby relict rock glaciers (Niedere Tauern Range, Austria). In: *Geografiska Annaler: Series A, Physical Geography* 105 (2), p. 1–24. DOI: 10.1080/04353676.2019.1670950.

Weiss, A. D. (2000): Topographic Position and Landforms Analysis. The Nature Conservancy, 2000.

Winkler, G.; Pauritsch, M.; Wagner, T.; Kellerer-Pirklbauer, A. (2016a): Relict rock glaciers as groundwater stores in alpine catchments of the Niedere Tauern Range. In: *Berichte der Wasserwirtschaftlichen Planung Steiermark*, 2016 (Band 87).

Winkler, G.; Wagner, T.; Pauritsch, M.; Birk, S.; Kellerer-Pirklbauer, A.; Benischke, R. et al. (2016b): Identification and assessment of groundwater flow and storage components of the relict Schöneben

Rock Glacier, Niedere Tauern Range, Eastern Alps (Austria). In: *Hydrogeol J* 24 (4), p. 937–953. DOI: 10.1007/s10040-015-1348-9.

Wu, Q. B.; Li, M. Y.; Liu, Y. Z. (2009): The cooling effect of crushed rock structures on permafrost under an embankment. In: *Science in Cold and Arid Regions* (1), p. 39–50.

Zehner, P.; Schlunder, E. U. (1970): Thermal conductivity of granular materials at moderate temperatures. In: *Chem Ing Tech*, 1970 (42), p. 933–941.

Zhang, T. (2005): Influence of the seasonal snow cover on the ground thermal regime: An overview. In: *Rev. Geophys.* 43 (4), p. 1. DOI: 10.1029/2004RG000157.

Table of Figures

Tables

Appendix 1: Correlation coefficients

Table 5 Correlation coefficients calculated between the loggers of each rock glacier (SRG, RGB, RGH and RGT). Results show a homogenous distribution of the GST for all rock glaciers except for RGT3 and RGB. Green numbers indicate a high correlation coefficient (r > 0,7); medium correlation coefficients (0,5 < r < 0,8) are shown as yellow values and low correlation coefficients (r < 0,4) are underlined as red values.

SRG	S_MTD3	S_MTD1	S_MTD4	S_MTD5	S_MTD2
S_MTD3					
S_MTD1	0,972				
S_MTD4	0,963	0,95			
S_MTD5	0,963	0,944	0,977		
S_MTD2	0,911	0,923	0,907	0,911	

RGB	KW 1	KW 2	KW 3	KW 4	KW 6	KW 7	KW 8	KW 10	KW 11	KW 12	KW 13
KW 1											
KW 2	1										
KW 3	0,734	0,734									
KW 4	0,922	0,922	0,806								
KW 6	0,808	0,808	0,951	0,883							
KW 7	0,863	0,863	0,847	0,934	0,902						
KW 8	0,764	0,764	0,912	0,846	0,944	0,852					
KW 10	0,820	0,820	0,884	0,814	0,869	0,809	0,849				
KW 11	0,736	0,736	0,943	0,793	0,926	0,845	0,916	0,916			
KW 12	0,832	0,832	0,927	0,886	0,954	0,875	0,908	0,892	0,914		
KW 13	0,594	0,594	0,822	0,683	0,802	0,739	0,798	0,759	0,832	0,797	

RGH	KW 14	KW 15	KW 16	KW 17	S 9	T 3	T 4	TS 19	WH 1	WH 2	WH 3	Z 1	Z 2	Z 3
KW14														
KW 15	0,967													
KW 16	0,972	0,977												
KW 17	0,957	0,932	0,947											
S 9	0,964	0,953	0,972	0,950										
T 3	0,951	0,922	0,924	0,929	0,940									
T 4	0,976	0,968	0,958	0,950	0,968	0,964								
TS 19	0,953	0,956	0,968	0,931	0,963	0,934	0,963							
WH 1	0,963	0,943	0,933	0,961	0,937	0,967	0,971	0,932						
WH 2	0,951	0,930	0,954	0,933	0,975	0,920	0,946	0,940	0,917					
WH 3	0,979	0,972	0,964	0,955	0,964	0,946	0,974	0,942	0,962	0,936				
Z 1	0,948	0,933	0,936	0,931	0,966	0,965	0,971	0,952	0,955	0,943	0,945			
Z 2	0,967	0,970	0,987	0,943	0,965	0,915	0,947	0,955	0,926	0,958	0,957	0,919		
Z 3	0,940	0,942	0,949	0,931	0,956	0,913	0,945	0,956	0,927	0,959	0,930	0,946	0,953	

RGT1	T 11	TS 14A	T 24A							
T 11										
TS 14A	0,965									
T 24A	0,972	0,936								
RGT2	T 3A	T 4	T 8	TS 23	T 16	T 31	TS 17A	TS 25	T 18	TS 12	TS 28
T 3A											
T 4	0,794										
T 8	0,870	0,899									
TS 23	0,783	0,878	0,834								
T 16	0,746	0,780	0,824	0,689							
T 31	0,828	0,920	0,884	0,924	0,743						
TS 17A	0,875	0,859	0,909	0,905	0,804	0,928					
TS 25	0,873	0,818	0,916	0,824	0,810	0,858	0,950				
T 18	0,846	0,821	0,887	0,826	0,789	0,880	0,951	0,958			
TS 12	0,827	0,926	0,921	0,915	0,736	0,948	0,923	0,878	0,888		
TS 28	0,885	0,847	0,915	0,843	0,844	0,885	0,957	0,968	0,940	0,887	
RGT3	T 9	T 27	T 32	T 33	T 38	TS 17	TS 21A	TS 22A	T19		
T 9											
T 27	0,672										
T 32	0,964	0,727									
T 33	0,901	0,671	0,929								
T 38	0,410	0,920	0,458	0,427							
TS 17	0,890	0,727	0,933	0,936	0,503						
TS 21A	0,662	0,955	0,711	0,631	0,883	0,668					
TS 22A	0,648	0,984	0,709	0,639	0,917	0,694	0,965				
T19	0,964	0,714	0,968	0,935	0,465	0,933	0,680	0,689			

Appendix 2: Temperature range

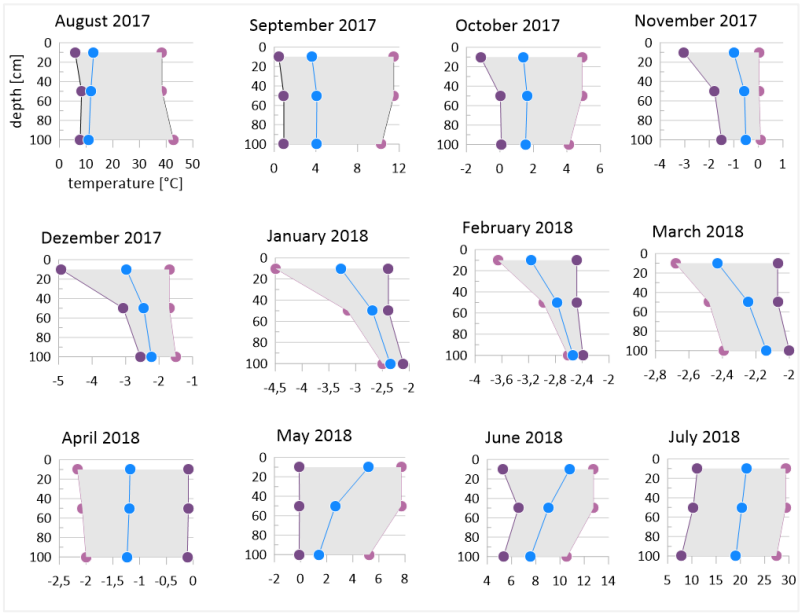

coarse grained material

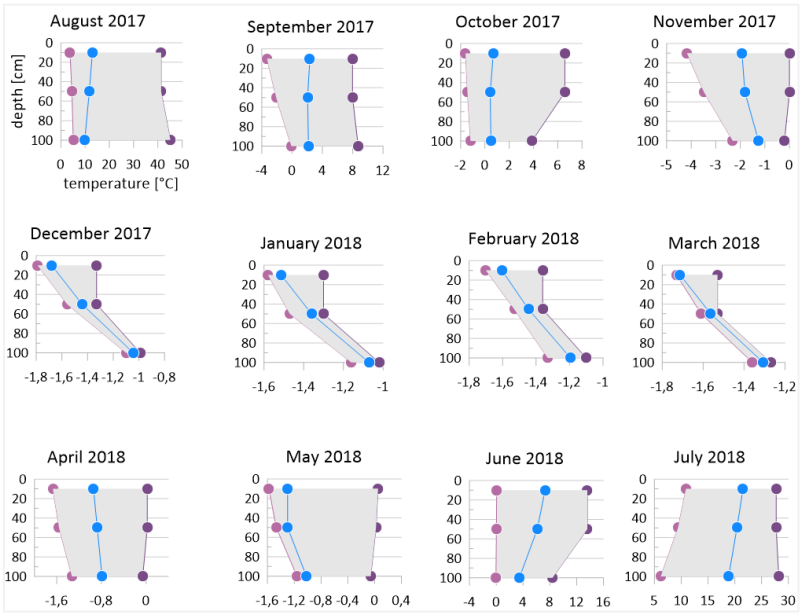

fine grained material

Figure 39 Monthly mean of the ground surface- and ground temperature calculated for the two logger profiles installed on RGB. Blue line indicates the monthly mean; violet lines indicate the daily maximum and minimum recorded in the corresponding month. The grey area shows the range of the data collected within one month.

Figure 40 Monthly mean of the ground surface- and ground temperature calculated for the logger profiles installed on SRG. Blue line indicates the monthly mean; violet lines indicate the daily maximum and minimum recorded in the corresponding month. The grey area shows the range of the data collected within one month.

Appendix 3: Cross-correlation

Table 6 Time lags and R(k) max calculated for each logger at SRG and RGB. Results show how fast (time lags in hours) and how intense (R(k) max), the upper layer of the two rock glaciers react to external temperature changes. "GST" indicates results of the ground surface temperature and "GT" those of the ground temperature at SRG. "C1"/"F1", "C2"/"F2" and "C3"/"F3" show the results of the ground surface temperature (0,10m depth), the ground middle temperature (0,50m depth) and the ground temperature (1,0m depth), respectively, at RGB.

Schöneben Rock Glacier		autumn	winter	spring	summer
	lag [h]	3	81	2	2
SMTD1 - GST	R(k) max	0,79	0,58	0,87	0,93
	lag [h]	12	146	6	7
SMTD1 - GT	R(k) max	0,87	0,43	0,81	0,86
	lag [h]	3	91	1	1
SMTD2 - GST	R(k) max	0,89	0,59	0,81	0,93
	lag [h]	14	164	2	7
SMTD2 - GT	R(k) max	0,81	0,46	0,77	0,85
	lag [h]	3	107	1	0
SMTD3 - GST	R(k) max	0,76	0,52	0,81	0,93
	lag [h]	9	119	4	7
SMTD3 - GT	R(k) max	0,78	0,46	0,78	0,81
	lag [h]	2	160	0	0
SMTD4 - GST	R(k) max	0,87	0,36	0,75	0,94
	lag [h]	20	168	3	9
SMTD4 - GT	R(k) max	0,73	0,24	0,71	0,90
	lag [h]	3	82	0	1
SMTD5 - GST	R(k) max	0,82	0,50	0,79	0,92
	lag [h]	18	168	3	7
SMTD5 - GT	R(k) max	0,75	0,10	0,76	0,91

Bergli Rock Glacier		autumn	winter	spring	summer
C1	lag [h]	**12**	**-76**	**17**	**124**
	R(k) max	**0,50**	**0,09**	**0,45**	**0,26**
C2	lag [h]	**20**	**-41**	**47**	**-129**
	R(k) max	**0,49**	**0,13**	**0,43**	**0,19**
C3	lag [h]	**28**	**-53**	**46**	**-110**
	R(k) max	**0,50**	**0,14**	**0,41**	**0,20**
F1	lag [h]	**6**	**90**	**44**	**122**
	R(k) max	**0,58**	**0,11**	**0,30**	**0,28**
F2	lag [h]	**9**	**82**	**44**	**124**
	R(k) max	**0,55**	**0,10**	**0,31**	**0,24**
F3	lag [h]	**16**	**168**	**17**	**-114**
	R(k) max	**0,53**	**0,12**	**0,34**	**0,21**